The Systems Biology of MHC Class II Antigen Presentation

Petra Paul

The Systems Biology of MHC Class II Antigen Presentation

Proefschrift

ter verkrijging van
de graad van Doctor aan de Universiteit Leiden,
op gezag van Rector Magnificus prof.mr. P.F. van der Heijden,
volgens besluit van het College voor Promoties

te verdedigen op donderdag 6 september 2012
klokke 11.15 uur

door
Petra Paul

geboren te Wenen, Oostenrijk
in 1980

Promotiecommissie

Promotor:	Prof. Dr. J. J. Neefjes
Referent:	Prof. Dr. Tom H. M. Ottenhoff
Overige leden:	Prof. Dr. J. Borst *Universiteit van Amsterdam*
	Prof. Dr. M. van Ham *Universiteit van Amsterdam*
	Prof. Dr. H. Overkleeft
	Prof. Dr. E. J. H. J. Wiertz *Universiteit Utrecht*

Cover and Art Work: Wilhelm Paul

The research described in this thesis was performed at the Department of Cell Biology II at the Netherlands Cancer Institute (Antoni van Leeuwenhoek Ziekenhuis, NKI/AvL) under the supervision of Prof. Dr. J. Neefjes and was supported by an EEC Marie Curie Research Training Network, an ERC program grant, the Dutch Cancer Society, NWO ALW and CW and the Center for Biomedical Genetics (CBG).

Financial support for the publication of this thesis was provided by: The Netherlands Cancer Institute and BD Biosciences.

Table of Contents

Introduction

Towards a Systems Understanding of MHC Class II Antigen Presentation

Adapted from
Neefjes J, Jongsma ML, Paul P, Bakke O

Nature Reviews Immunology, 2011 Nov 11;11(12):823-36

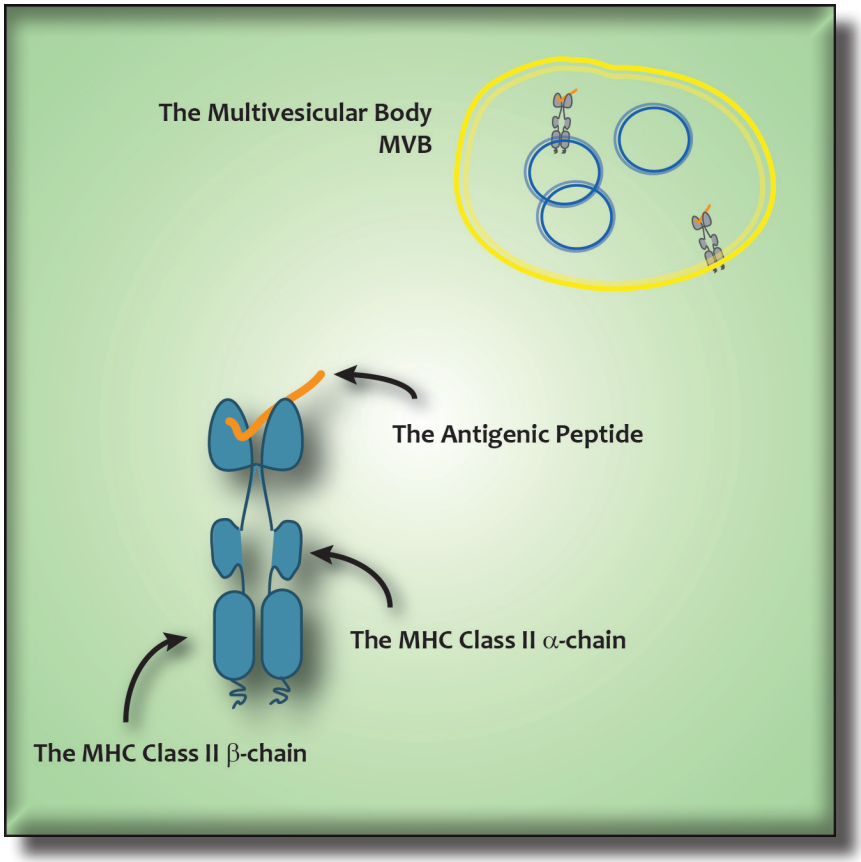

The molecular details of antigen processing and presentation by MHC class II molecules have been studied extensively for almost three decades. Although the basics of these processes were laid out some ten years ago, the recent years have revealed many details and provided new insights into their control and specificity. MHC molecules employ various biochemical reactions in order to achieve successful presentation of antigenic fragments to the immune system. Here we present a timely evaluation of the biology of antigen presentation and a survey of issues considered unresolved. The continuing flow of new details into the biology of MHC class II antigen presentation is exciting and builds a system involving several cell biological processes, which is being discussed in this chapter.

Introduction

Major Histocompatibility class I and II molecules (MHC-I and MHC-II) are similar in function: they present peptides at the cell surface to CD8+ and CD4+ T cells, respectively. These peptides originate from different sources - intracellular for MHC-I and exogenous for MHC-II - and are obtained via different pathways [1]. An interesting link, termed cross-presentation, exists between the two pathways, whereby exogenous antigens are presented by MHC-I [2]. In addition, cytosolic proteins can be presented by MHC-II when proteins are degraded through the autophagy or other pathways [3]. Furthermore, the various mechanisms that pathogens have evolved to manipulate the MHC-I and MHC-II pathways have provided new insights into the biology of antigen presentation [4]; however, we will not further discuss these topics, as they have recently been reviewed [2-4].

MHC-II: like and unlike MHC-I Molecules

MHC-I and MHC-II molecules overlap in a number of characteristics: high polymorphism, similar 3D structure due to the fact that they originate from one common founder gene by simple gene duplication, location in one gene locus and presentation of peptides to the immune system. Yet, these molecules show a different tissue distribution and differ in the types of antigenic peptides presented as a result of their different cell biology.

Like MHC-I, MHC-II is encoded by three polymorphic genes (HLA-DR, HLA-DQ and HLA-DP in humans) that bind different peptides. Some of the MHC-II alleles are known to be the strongest genetic markers associated to autoimmune diseases, possibly due to the peptides they present [5]. Although the different alleles appear to associate differentially with the chaperone HLA-DM (see later) [6], the effects of MHC-II polymorphism on their cell biology is poorly studied when compared to MHC-I. The MHC-II pathway described below is mainly based on studies of HLA-DR and murine MHC-II (I-A and I-E). Of note, the pathway may differ in details for other MHC-II molecules.

The Basics of MHC-II Antigen Presentation

While MHC-I is ubiquitously expressed, MHC-II molecules are primarily expressed by professional APCs, such as dendritic cells (DCs), macrophages and B cells. It has been concluded from the work of many groups that the transmembrane α- and β-chains of MHC-II are assembled in the ER and associate with the

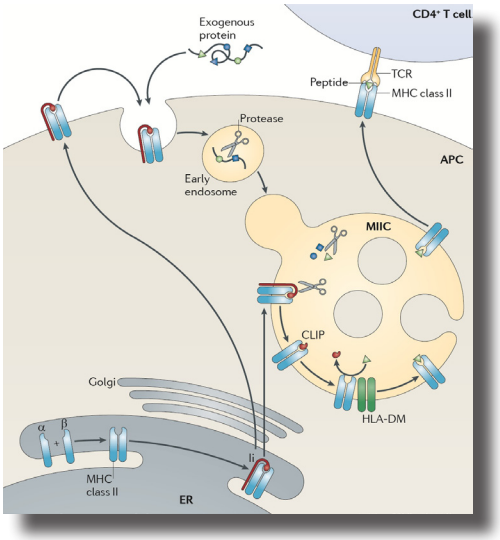

Figure 1 | The Basics MHC Class II Antigen Presentation Pathway

MHC-II α- and β-chains assemble in the ER and form a complex with the Ii. The MHC-II/Ii heterotrimer is transported through the Golgi to the MIIC, either directly and/or via the plasma membrane. Endocytosed proteins and the Ii are degraded here by resident proteases. The CLIP fragment of Ii remains in the peptide-binding groove of MHC-II and is exchanged for proper peptide with the help of the dedicated chaperone HLA-DM. MHC-II is then transported to the plasma membrane for presentation of antigenic fragments to CD4+ T cells.

CLIP, Class II associated Invariant chain Peptide. ER, Endoplasmic Reticulum. Ii, Invariant chain. MIIC, MHC II Compartment. TCR, T-cell receptor.

invariant chain (Ii). The resulting MHC-II-Ii complex is transported to late endosomal compartments, termed MIIC (MHC class II compartment). Here, Ii is digested, leaving a residual class II-associated Ii peptide (CLIP) in the peptide-binding groove of MHC-II. In the MIIC, MHC-II requires HLA-DM (H2-DM in mice) to facilitate the exchange of the CLIP fragment for a specific peptide derived from proteins degraded in the endosomal pathway. MHC-II is then transported to the plasma membrane to present its peptide cargo to CD4+ T cells (Figure 1). In B cells, a modifier of HLA-DM is expressed called HLA-DO (H2-O in mice) which associates with HLA-DM and restricts HLA-DM activity to more acidic compartments thus modulating peptide binding to MHC-II [7].

Cross-presentation aside, MHC-I presents peptides of cytosolic origin, whereas MHC-II carries peptides derived from antigens degraded in the endocytic pathway. Their combined specificities cover antigens from almost all cellular compartments. However, essential differences in the pathways complicate this basic paradigm. In addition, various issues are less well understood and no numbers to calculate the reaction efficiencies leading to MHC-II peptide loading have been reported.

The Complexity of MHC-II Antigen Presentation

MHC-II Expression

Unlike MHC-I, the expression of MHC-II is restricted to APCs. However, MHC-II expression can be induced by IFNγ and other stimuli in non-APCs, including mesenchymal stromal cells [8], fibroblasts and endothelial cells [9], and in epithelial cells and enteric glial cells in Crohn's disease [10, 11] and eosinophilic esophagitis [12]. Also dermatoses, such as psoriasis [13], can induce MHC-II expression by keratinocytes [14]. Non-APCs may express MHC-II in the absence of co-stimulatory molecules that may drive or attenuate local T cell responses. The question is, how expression of MHC-II is controlled in APC and non-APCs.

The master regulator of MHC-II expression is class II transactivator (CIITA). CIITA is recruited by the MHC-II enhanceosome (which contains cyclic-AMP-responsive-element-binding protein (CREB), nuclear transcription factor Y (NFY) and the regulatory factor X (RFX) complex) to the X1, X2, Y-box elements at the MHC-II locus (reviewed in [15]). CIITA expression is regulated in a more complex manner, yielding CIITA isoforms I, III and IV [16, 17], which are expressed in different cell types. Transcriptional regulation of MHC-II in DCs is controlled by an additional layer of regulation. In immature DCs, four factors (PU.1, IRF8, NF-κB and SP1) bind to the type I CIITA promoter resulting in high CIITA transcription and, as a result, high MHC-II transcription. During DC maturation, this complex is replaced by a complex containing PR domain zinc finger protein 1 (PRDM1) and B-lymphocyte-induced maturation protein 1 (BLIMP1) that inhibits CIITA transcription [18] (Figure 2B). In addition, CIITA requires phosphorylation [19, 20] and mono-ubiquitination [21, 22] before being active as the MHC-II transcription factor in APCs.

By combining the results of a genome-wide small interfering RNA (siRNA) screen with quantitative PCR, five upstream regulators of CIITA (CDCA3, RMND5B, CNOT1, MAPK1 and PLEKHA4) were recently identified. By determining how these factors controlled the expression of each other, a complex feedback mechanism in control of CIITA and MHC-II transcription was uncovered [23 and Chapter 1 of this thesis] (Figure 2A). In fact, a complex transcriptional feedback mechanism is the only mechanism possible to explain how a master regulator of transcription (CIITA) is controlled by the next factor that is controlled by the next ad infinitum. However, the factors constituting the feedback mechanism should also be controlled. Further systems biology analyses showed that feedback control of CIITA expression is determined by the combined activities of transforming growth factor β (TGFβ) signalling and chromatin modifications leading to MHC-II transcription in APCs [23]. Tissue specific regulation of MHC-II expression is then the consequence of two general terms; chromatin modifications that include epigenetics, and signalling by external factors. The latter has been noticed earlier as a series of cell types only express MHC-II under inflammatory conditions (see later). In summary, transcription of MHC-II is controlled by the master regulator CIITA, which in turn is regulated by post-translational modifications and factors mainly, but not exclusively, active in immune cells. Under defined conditions of signalling and chromatin modifications, CIITA and MHC-II can be expressed in non-immune cells, often in response to infections or inflammation.

MHC-II Transport from ER to the MIIC

Although both MHC-I and MHC-II are assembled in the ER, MHC-I needs to be loaded with peptide to leave the ER, whereas MHC-II associates with Ii [24]. Four different splice variants of Ii exist, with variation in the cytoplasmic tail (the p33 and p35 variants) or inclusion of an additional exon encoding a protease inhibitor cystatin (the p43 and p45 variants) [25, 26]. While the α and β chain of MHC-II are ER-bound, the assembled MHC-II αβ heterodimers is already slowly leaving the ER, which is further accelerated by Ii binding. It is believed that the CLIP region

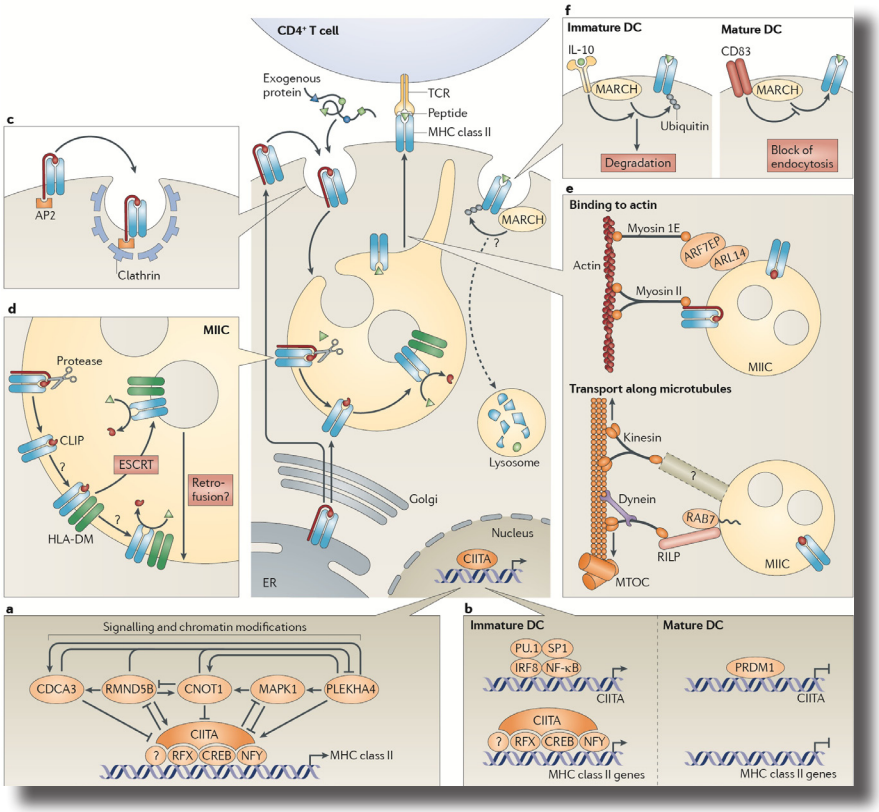

Figure 2 | Complexity of the MHC Class II Antigen Presentation Pathway

Insights in the various steps of the MHC-II pathway are shown in different boxes projected on the basic pathway of Figure 1. a | MHC-II transcription is controlled by master regulator CIITA ensuring tissue specific expression. CIITA is controlled by a feedback loop of factors that are subsequently controlled by two general processes: (TGFβ) signaling and chromatin modifications. b | CIITA expression is differentially controlled in imDC (via an activating transcriptional complex) and mDC (via an inhibitory complex). Consequently, CIITA (with other factors) induces transcription of MHC-II in imDC unlike in mDC. c | Adaptor proteins binding the Ii are known. AP2 drives internalization of MHCII-Ii complexes via CCV at the plasma membrane for endocytosis and transport to the MIIC. d | In the MIIC, Ii is degraded and MHC-II interacts with HLA-DM. Most HLA-DM and MHC-II locate and interact in the internal structures formed by the ESCRT machinery. The mechanism of back-fusion of internal DM and MHC-II to the limiting membrane is hypothetical. e | MHC-II or its tubular extensions are transported by the microtubule-based motor proteins dynein and kinesin. These have receptors on the MIIC, like RAB7-RILP for the dynein motor. The final step involves actin-based myosin motors that interact with the MIIC via Ii (MYOII) or the GTPase ARL14 (MYO1E). The latter mechanism controls MIIC secretion in imDC. f | In imDCs, internalization of MHC-II from the plasma membrane may require the ubiquitin ligase MARCH1 which is controlled by IL10. CD83 on mDC prevents this ubiquitin modification of MHC-II which stabilizes MHC-II cell surface expression.

AP2, Adaptor Protein-2. CCV, Clathrin Coated Vesicle. CIITA, Class II TransActivator. imDCs, immature Dendritic Cell. mDCs, mature Dendritic Cell. Ii, invariant chain. MHC, Major Histocompatibility Complex. MIIC, MHC II Compartment. MTOC, Microtubuli organizing centre. TCR, T-cell receptor.

of Ii blocks the peptide-binding groove of MHC-II, thus preventing binding of other peptides in the ER. Indeed, the levels of endogenous antigen presentation is higher in Ii knockout mice [27], but biochemical analyses of the same mice suggest this is not an efficient process, as most MHC-II are not converted into a stable peptide-loaded form in the absence of Ii [28, 29]. Yet, particular antigens can access MHC-II after TAP-dependent translocation in the ER [30] but the vast majority of peptides will fail

to enter MHC-II due to Ii.

The cytoplasmic tail of Ii contains two classical di-leucine sorting motifs that direct MHC-II to endosomal compartments (Figure 2C). These sorting motifs are recognized by the sorting adaptors AP1 (a trans-Golgi network adaptor) and AP2 (a plasma membrane adaptor) [31]. Ii may direct MHC-II directly from the trans-Golgi network to MIIC or by endocytosis from the plasma membrane. Endocytosis may be preferred in human cervical carcinoma cells (HeLa cells) and immature DCs (AP2 dependent) [32, 33], whereas direct sorting may be dominant in mature DC (AP1 dependent) [34]. In summary, Ii is essential for various steps in the life of MHC-II, but may take different routes to its final destination, which is the endosomal pathway where Ii is degraded before MHC-II finally acquires its final peptide.

The MHC-II Peptide-loading Compartment

While MHC-I binds peptides in a partially folded state stabilized by chaperones in the ER, this is probably different for MHC-II, as endosomes are not known to contribute to folding. The location of MHC-II peptide loading has been a matter of debate since the MIIC was visualized by electron microscopy in 1990 [35]. At that time, the MIIC was shown to contain MHC-II and Ii, to be multilamellar in morphology, to be acidic and to contain lysosomal proteases and CD63, which defined it as late endosomal [35]. Other structures were subsequently identified and a revised definition for the MIIC was required. The MHC-II chaperone HLA-DM was found to localize in late endosomes [36], where it stabilizes MHC-II either bound to or devoid of the CLIP peptide (thus preventing aggregation and degradation of MHC-II) until high affinity peptides bind [37] (Figure 2D). The late endosomal tetraspanin proteins [38] which interact with HLA-DM and MHC-II, and probably induce the formation of a proteinacious network, were identified, as were the proteases cathepsin S and cathepsin L that degrade Ii [39]. An *in vitro* reconstitution experiment defined the molecules minimally required for the MIIC as MHC-II, HLA-DM and cathepsins [40] and the combined data suggest that a late endosomal structure with (at least) these three factors would fulfill the criteria for the MIIC.

A complicating factor is that the MIIC is not homogeneous but exists in multiple morphologies (multivesicular, mixed and multilamellar) that may represent different maturation states. MHC-II, HLA-DM and other molecules are located mainly in the internal structures of the MIIC and have to be ubiquitinated and sorted by the endosomal sorting complex required for transport (ESCRT) machinery on the limiting membrane [41]. Fluorescence resonance energy transfer (FRET) studies have suggested that HLA-DM interacts with MHC-II on the internal vesicles of the MIIC and not on the limiting membrane [42]. The internal vesicles carrying MHC-II and HLA-DM are thought to fuse back to the limiting membrane of MIIC to prevent secretion in the form of exosomes and to be embedded in the plasma membrane. This process of 'retrofusion' has not yet been defined. Another model proposes that peptide-loaded MHC-II appearing on the plasma membrane in DCs originate from the limiting membrane and that MHC-II on internal vesicles are destined for degradation [43]. However, as most of the MHC-II is found on internal vesicles, a major loss of MHC-II would be expected to occur, but this was not observed in biochemical experiments [44]. The molecular mechanisms of retrofusion (if any) need to be defined to explain this contradiction.

Although the intracellular location for peptide loading of MHC-II seems to be in the MIIC, many issues have yet to be resolved. These include the entry of MHC-II via earlier endosomes into the MIIC and the functional role of Ii to mediate fusion of early endosomes [45] and regulate intracellular transport of MHC-II [46]. MHC-II will probably present different peptides when sampling these in different parts of the endosomal pathway with different help of HLA-DM [47]. Finally, degradation of antigens is strongly delayed in immature DCs possibly as a mechanism to store antigens for presentation over long periods of time [48]. Whereas the minimal MIIC has been defined, the consequences of different MIIC morphology, different proteolytic activities, controlled acidification during DC maturation, retrofusion and other processes need to be defined for a more complete understanding of the intracellular process of MHC-II antigen loading.

MHC-II Transport from MIIC towards the Plasma Membrane

Late endosomal compartments such as MIIC are not typical recycling structures; yet MHC-II, HLA-DM, tetraspanins and other molecules are transported from the MIIC to the plasma membrane. The content of MIIC, including MHC-II, is released after a specific time period. This release is controlled by factors such as cholesterol, cytosolic pH, kinases and GTPases.

Fast transport of MIIC and other vesicles is driven by the microtubule-based motors dynein (for inward transport) and the kinesin family (for outward transport), whereas slow vesicle transport involves the actin-based myosin motor family. Motor proteins require vesicle receptors that are subsequently controlled by other processes. The molecular basis for this part of cell biology is largely undefined with few exceptions. Inward transport of MIIC by the

dynein motor is controlled by the RAB7-interacting lysosomal protein (RILP) on MIIC (Figure 2E), which is further controlled by the cholesterol-sensor OSBP-related protein 1L (ORP1L) and the ER-resident protein VAMP-associated protein A (VAPA) [49]. This may explain the effect of cholesterol on MHC-II antigen presentation [50].

DCs may be unique in that MHC-II transport from MIIC is regulated by maturation signals, which induce higher MHC-II surface expression at the cost of the intracellular pool of MHC-II [51, 52]. Lipopolysaccharide triggers the formation of tubules that originate from MIIC in DCs, generating a complex network of moving vesicles and tubules that may all fuse to the plasma membrane [53-55]. What controls MHC-II transport in DCs? Two actin-based motors have been implicated. The common actin motor myosin II (MYOII) may interact with Ii to control MHC-II transport in DCs [56] (Figure 2E). Another pathway controlling MHC-II transport in DCs was identified using an integrated siRNA and cell biology screen. First, siRNAs affecting MHC-II expression were defined, then downregulation of the target genes upon maturation of DCs was determined and the finally remaining candidates were silenced in immature DCs. Some of these induced redistribution of MHC-II corresponding to maturated DCs, while the cells remained immature in respect to other activation markers [23]. The candidates included GTPase ADP-ribosylation factor-like protein 14 (ARL14; also known as ARF7) that locates on MIIC, recruits the effector ARF7EP, which acts as a receptor for the motor protein myosin1E (MYO1E) [23 and Chapter 1 of this thesis]. This pathway controls MHC-II export in DCs (Figure 2E). How maturation signals by LPS control these pathways is unclear, yet they may show some resemblance to the induced secretion of other lysosome-related organelles, such as cytolytic granules, melanosomes and Weibel-Palade bodies [57].

The End of an MHC-II Molecule

Similar to MHC-I, MHC-II do not have an infinite life. However, MHC-II is relatively stable (it has already survived late endosomal conditions) and does not dissociate at the plasma membrane. In addition, the half-life of MHC-II greatly increases upon DC maturation [51, 52]. How is it then finally degraded? MHC-II (like MHC-I) can be ubiquitylated by MARCH1 [58]. Since the expression levels of MARCH1– and ubiquitiylation of MHC-II – decrease when DCs mature, ubiquitylation was proposed to control MHC-II half-life [59]. Interleukin-10 (IL-10) downregulates surface expression of MHC-II and controls the expression of MARCH1 [60, 61]. In addition, the co-stimulatory molecule CD83 is highly expressed by mature DCs and inhibits the interaction between MARCH1 and MHC-II, thereby preventing MHC-II ubiquitiylation [62]. These observations suggest a causal link between ubiquitylation and MHC-II half-life (Figure 2F). However, this link has recently been challenged. Mice engineered to express MHC-II with mutations that prevent its ubiquitylation still show normal antigen presentation by MHC-II, although MHC-II expression at the plasma membrane was slightly elevated [63]. Therefore, MHC-II ubiquitylation may be involved in sorting within the endosomal pathway rather than endocytosis and degradation [48, 64].

In summary, MHC-II is extraordinary stable but still displays cell type-specific half-lives. The control of MHC-II degradation has not been established but could involve ubiquitylation [63] . Most likely, MHC-II ends like any other lysosomal protein by lysosomal proteolysis, but the exact mechanism is unresolved.

The Systems of MHC-II Antigen Presentation

Although the system of antigen presentation is understood at a high level of detail, this in fact only represents sketches of the total biology. For a further understanding, modern technologies such as siRNA screens allow genome-wide consideration of relevant molecular relationships. This can yield comprehensive lists of new molecules involved in any process. An integration of siRNA data with flow cytometry, microscopy and transcriptional information from qPCR and microarray yielded various novel pathways, placing novel GTPases and motor proteins in the control of MHC-II transport [23]. Such experimental data sets can be integrated with others derived from siRNA screens, genetic screens, expression and protein-protein interaction data bases to build pathways *in silico*. These pathways then have to be experimentally validated to avoid noise in our understanding of the MHC-I and MHC-II antigen presentation pathway.

Outside-in Signalling by MHC-II

MHC-II mediate inside-out signalling when presenting peptides to T cells, but recent data suggest that MHC-II also functions as a signalling receptor, resulting in outside-in signalling (reviewed in [65]). This can lead to apoptosis of activated APCs and results in the termination of immune responses [66]. By contrast, engagement of MHC-II on melanoma cells by its ligand lymphocyte activation gene 3 (LAG3) expressed by infiltrating lymphocytes can prevent cell death by activating survival pathways [67]. Since MHC-II has short cytoplasmic tails without detectable signalling motifs, adaptor molecules

must be involved to transduce the outside-in signals [65]. Toll-like receptor (TLR) activation induces the association of CD40 and Bruton's tyrosine kinase (BTK) with intracellular MHC-II, resulting in prolonged BTK activation and TLR signalling-specific gene transcription [68]. In addition to CD40, the B cell receptor complex components CD79a and CD79b [69], the IgE receptor [70] and CD19 [71] have been reported to be involved in MHC-II-associated signal transduction. Signalling through MHC-II is a new concept and consequences of this have to be revealed in the future.

Conclusions and Perspectives

The biology of MHC-I and MHC-II has been studied extensively due to their fundamental role in controlling immune responses and their involvement in transplantation, infection, vaccination and autoimmunity. Understanding MHC-I and MHC-II antigen presentation can be – and in fact already is – translated into treatment options [72-74]. Deeper understanding of antigen presentation by MHC-I and MHC-II should result in additional targets for therapeutic manipulation of the immune system.

Many groups have recently uncovered new steps in the antigen processing and presentation system. However, many unknowns and controversies remain. Whether immunodominance of peptides can be predicted and why particular MHC-I or MHC-II alleles are associated with autoimmune diseases is mostly unclear (except for the known link between gluten, HLA-DQ2 and HLA-DQ8 and celiac disease [75]) but we hope they will be resolved in the coming years.

References

1. Vyas, J.M., A.G. Van der Veen, and H.L. Ploegh, *The known unknowns of antigen processing and presentation.* Nat Rev Immunol, 2008. **8**(8): p. 607-618.
2. Kurts, C., B.W. Robinson, and P.A. Knolle, *Cross-priming in health and disease.* Nat Rev Immunol, 2010. **10**(6): p. 403-414.
3. Crotzer, V.L. and J.S. Blum, *Autophagy and adaptive immunity.* Immunology, 2010. **131**(1): p. 9-17.
4. Horst, D., et al., *Viral evasion of T cell immunity: ancient mechanisms offering new applications.* Curr Opin Immunol, 2011. **23**(1): p. 96-103.
5. Fernando, M.M., et al., *Defining the role of the MHC in autoimmunity: a review and pooled analysis.* PLoS Genet, 2008. **4**(4): p. e1000024.
6. Anders, A.K., et al., *HLA-DM captures partially empty HLA-DR molecules for catalyzed removal of peptide.* Nat Immunol, 2011. **12**(1): p. 54-61.
7. Denzin, L.K., et al., *Right place, right time, right peptide: DO keeps DM focused.* Immunol Rev, 2005. **207**: p. 279-292.
8. Romieu-Mourez, R., et al., *Regulation of MHC class II expression and antigen processing in murine and human mesenchymal stromal cells by IFN-gamma, TGF-beta, and cell density.* J Immunol, 2007. **179**(3): p. 1549-1558.
9. Geppert, T.D. and P.E. Lipsky, *Antigen presentation by interferon-gamma-treated endothelial cells and fibroblasts: differential ability to function as antigen-presenting cells despite comparable Ia expression.* J Immunol, 1985. **135**(6): p. 3750-3762.
10. Bland, P., *MHC class II expression by the gut epithelium.* Immunol Today, 1988. **9**(6): p. 174-178.
11. Koretz, K., et al., *Metachromasia of 3-amino-9-ethylcarbazole (AEC) and its prevention in immunoperoxidase techniques.* Histochemistry, 1987. **86**(5): p. 471-478.
12. Mulder, D.J., et al., *Antigen presentation and MHC class II expression by human esophageal epithelial cells: role in eosinophilic esophagitis.* Am J Pathol, 2011. **178**(2): p. 744-753.
13. Schonefuss, A., et al., *Upregulation of cathepsin S in psoriatic keratinocytes.* Exp Dermatol, 2010. **19**(8): p. e80-e88.
14. Tjernlund, U.M., et al., *Anti-Ia-reactive cells in mycosis fungoides: a study of skin biopsies, single epidermal cells and circulating T lymphocytes.* Acta Derm Venereol, 1981. **61**(4): p. 291-301.
15. Choi, N.M., P. Majumder, and J.M. Boss, *Regulation of major histocompatibility complex class II genes.* Curr Opin Immunol, 2011. **23**(1):

p.81-87.
16. Muhlethaler-Mottet, A., et al., *Expression of MHC class II molecules in different cellular and functional compartments is controlled by differential usage of multiple promoters of the transactivator CIITA.* EMBO J, 1997. **16**(10): p. 2851-2860.
17. Reith, W., S. LeibundGut-Landmann, and J.M. Waldburger, *Regulation of MHC class II gene expression by the class II transactivator.* Nat Rev Immunol, 2005. **5**(10): p. 793-806.
18. Smith, M.A., et al., *Positive regulatory domain I (PRDM1) and IRF8/PU.1 counter-regulate MHC class II transactivator (CIITA) expression during dendritic cell maturation.* J Biol Chem, 2011. **286**(10): p. 7893-7904.
19. Sisk, T.J., et al., *Phosphorylation of class II transactivator regulates its interaction ability and transactivation function.* Int Immunol, 2003. **15**(10): p. 1195-1205.
20. Greer, S.F., et al., *Serine residues 286, 288, and 293 within the CIITA: a mechanism for down-regulating CIITA activity through phosphorylation.* J Immunol, 2004. **173**(1): p. 376-383.
21. Bhat, K.P., A.D. Truax, and S.F. Greer, *Phosphorylation and ubiquitination of degron proximal residues are essential for class II transactivator (CIITA) transactivation and major histocompatibility class II expression.* J Biol Chem, 2010. **285**(34): p. 25893-25903.
22. Greer, S.F., et al., *Enhancement of CIITA transcriptional function by ubiquitin.* Nat Immunol, 2003. **4**(11): p. 1074-1082.
23. Paul, P., et al., *A Genome-wide multidimensional RNAi screen reveals pathways controlling MHC class II antigen presentation.* Cell, 2011. **145**(2): p. 268-283.
24. Busch, R., et al., *Accessory molecules for MHC class II peptide loading.* Curr Opin Immunol, 2000. **12**(1): p. 99-106.
25. Bertolino, P. and C. Rabourdin-Combe, *The MHC class II-associated invariant chain: a molecule with multiple roles in MHC class II biosynthesis and antigen presentation to CD4+ T cells.* Crit Rev Immunol, 1996. **16**(4): p. 359-379.
26. Landsverk, O.J., O. Bakke, and T.F. Gregers, *MHC II and the endocytic pathway: regulation by invariant chain.* Scand J Immunol, 2009. **70**(3): p. 184-193.
27. Bodmer, H., et al., *Diversity of endogenous epitopes bound to MHC class II molecules limited by invariant chain.* Science, 1994. **263**(5151): p. 1284-1286.
28. Viville, S., et al., *Mice lacking the MHC class II-associated invariant chain.* Cell, 1993. **72**(4): p. 635-648.
29. Bikoff, E.K., et al., *Defective major histocompatibility complex class II assembly, transport, peptide acquisition, and CD4+ T cell selection in mice lacking invariant chain expression.* J Exp Med, 1993. **177**(6): p. 1699-1712.
30. Tewari, M.K., et al., *A cytosolic pathway for MHC class II-restricted antigen processing that is proteasome and TAP dependent.* Nat Immunol, 2005. **6**(3): p. 287-294.
31. Hofmann, M.W., et al., *The leucine-based sorting motifs in the cytoplasmic domain of the invariant chain are recognized by the clathrin adaptors AP1 and AP2 and their medium chains.* J Biol Chem, 1999. **274**(51): p. 36153-36158.
32. Dugast, M., et al., *AP2 clathrin adaptor complex, but not AP1, controls the access of the major histocompatibility complex (MHC) class II to endosomes.* J Biol Chem, 2005. **280**(20): p. 19656-19664.
33. McCormick, P.J., J.A. Martina, and J.S. Bonifacino, *Involvement of clathrin and AP-2 in the trafficking of MHC class II molecules to antigen-processing compartments.* Proc Natl Acad Sci U S A, 2005. **102**(22): p. 7910-7915.
34. Santambrogio, L., et al., *Involvement of caspase-cleaved and intact adaptor protein 1 complex in endosomal remodeling in maturing dendritic cells.* Nat Immunol, 2005. **6**(10): p. 1020-1028.
35. Peters, P.J., et al., *Segregation of MHC class II molecules from MHC class I molecules in the Golgi complex for transport to lysosomal compartments.* Nature, 1991. **349**(6311): p. 669-676.
36. Sanderson, F., et al., *Accumulation of HLA-DM, a regulator of antigen presentation, in MHC class II compartments.* Science, 1994. **266**(5190): p. 1566-1569.
37. Kropshofer, H., et al., *Editing of the HLA-DR-peptide repertoire by HLA-DM.* EMBO J, 1996. **15**(22): p. 6144-6154.
38. Engering, A. and J. Pieters, *Association of distinct tetraspanins with MHC class II molecules at different subcellular locations in human immature dendritic cells.* Int Immunol, 2001. **13**(2): p. 127-134.
39. Hsing, L.C. and A.Y. Rudensky, *The lysosomal cysteine proteases in MHC class II antigen presentation.* Immunol Rev, 2005. **207**: p. 229-241.
40. Hartman, I.Z., et al., *A reductionist cell-free major histocompatibility complex class II antigen processing system identifies immunodominant epitopes.* Nat Med, 2010. **16**(11): p. 1333-1340.
41. Raiborg, C. and H. Stenmark, *The ESCRT machinery in endosomal sorting of ubiquitylated membrane proteins.* Nature, 2009. **458**(7237): p. 445-452.

42. Zwart, W., et al., *Spatial separation of HLA-DM/HLA-DR interactions within MIIC and phagosome-induced immune escape.* Immunity, 2005. **22**(2): p. 221-233.
43. ten Broeke, T., et al., *Endosomally Stored MHC Class II Does Not Contribute to Antigen Presentation by Dendritic Cells at Inflammatory Conditions.* Traffic, 2011.
44. Neefjes, J.J., et al., *The biosynthetic pathway of MHC class II but not class I molecules intersects the endocytic route.* Cell, 1990. **61**(1): p. 171-183.
45. Nordeng, T.W., et al., *The cytoplasmic tail of invariant chain regulates endosome fusion and morphology.* Mol Biol Cell, 2002. **13**(6): p. 1846-1856.
46. Landsverk, O.J., et al., *Invariant chain increases the half-life of MHC II by delaying endosomal maturation.* Immunol Cell Biol, 2011. **89**(5): p. 619-629.
47. Strong, B.S. and E.R. Unanue, *Presentation of Type B Peptide-MHC Complexes from Hen Egg White Lysozyme by TLR Ligands and Type I IFNs Independent of H2-DM Regulation.* J Immunol, 2011.
48. Trombetta, E.S., et al., *Activation of lysosomal function during dendritic cell maturation.* Science, 2003. **299**(5611): p. 1400-1403.
49. Rocha, N., et al., *Cholesterol sensor ORP1L contacts the ER protein VAP to control Rab7-RILP-p150 Glued and late endosome positioning.* J Cell Biol, 2009. **185**(7): p. 1209-1225.
50. Kuipers, H.F., et al., *Statins affect cell-surface expression of major histocompatibility complex class II molecules by disrupting cholesterol-containing microdomains.* Hum Immunol, 2005. **66**(6): p. 653-665.
51. Cella, M., et al., *Inflammatory stimuli induce accumulation of MHC class II complexes on dendritic cells.* Nature, 1997. **388**(6644): p. 782-787.
52. Pierre, P., et al., *Developmental regulation of MHC class II transport in mouse dendritic cells.* Nature, 1997. **388**(6644): p. 787-792.
53. Boes, M., et al., *T-cell engagement of dendritic cells rapidly rearranges MHC class II transport.* Nature, 2002. **418**(6901): p. 983-988.
54. Wubbolts, R., et al., *Direct vesicular transport of MHC class II molecules from lysosomal structures to the cell surface.* J.Cell Biol., 1996. **135**(3): p. 611-622.
55. Kleijmeer, M., et al., *Reorganization of multivesicular bodies regulates MHC class II antigen presentation by dendritic cells.* J Cell Biol, 2001. **155**(1): p. 53-63.
56. Vascotto, F., et al., *The actin-based motor protein myosin II regulates MHC class II trafficking and BCR-driven antigen presentation.* J Cell Biol, 2007. **176**(7): p. 1007-1019.
57. Saftig, P. and J. Klumperman, *Lysosome biogenesis and lysosomal membrane proteins: trafficking meets function.* Nat Rev Mol Cell Biol, 2009. **10**(9): p. 623-635.
58. de Gassart, A., et al., *MHC class II stabilization at the surface of human dendritic cells is the result of maturation-dependent MARCH I down-regulation.* Proc Natl Acad Sci U S A, 2008. **105**(9): p. 3491-3496.
59. Shin, J.S., et al., *Surface expression of MHC class II in dendritic cells is controlled by regulated ubiquitination.* Nature, 2006. **444**(7115): p. 115-118.
60. Thibodeau, J., et al., *Interleukin-10-induced MARCH1 mediates intracellular sequestration of MHC class II in monocytes.* Eur J Immunol, 2008. **38**(5): p. 1225-1230.
61. Koppelman, B., et al., *Interleukin-10 down-regulates MHC class II alphabeta peptide complexes at the plasma membrane of monocytes by affecting arrival and recycling.* Immunity, 1997. **7**(6): p. 861-871.
62. Tze, L.E., et al., *CD83 increases MHC II and CD86 on dendritic cells by opposing IL-10-driven MARCH1-mediated ubiquitination and degradation.* J Exp Med, 2011. **208**(1): p. 149-165.
63. McGehee, A.M., et al., *Ubiquitin-dependent control of class II MHC localization is dispensable for antigen presentation and antibody production.* PLoS One, 2011. **6**(4): p. e18817.
64. Walseng, E., et al., *Ubiquitination regulates MHC class II-peptide complex retention and degradation in dendritic cells.* Proc Natl Acad Sci U S A, 2010. **107**(47): p. 20465-20470.
65. Al Daccak, R., N. Mooney, and D. Charron, *MHC class II signaling in antigen-presenting cells.* Curr Opin Immunol, 2004. **16**(1): p. 108-113.
66. Drenou, B., et al., *A caspase-independent pathway of MHC class II antigen-mediated apoptosis of human B lymphocytes.* J Immunol, 1999. **163**(8): p. 4115-4124.
67. Hemon, P., et al., *MHC class II engagement by its ligand LAG-3 (CD223) contributes to melanoma resistance to apoptosis.* J Immunol, 2011. **186**(9): p. 5173-5183.
68. Liu, X., et al., *Intracellular MHC class II molecules promote TLR-triggered innate immune responses by maintaining activation of the kinase Btk.* Nat Immunol, 2011. **12**(5): p. 416-424.
69. Lang, P., et al., *TCR-induced transmembrane signaling by peptide/MHC class II via associated Ig-alpha/beta dimers.* Science, 2001. **291**(5508): p. 1537-1540.
70. Bonnefoy, J.Y., et al., *The low-affinity receptor for IgE (CD23) on B lymphocytes is spatially associated with HLA-DR antigens.* J Exp Med, 1988. **167**(1): p.

57-72.
71. Bradbury, L.E., et al., *The CD19/CD21 signal transducing complex of human B lymphocytes includes the target of antiproliferative antibody-1 and Leu-13 molecules.* J Immunol, 1992. **149**(9): p. 2841-2850.
72. van der Burg, S.H. and C.J. Melief, *Therapeutic vaccination against human papilloma virus induced malignancies.* Curr Opin Immunol, 2011. **23**(2): p. 252-257.
73. Mitea, C., et al., *A universal approach to eliminate antigenic properties of alpha-gliadin peptides in celiac disease.* PLoS One, 2010. **5**(12): p. e15637.
74. Baugh, M., et al., *Therapeutic dosing of an orally active, selective cathepsin S inhibitor suppresses disease in models of autoimmunity.* J Autoimmun, 2011. **36**(3-4): p. 201-209.
75. Fallang, L.E., et al., *Differences in the risk of celiac disease associated with HLA-DQ2.5 or HLA-DQ2.2 are related to sustained gluten antigen presentation.* Nat Immunol, 2009. **10**(10): p. 1096-1101.

Chapter 1

A Genome-wide Multi-Dimensional RNAi Screen Reveals Pathways Controlling MHC Class II Antigen Presentation

Petra Paul*, Tineke van den Hoorn*, Marlieke L.M. Jongsma*, Mark J. Bakker, Rutger Hengeveld, Lennert Janssen, Peter Cresswell, David A. Egan, Marieke van Ham, Anja ten Brinke, Huib Ovaa, Roderick L. Beijersbergen, Coenraad Kuijl and Jacques Neefjes

* equal contribution

Cell. 2011 Apr 15;145(2):268-83

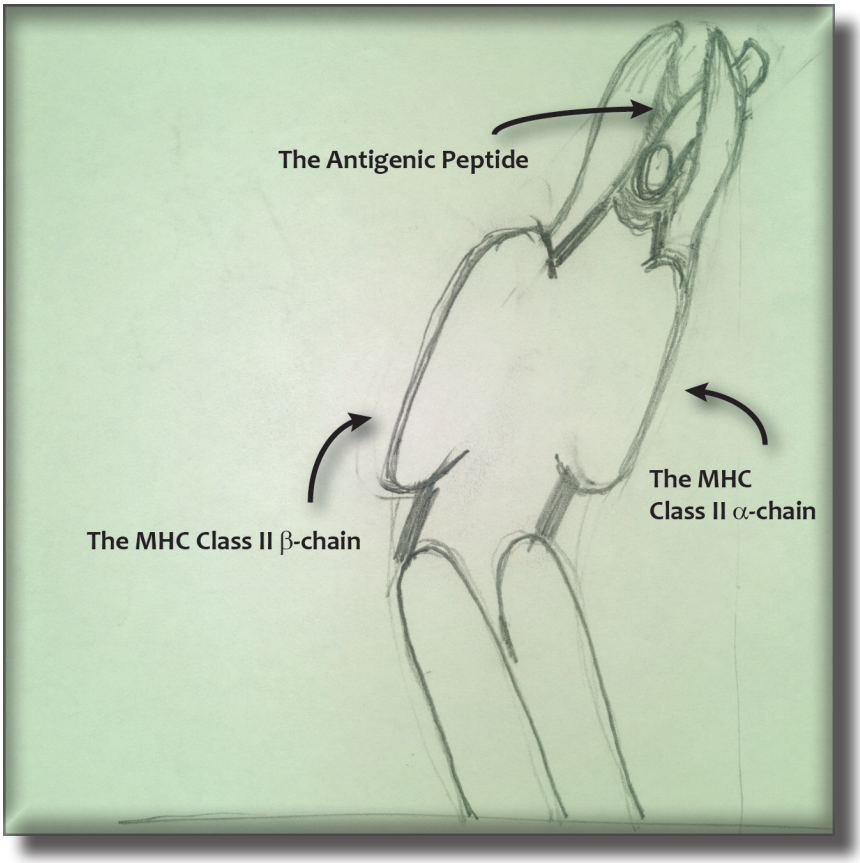

MHC class II molecules (MHC-II) present peptides to T helper cells to facilitate immune responses and are strongly linked to autoimmune diseases. To unravel processes controlling MHC-II antigen presentation, we performed a genome-wide flow cytometry-based RNAi screen detecting MHC-II expression and peptide loading followed by additional high-throughput assays. All datasets were integrated to answer two fundamental questions: what regulates tissue-specific MHC-II transcription and what controls MHC-II transport in dendritic cells. MHC-II transcription was controlled by nine regulators acting in feedback networks with higher order control by signalling pathways including TGFβ. MHC-II transport was controlled by the GTPase ARL14/ARF7, which recruits the motor myosin 1E via an effector protein ARF7EP. This complex controls movement of MHC-II vesicles along the actin cytoskeleton in human dendritic cells (DCs). These genome-wide systems analyses have thus identified factors and pathways controlling MHC-II transcription and transport, defining targets for manipulation of MHC-II antigen presentation in infection and autoimmunity.

Introduction

Major Histocompatibility Complex class II molecules (MHC-II) present peptides to $CD4^+$ T cells that initiate and control immune responses. The expression of MHC-II is mostly restricted to professional antigen presenting cells (APCs), such as B cells and dendritic cells (DCs), and controlled by a transcriptional complex that includes the MHC-II transactivator CIITA [1]. Careful regulation of expression is needed to prevent uncontrolled immune responses. Various allelic forms of MHC-II are associated with autoimmune diseases [2]. The successful presentation of peptides at the cell surface involves a series of subcellular events: In the ER, MHC-II associates with the invariant chain (Ii) that fills the peptide-binding groove and mediates transport to late endosomal compartments called MHC-II compartments (MIICs) [3, 4]. There, Ii is degraded leaving a fragment called CLIP in the peptide-binding groove of MHC-II [5]. In parallel, endocytosed antigens are degraded into peptides, which compete with CLIP for binding to MHC-II in a process catalyzed by the chaperone HLA-DM (DM) [6, 7] in the intraluminal vesicles of the MIIC [8]. Ultimately, MHC-II-containing vesicles and tubules fuse with the plasma membrane [9-11] to present the peptide-loaded MHC-II to $CD4^+$ T cells.

Various factors controlling MHC-II expression have been identified, such as cytokines that can inhibit (IL-10) [12] or upregulate (interferon-γ) [13] MHC-II expression. Certain activation signals, such as TLR signalling can also upregulate its expression in B cells and DCs [14]. IL-10 signalling may upregulate MARCH I, which ubiquitinates and shortens MHC-II half-life [15]. Other factors such as pH [16], kinases [17] and cholesterol [18] affect MHC-II expression and antigen presentation.

As a first step towards a systems-understanding of MHC-II antigen presentation, we performed a multi-dimensional RNAi screen where we investigated cell surface expression of MHC-II, as well as peptide loading, transcriptional control and intracellular distribution in an integrated manner. Combining these phenotypic analyses yielded factors and pathways controlling MHC-II transcription and transport in DCs and defined targets for manipulation of MHC-II antigen presentation in infection and autoimmunity.

Results

Genome-wide RNAi Screen identifies 276 Candidate Genes affecting MHC-II Expression and Peptide Loading

MHC-II is selectively expressed by APCs. To identify proteins and networks involved in MHC-II expression and peptide loading, we selected the human melanoma cell line MelJuSo, which expresses peptide-loaded MHC-II and all components required for MHC-II antigen presentation [11]. Whereas MelJuSo is not an immune cell type, it does express many immune-specific genes and proteins controlling MHC-II transport similar to DCs. APCs express Toll-like receptors (TLRs) recognizing double-stranded siRNA resulting in activation signals that might increase MHC-II expression [19, 20]. MelJuSo lacks these TLRs and in addition exhibits transfection efficiencies greater than 95%, as well as stable MHC-II expression and peptide loading capacity (data not shown). These features, which are essential for reliable RNAi screens, are not shared by any primary APC tested.

To visualize the effects of gene knockdown on MHC-II expression and peptide loading, we used two monoclonal antibodies (Figure 1A). Cy5-conjugated CerCLIP, which recognizes human MHC-II loaded with the residual Ii-derived CLIP fragment, and Cy3-conjugated L243, which recognizes peptide-loaded MHC-II (called HLA-DR). CLIP-loaded MHC-II reflects an inefficiency of the loading of antigenic peptide on the mature receptor [21], whereas L243 detects correctly loaded MHC-II on the plasma membrane [22]. MelJuSo cells were transfected with pools of siRNAs (four duplexes per target gene) in 96-well format targeting 21,245 human genes in total. Three days post-transfection, cells were analyzed by flow

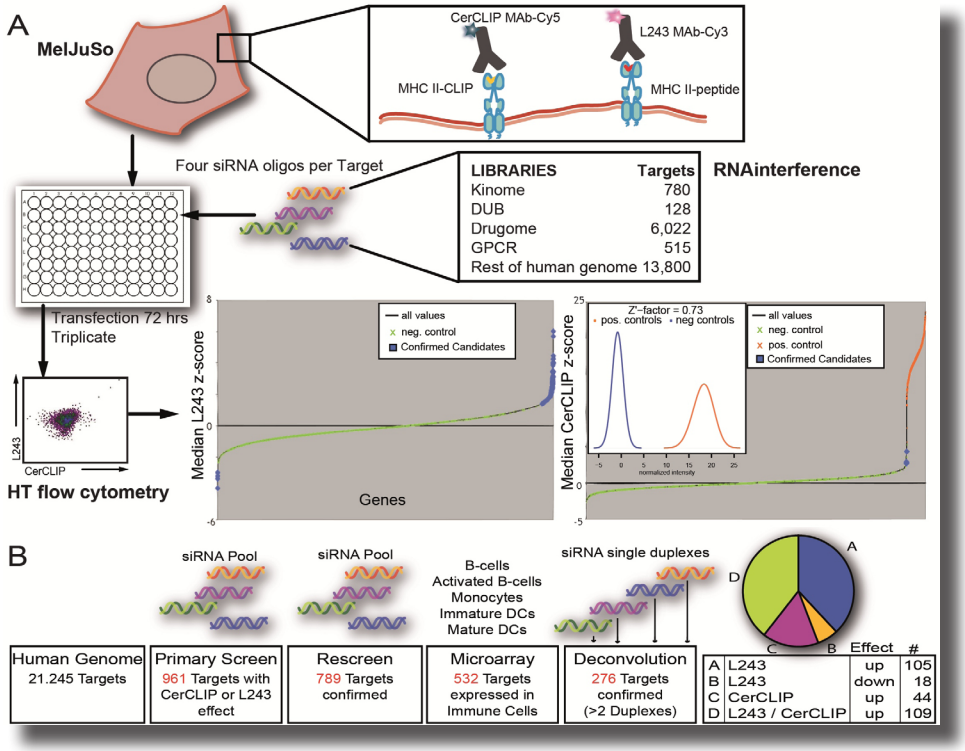

Figure 1 | A genome-wide Flow Cytometry-based RNAi Screen

A | MelJuSo transfected with siRNA were analysed for surface expression of peptide- versus CLIP-loaded MHC-II by high-throughput flow cytometry using monoclonal antibodies (L243-Cy3 and CerCLIP-Cy5). The graphs show representative z-scores of siRNAs without effect (|z|<3; black line), untreated cells (green), HLA-DM-silencing (orange) and candidates after normalization (|z|>3; blue). Inlay in the CerCLIP plot shows the Z'-factor for the analysis of the kinase sublibrary, representing the detection window between negative (blue) and positive controls (red).

B | Scheme showing the different confirmation steps in the screening procedure resulting in 276 candidate genes influencing MHC-II expression and peptide loading. Indicated is the distribution of four phenotypes detected by flow cytometry. See also Table S1 and S2 in Chapter 2 of this thesis.

cytometry to determine peptide loading as well as expression levels of MHC-II. The primary screen (performed in triplicate) achieved an excellent "screening window" (difference of negative and positive control) defined by the Z' factor [23]. All parts yielded Z'>0.5 (Figure 1A; Z' for the kinase sub-library). Results were z-score normalized. Genes whose silencing resulted in a change of L243 or CerCLIP staining by |z|>3 (p<0.0027) were considered candidates for follow up. These genes were re-screened in triplicate, resulting in 789 candidate proteins with potential functions in controlling MHC-II expression and peptide loading (Figure 1B).

To determine which of the 789 candidates identified in the screen were expressed in APCs, we performed microarray gene expression analysis on human primary monocytes, monocyte-derived (activated and immature) DCs and naïve or CD40L-activated B cells (Table S1, see Chapter 2 of this thesis). Of the candidate genes identified in MelJuSo cells, 532 genes were expressed in one or more human primary APC type. Correcting for off-target effects (see Experimental Procedures) resulted in 276 confirmed candidates (Table S2, see Chapter 2 of this thesis). These candidates could be divided into four groups based on differential staining with L243 or CerCLIP, which allowed the distinction between effects on MHC-II expression versus effects on peptide loading, respectively. Most candidate proteins identified in the screen appeared to affect MHC-II surface expression; only 45 genes specifically affected peptide loading (CLIP up; Figure 1B).

Candidate Proteins include known MHC-II Pathway Components and Proteins associated with Autoimmunity

To annotate the function of the 276 identified genes, we used database tools to determine tissue distribution, potential function, association with autoimmune diseases and established function in the MHC-II antigen presentation pathway. First, as a validation of our method, we interrogated the dataset for proteins already known to be involved in MHC-II antigen presentation. Thirteen candidates have been reported in literature to control MHC-II antigen presentation (Figure 2A, green/yellow proteins), including the MHC-II transcriptional regulator CIITA, the HLA-DRA and DRB chains, DM and the IL-10 receptor. Another set of 13 proteins might indirectly correlate to the pathway through inhibitors or as targets of pathogenic immune regulators (Figure 2A, blue proteins). For example, FKBP3 (FK506-binding protein 3) may be the target of FK506 [24]. The target(s) for general kinase inhibitor Staurosporine [17] can be included in the 28 serine/threonine kinases we identified in our screen. Also, the immunodeficiency virus (HIV) protein Tat has been postulated to control HIV-Tat Interacting Protein (HTATIP) [25] (Figure 2A), which we picked up in our screen as a regulator of MHC-II peptide loading. Hence, some 10% (26 of 276) of our primary screen candidates have already been implicated in controlling MHC-II expression and peptide loading. In our initial screen however, we did not identify all factors that had been reported in literature to control MHC-II function. We thus retested these separately, which revealed that most of them yielded effects below our cut-off of $|z|>3$ (Figure S1, see Chapter 2 of this thesis).

Second, to determine which candidate genes were selectively expressed in immune tissues, we interrogated a gene expression database of 79 human tissues [26], and compared expression levels of each candidate between immune and other tissues. The expression of CIITA is limited to antigen presenting cells, therefore we used its expression as a standard for immune-specificity (Figure 2B). Sixty-nine of the 276 candidates identified by the RNAi screen exhibited selective expression in immune tissues (Table S1, see Chapter 2 of this thesis).

Another interesting group in which some of our candidates could be placed were associated with autoimmunity. Genetic association studies have revealed that MHC-II is the strongest autoimmunity-associated factor [2] possibly triggering the immune response by presenting autoantigens. Comparing our candidates involved in MHC-II regulation with a database containing genes linked to autoimmune diseases **(http://geneticassociationdb.nih.gov)** showed that 8% (21 of 276) were associated with autoimmune diseases (Figure 2C). This association, together with their immune tissue-specific expression pattern, makes some of them attractive therapeutic targets for manipulating MHC-II function.

A standard protocol in genome-wide screening is pathway analysis based on literature. We first subclustered candidates into four groups based on their flow cytometry parameters (Figure 1B) before functional annotation by Ingenuity Pathway Analysis (**www.ingenuity.com**, Figure 2D; Table S2, see Chapter 2 of this thesis). Many enzyme classes are found to be involved in MHC-II antigen presentation, but the majority of genes had no ascribed function. The four groups were then analyzed by Ingenuity Pathways Analysis and STRING [27] for established protein interactions and yielded several networks consisting of annotated proteins only (Figure S2, see Chapter 2 of this thesis). Analysis of these networks revealed clusters of proteins already known to be involved in MHC-II antigen presentation. No novel clusters regulating MHC-II became apparent from this network analysis. As most proteins had unknown functions, these pathways only covered a small fraction of candidate proteins. Hence, network analysis using different database tools was unsatisfactory in terms of describing the systems biology of MHC-II antigen presentation.

Therefore, we aimed at placing candidates in functional networks following secondary high-throughput screens. We broke down MHC-II antigen presentation in three processes: peptide loading (1), transcriptional regulation (2), and the general cell biology of MHC-II (3). The latter category consists of the assembly, intracellular transport, processing in the MIIC, endo- and exocytosis. Factors affecting peptide loading (1) were already identified by the antibody CerCLIP in the primary screen.

After genome-wide screening we were able to confirm our strategy by identifying known members of the MHC-II pathway. Furthermore, we have highlighted interesting therapy targets displaying immune-tissue specific expression and association to autoimmune diseases. Secondary high-throughput assays are needed to decipher the candidates involved in the transcriptional regulation and general cell biology of MHC-II.

Nine Candidates are implicated in Transcriptional and Higher Order Control of MHC-II Expression

MHC-II mRNA expression is controlled by CIITA. To determine whether the 276 candidate genes identified in the earlier RNAi screen affected MHC-II transcription, we silenced the 276 candidates in

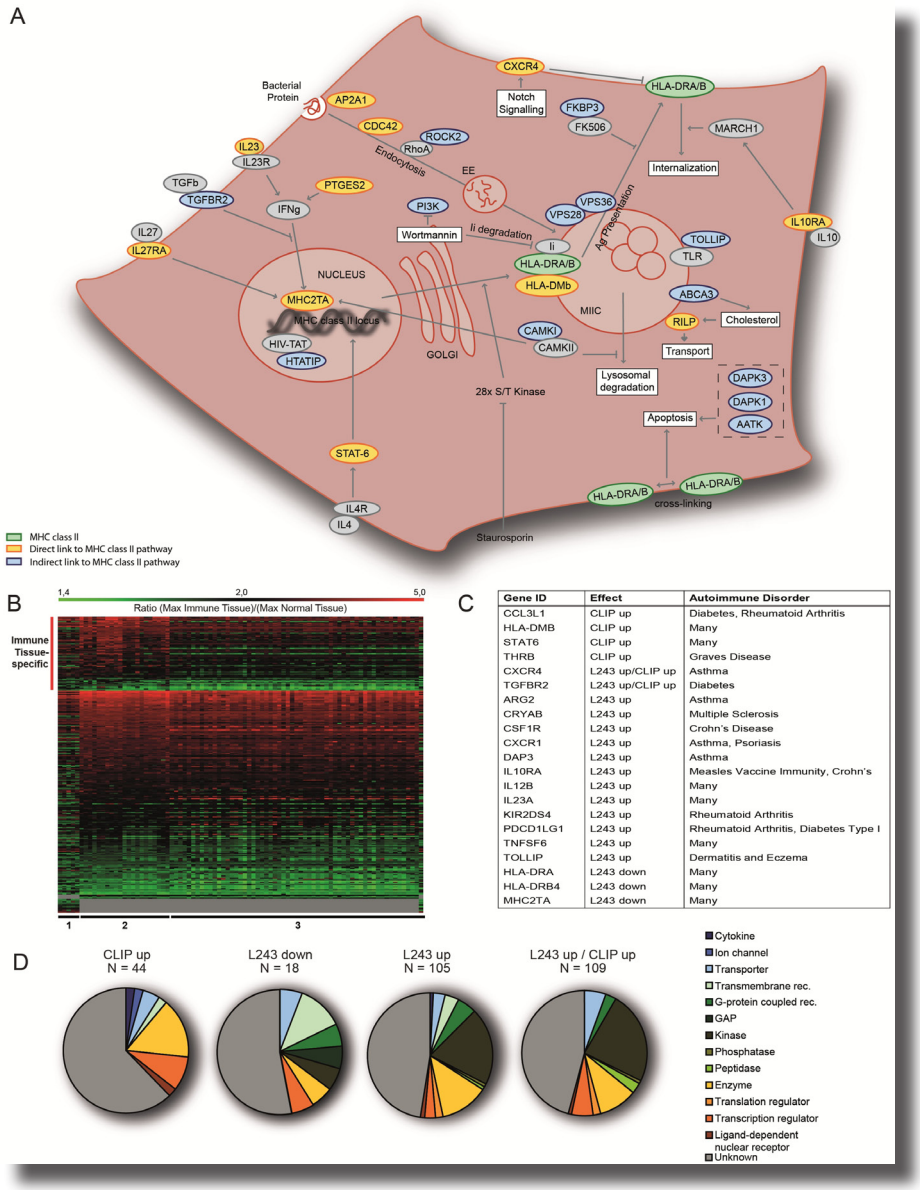

Gene ID	Effect	Autoimmune Disorder
CCL3L1	CLIP up	Diabetes, Rheumatoid Arthritis
HLA-DMB	CLIP up	Many
STAT6	CLIP up	Many
THRB	CLIP up	Graves Disease
CXCR4	L243 up/CLIP up	Asthma
TGFBR2	L243 up/CLIP up	Diabetes
ARG2	L243 up	Asthma
CRYAB	L243 up	Multiple Sclerosis
CSF1R	L243 up	Crohn's Disease
CXCR1	L243 up	Asthma, Psoriasis
DAP3	L243 up	Asthma
IL10RA	L243 up	Measles Vaccine Immunity, Crohn's
IL12B	L243 up	Many
IL23A	L243 up	Many
KIR2DS4	L243 up	Rheumatoid Arthritis
PDCD1LG1	L243 up	Rheumatoid Arthritis, Diabetes Type I
TNFSF6	L243 up	Many
TOLLIP	L243 up	Dermatitis and Eczema
HLA-DRA	L243 down	Many
HLA-DRB4	L243 down	Many
MHC2TA	L243 down	Many

Figure 2 | Candidate Gene Annotation

A | A literature-based model representing proteins directly (yellow) and indirectly (blue) involved in the MHC-II pathway (green). See also Figure S1 in Chapter 2 of this thesis. EE = Early Endosome; MIIC = MHC class II containing Compartment; Ii = invariant chain

B | Gene expression ratios of the candidate genes in the primary human immune cells (1) used in our selection procedure (Figure 1B) and immune tissues (2) versus non-immune tissues (3). Grey areas indicate absence of probes on the expression arrays. Expression levels of (2) and (3) were obtained from the BioGPS application.

C | Genes from the screen that are associated to autoimmune diseases based on the Genetic Association Database.

D | Functional annotation of the candidate genes involved in the various effects on MHC-II antigen presentation. Annotation retrieved from Ingenuity Pathways Analysis.

See also Figure S2 and Table S1 and S2 in Chapter 2 of this thesis.

MelJuSo cells and performed quantitative PCR for mRNA of MHC-II (HLA-DRA), CIITA, and Ii. To check whether the candidates from our screen controlled the entire MHC locus, MHC class I transcription (HLA-A/B/C) was assessed [28].

The silencing of nine candidate proteins affected transcription of one or several of the tested genes (Figure 3A, Table S3, see Chapter 2 of this thesis). Silencing of three candidate genes (CIITA itself, RMND5B and PLEKHA4) down-regulated CIITA and HLA-DR mRNA levels: The protein RMND5B has an unknown function and PLEKHA4 has so far only been described as a phosphoinositide binding protein. The silencing of three other genes (KIAA1007 [CNOT1], CDCA3 and MAPK1) up-regulated both CIITA and HLA-DR transcription. CNOT1 is part of a transcription regulatory complex called CCR4-NOT. This complex contains also another protein identified in our primary screen, called CNOT2. MAPK1, is a key signalling intermediate in many well-studied pathways and the function of CDCA3 is yet unknown. MAPK1 (and CIITA itself) were the only genes shown to affect the whole MHC-locus, as measured by MHC class I (MHC-I) expression.

Knockdown of unknown EFHD2 and HTATIP increased the expression levels of HLA-DR and Ii. Silencing of only one gene (IL27RA, the IL-27 receptor) affected MHC-I expression independently of CIITA. This probably represents a more locus-specific effect. IL-27RA has been implicated in Th1-type as well as innate immune responses. For a full description of the candidates that affect MHC-II transcription see Table S3 in Chapter 2 of this thesis.

These nine candidate genes, including CNOT2, can affect each other's expression as well as that of CIITA, HLA-DR, Ii and MHC-I. To define potential interconnections, we performed a 'cross-correlative qPCR': Each candidate was silenced and the effect on expression of the other candidates was determined by qPCR (Figure 3B). Most siRNAs affected the expression of one or more other candidate genes, suggesting that they act in complex networks (Figure 3C). These networks can be either defined as controlling the CIITA expression (network 1), the MHC locus (network 2) or the selective transcription of HLA-DR and Ii (group 3).

We performed literature analysis to define higher order regulation of the transcriptional network controlling MHC-II expression. Seven of the candidates affecting MHC-II transcription have already been annotated to pathways. FLJ22318/RMND5B (human homologue of yeast Required for Meiotic Nuclear Division 5B protein), on the other hand, is not functionally annotated, but an interaction with SMAD4 has been reported [29]. SMAD-proteins transduce signals from the TGFβ receptor to the nucleus to downregulate MHC-II expression [30]. To understand the role of this unknown factor, we tested whether RMND5B is involved in TGFβ signaling. Following exposure to TGFβ for three days, MHC-II was downregulated in MelJuSo. RMND5B silencing further downregulated MHC-II expression as detected by flow cytometry and qPCR (Figure 3D, E). RMND5B might thus act as an inhibitor of SMADs. SMAD4 translocates from cytosol to nucleus upon TGFβ exposure [31], which was also observed for RMND5B in MelJuSo (Figure 3F). Although we failed to show a direct interaction with SMAD4, we placed RMND5B in a network controlled by TGFβ signaling, which controls MHC-II expression.

We have defined a transcriptional network controlling MHC-II expression. Furthermore, we described a network of higher order control based on proteins annotated in literature (Figure 3G; for references Figure S3 in Chapter 2 of this thesis). These networks should in principle explain the immune tissue-selective expression of MHC-II. The data show that CIITA expression is controlled by a complex transcriptional feedback mechanism, which in turn is controlled by a series of general biological processes such as chromatin modification, the cell cycle and a number of different signaling events including those mediated by TGFβ and RMND5B. The combined input of events presumably determines the tissue selectivity of MHC-II expression.

Analysis of Networks with similar intracellular MHC-II Distribution Phenotypes selects Candidates for in-depth Study

Nine candidate genes were shown to control the transcription of MHC-II. This implies that the other 268 candidates could affect the intracellular distribution of MHC-II. This we evaluated by microscopy. A clonal MelJuSo cell line expressing MHC-II-GFP and mCherry-GalT2 (a Golgi marker) was transfected with siRNAs for the candidates. The nuclei (Hoechst) and early endosomes (anti-EEA1) were stained to detect all relevant intracellular compartments of MHC-II (Figure 4A and S4A, see Chapter 2 of this thesis). The resulting images were processed with CellProfiler software [32], which resulted in more than 100 parameters describing the features of nuclei, endosomes, Golgi and plasma membrane. Images were analyzed and scored using automated image analysis software (CPAnalyst2; see Supplemental Experimental Procedures for analysis parameters in Chapter 2 of this thesis) [33]. Particular phenotypes could be characterised in this manner: e.g. enlarged MHC-II positive vesicles, MHC-II redistribution to the plasma membrane, clustering or dispersion of early endosomes, and

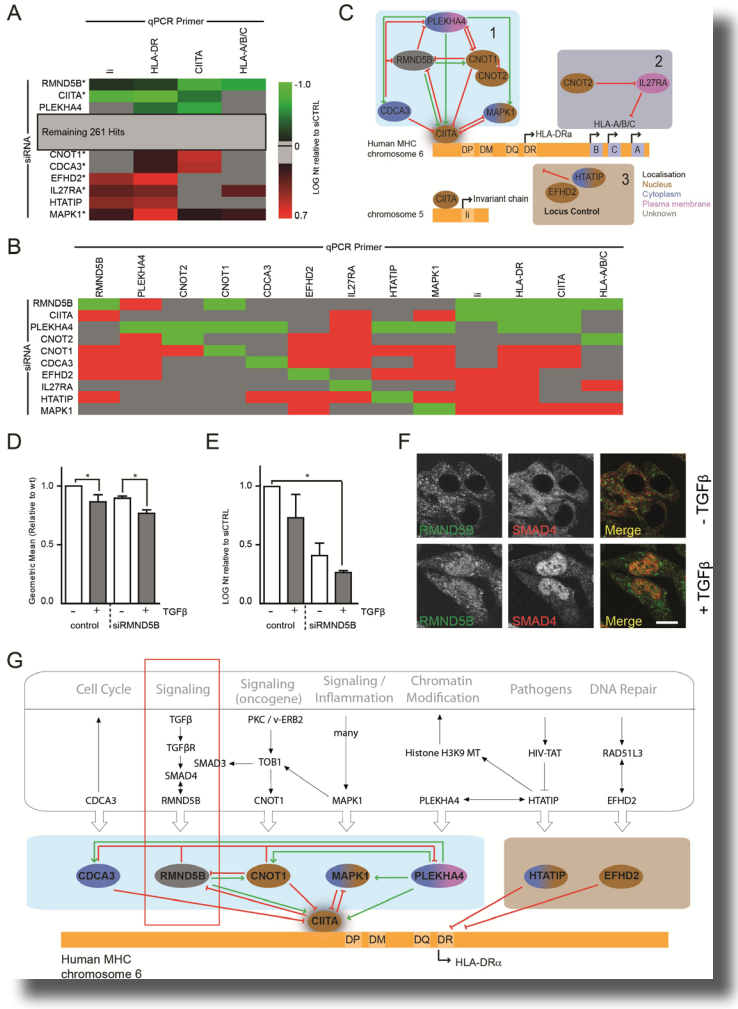

Figure 3 | MHC-II Transcription Control Networks and higher Order Control

A | The heatmap shows the log-transformed expression values (GAPDH as reference) relative to siControl-treated cells (FLJ22318 = RMND5B; KIAA1007 = CNOT1). Mean values of four independent experiments are shown. Stars show correlation between L243 phenotype (Table S2, in Chapter 2 of this thesis) and qPCR.

B | Upon silencing the genes defined under (A), the effect on the expression levels of the nine genes and the MHC-II factors were determined by qPCR. Confirmed effects of at least two experiments are shown (green = down-; red = up-regulation; gray = no effect).

C | Transcriptional networks deduced from the qPCR data controlling CIITA (1), the MHC locus (2) or MHC-II and Ii expression without CIITA involvement (3). Intracellular localisation of the proteins is represented in different colours. Red arrows: inhibition, green arrows: activation of transcription.

D | MHC-II expression on RMND5B silenced MelJuSo cells in presence or absence of TGFβ. Mean fluorescence intensity of three experiments plus standard deviation normalized to control siRNA conditions is plotted.
** p<0.05*

*E | RNA levels of HLA-DR upon RMND5B silencing and TGFβ treatment. LOG-transformed expression levels (relative to GAPDH) from two experiments normalized to control siRNA conditions plus standard deviation are plotted. *p<0.05*

F | Intracellular distribution of RMND5B and SMAD4 in MelJuSo in the presence or absence of TGFβ. (bar = 10 mm)

G | Higher order control of the transcriptional network, based on literature and experimental data (red box).

See also Figure S3 and Table S3 in Chapter 2 of this thesis.

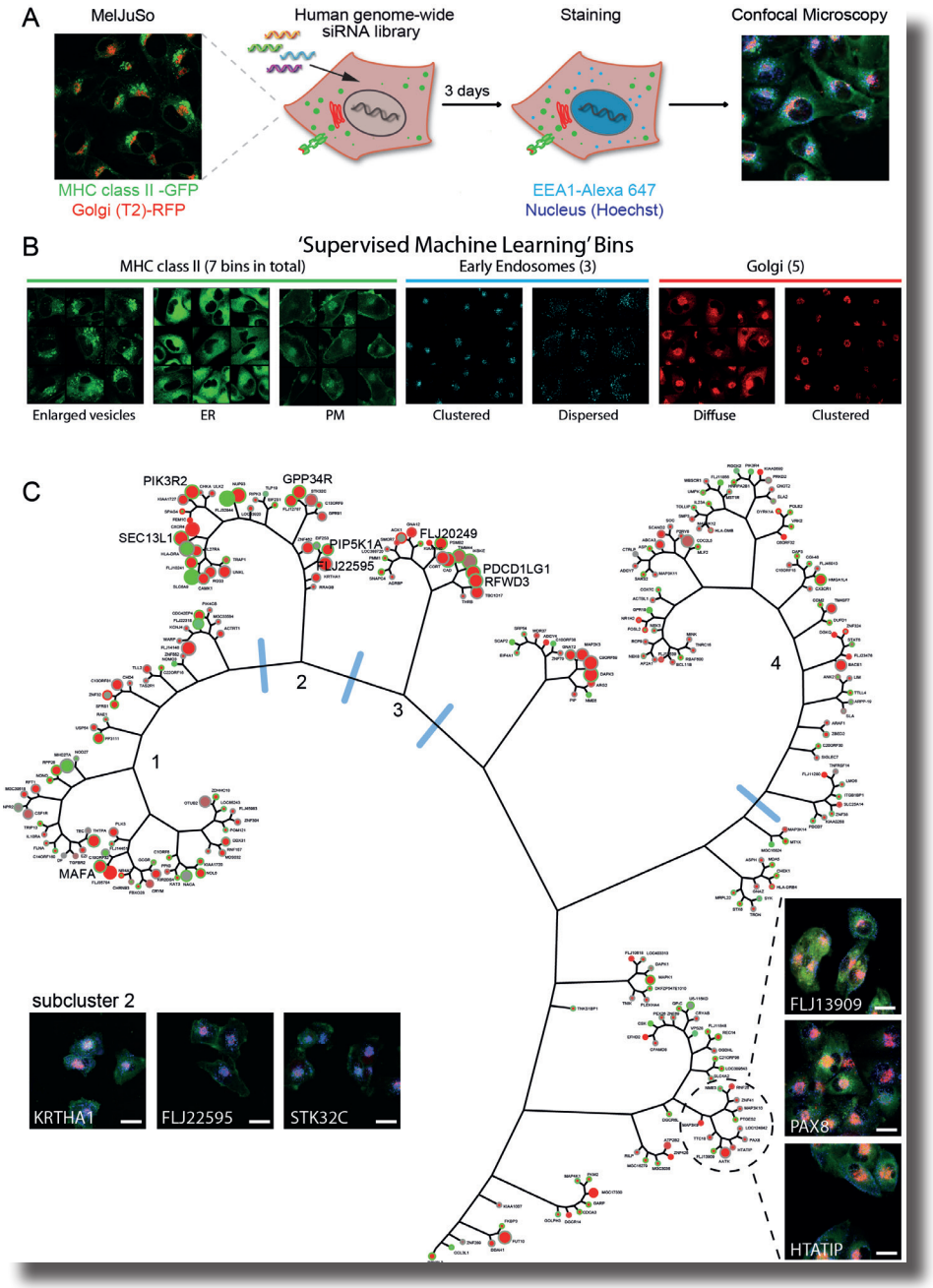

Figure 4| MHC-II Distribution Control: Automated Image Analysis

A | MelJuSo stably expressing MHC-II (HLA-DRB1-GFP, green) and a Golgi marker (mCherry-GalT2, red) were transfected with siRNA targeting the 276 candidate genes and stained for early endosomes (EEA1) in blue and nucleus (Hoechst, not shown).

B | Confocal images of all silenced genes were analysed using CellProfiler and CPAnalyst 2. In the process of 'supervised machine learning', siRNAs resulting in similar phenotypes were manually grouped into several bins for the different fluorescent channels. Shown are panels with representative images used for computer instruction. The minimal number of descriptive parameters for each group was determined.

Figure 4 | continued

C | Organic view of clustered genes based on phenotype determined by quantitative microscopy analysis. The color of the nodes indicates the z-score for the L243 staining (red: up-, green: down-regulation). The nodes' border color indicates the change in mRNA levels upon DC maturation (red: higher, green: lower expression). Node size represents a measure of mDC phenotype. A larger node is correlated to higher cell membrane MHC-II levels related to intracellular vesicles. Names in large font indicate selected candidates for further testing in DCs. Example images of genes from selected clusters are shown. (bar = 25 mm)
See also Figure S4 and S5, Table S4 in Chapter 2 of this thesis.

altered Golgi structure (Figure 4B). After several rounds of software training, the minimal number of parameters (out of the >100) needed to distinguish the phenotypes was determined (Figure S4B and Table S4, see Chapter 2 of this thesis). After z-score normalization, the siRNAs giving similar phenotypes were clustered (Figure 4C). Control siRNAs (positive and non-affecting) were clustered in distinct groups, thereby validating our method.

To obtain an overview of our data, we built a network tree integrating information of all the different screens. The fill-color of each gene shows the effect on MHC-II surface expression (L243, flow cytometry screen), while the color of the edge represents mRNA level changes going from immature (im)DCs to mature (m)DCs, as found by microarray. The size of the node correlates to an increase in the relative amount of MHC-II at the surface, an mDC-like phenotype [34, 35]. This feature was deduced from the microscopic analysis (Table S4, see Chapter 2 of this thesis). Candidate genes grouped in the same branch of the diagram, due to similar phenotypes generated, were postulated to act in the same functional pathways. We set an arbitrary threshold to distinguish four highly homologous clusters in our tree diagram (distance to root ≥153.6, genes per cluster ≥15, indicated by blue lines in Figure 4C, see also Figure S5 in Chapter 2 of this thesis). These clusters included also unknown proteins that might be functionally connected to known proteins present in the same cluster. These connections may be better understood after in-depth experimental validation.

To understand the function of the identified clusters, we determined the enrichment of Gene Ontology (GO) terms. As expected, all candidates identified by the screens were enriched for the GO cellular component term 'MHC-II protein complex' ($p=0.0028815$, Table S5, see Chapter 2 of this thesis). For a more extensive analyses, we applied the integrated functional gene network program Humannet v. 1 [36] that combines information from several expression and protein-protein interaction databases. We first measured the degree of connectivity between our candidates by the Area Under the Receiver Operating Characteristic (ROC) Curve (AUC) (Figure S6, see Chapter 2 of this thesis). The AUC of 0.6175 indicates that many connected genes (neighbours) also genuinely interact. Neighbours with a log-likelihood score ≥1 according to Humannet and a $|z| \geq 1.645$ ($p<0.1$) in our original flow cytometry screen were also included in this analysis (Table S6, see Chapter 2 of this thesis). These increased the number of proteins involved in the same functional pathway. Subsequent GO analysis of the expanded groups indicated that clusters 2 and 4 (Figure 4C) were enriched for 'MHC-II protein complex' (Table S5, see Chapter 2 of this thesis). When we combined this information with the microscopy phenotypes we noted that the genes in cluster 4 did not affect MHC-II distribution while those in cluster 2 showed MHC-II redistribution to the cell surface which resembles an mDC phenotype (Figure 6A). Cluster 2 has two areas where the genes cohered (Figure 5A), one was enriched for GO terms like 'MHC-II protein complex' (Figure 5B) and another for 'cytosolic ribosome' terms [cells with reduced intracellular MHC-II; (data not shown)].

The definition of clusters combined with functional annotation predicts connections between candidates within a network. This allows the addition of genes to these networks, which were not originally identified in our siRNA screen (for reasons of functional redundancy, effect below cut-off etc.). Our integrative bioinformatic approach enables us to select candidates for further biochemical studies based on their predicted functional relationships and effects observed in our various screens.

Six Proteins involved in MHC-II Redistribution in maturing DCs

To test whether our networks indeed predict processes essential in the immune system, we studied MHC-II distribution in DCs. DCs exposed to maturation signals redistribute MHC-II molecules and various activation markers from CD63-positive vesicles to the plasma membrane, enhancing their surface expression. This is an essential step in the acceleration of immune responses [34, 35] (Figure 6A). MHC-II distribution is visualized in a co-localisation pixel plot of CD63 versus MHC-II (Figure 6A, right panel). To select candidates potentially involved in the control of MHC-II redistribution in DCs, we used the following arguments. Firstly, the

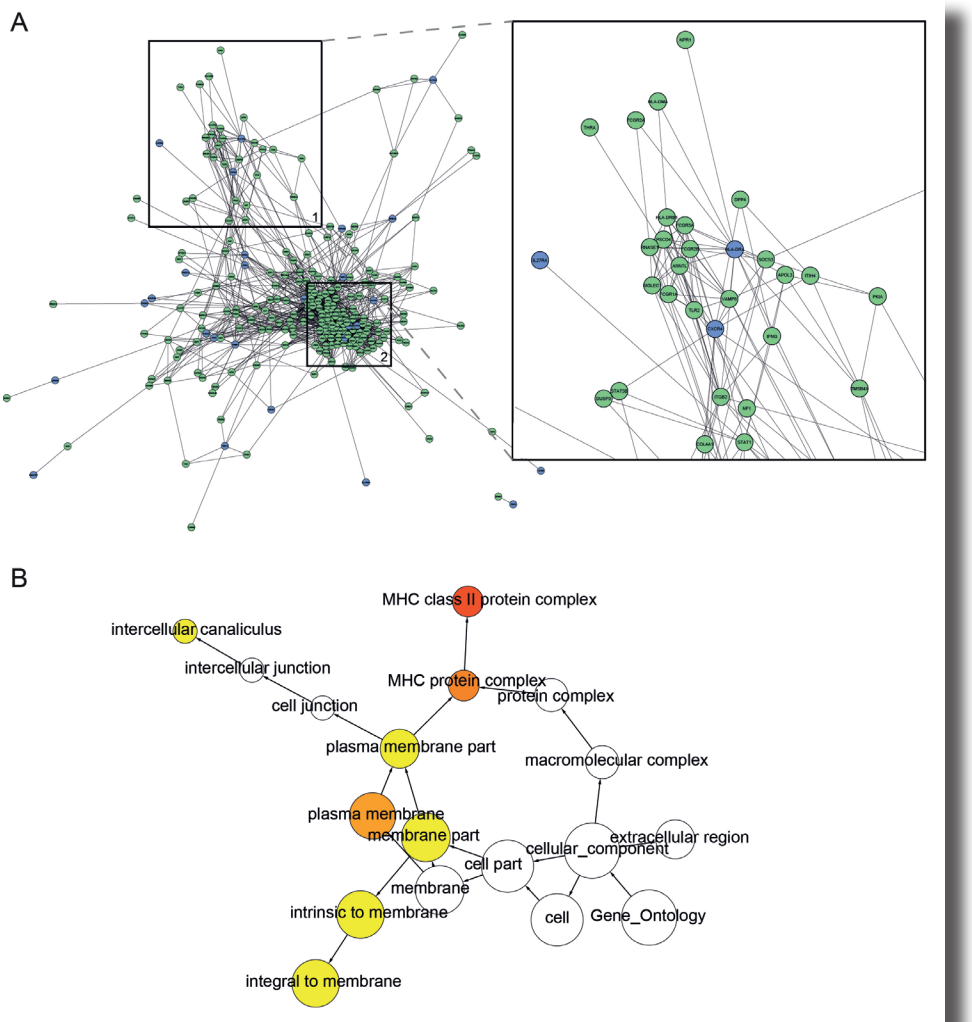

Figure 5 | MHC-II Distribution Control: Systems Analysis of Biological Pathways
A | Interaction network of genes from cluster 2 (Figure 4C). green: high scoring neighbours with |z|≥1.645 (p=0.1) in the original flow cytometry screen, blue: genes from cluster 2. Zoom in on Box 1 is shown.
B | Gene Ontology analysis of cellular components from the aggregated genes in Box 1. The colours represent enrichment for specific GO term (yellow to red: enriched).
See also Figure S6 and Table S5 and S6 in Chapter 2 of this thesis.

genes should up-regulate MHC-II expression at the cell surface (as in mDCs). Secondly, if upregulation is caused by silencing, the candidate should be downregulated in the microarray analyses from imDC to mDC. Lastly, silencing of genes should induce MHC-II transport to the plasma membrane as determined by microscopy (Figure 4C, Table S1, S2, see Chapter 2 of this thesis). Nine unrelated candidates fulfilled all criteria and we tested whether silencing these genes in imDCs could mimic the reduction in expression following activation and therefore alter the distribution of MHC-II (Figure 6B). Four individual shRNA sequences per gene were introduced into primary human monocytes, before differentiation into imDCs, detected by decreased monocyte marker CD14 and increased DC marker DC-SIGN expression. Typical activation markers for mDCs remained absent (Figure 6C). Seven out of nine selected candidates increased CerCLIP and/or MHC-II expression in imDCs six days after shRNA

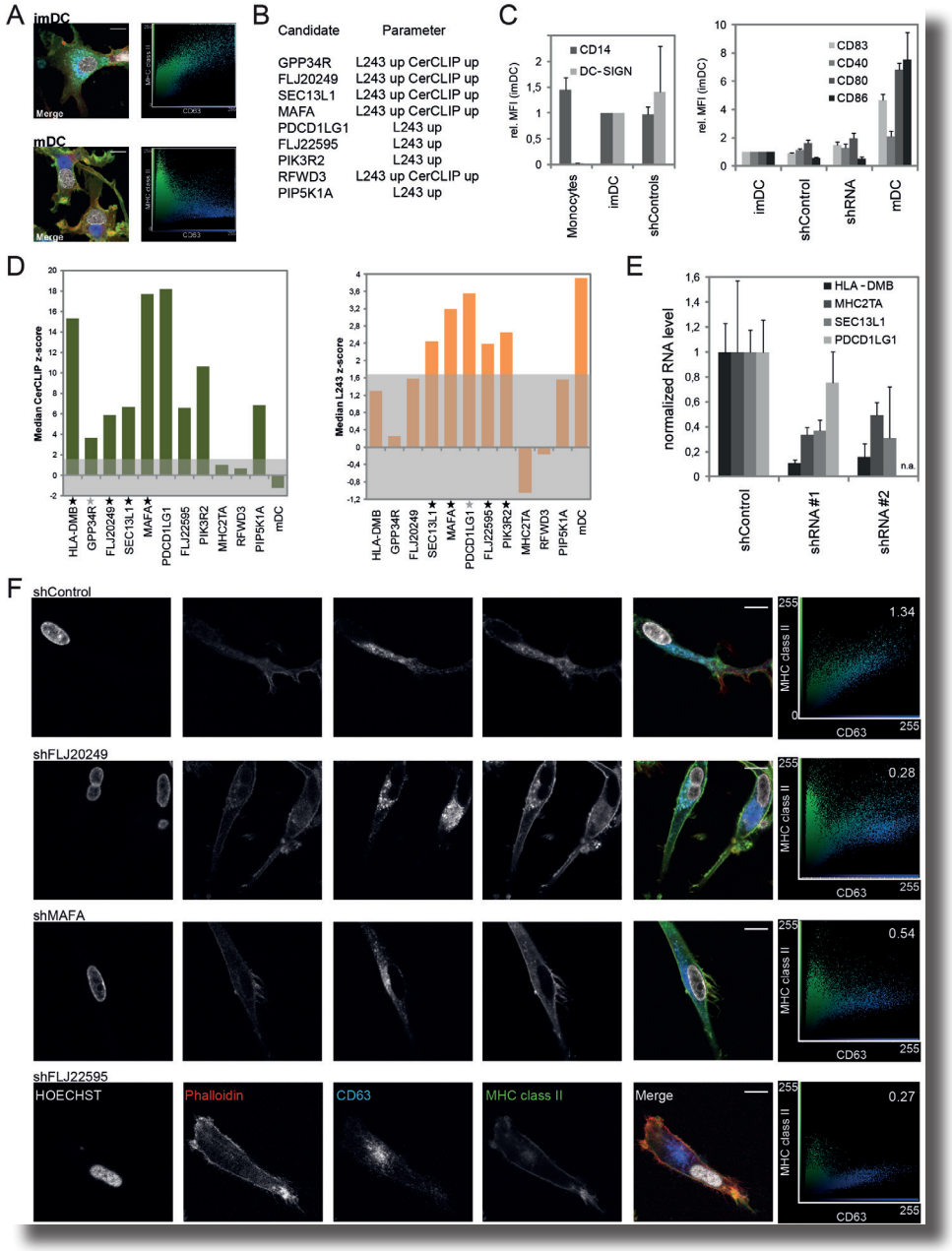

Figure 6 | MHC-II Redistribution in imDCs

A, F | Immature (imDCs) and maturated (mDCs) DCs (A) or manipulated imDCs (F) were stained for MHC-II (green), CD63 (blue), actin (phalloidin; red) and nucleus (Hoechst; white) and analyzed by confocal microscopy. Shown is the merge and the colocalisation plot per pixel for CD63 versus MHC-II (right panel) with the normalized correlation coefficient indicated (bar = 10 µm).

B | Selected candidate genes with primary screen phenotype (Table S2 in Chapter 2 of this thesis) are indicated.

C | Cell surface expression levels of monocyte (CD14), DC (DC-SIGN) and maturation markers (CD83, CD40, CD80, CD86) are plotted as averages of three donors plus standard deviation relative to levels on imDC. Four individual shRNA control vectors (shControl) or shRNAs targeting various candidate genes (shRNA) have been averaged.

Figure 6 | continued

D | Median z-score of three donors in flow cytometry after silencing candidates in imDCs plotted for one representative shRNA construct per gene. The grey box highlights the cut-off. Stars indicate confirmation of phenotype as observed in MelJuSo cells (black confirmation by >1 shRNA constructs, grey by one shRNA construct).

E | Knockdown levels determined by qPCR represented as normalized RNA levels relative to control shRNA treated cells of one donor. Two representative constructs are shown per gene. Averages plus standard deviations are plotted. n.a. not analyzed

F | Representative microscopy images of three confirmed candidates silenced by lentiviral shRNA in imDC with intracellular effects on MHC-II redistribution. The colocalisation coefficient was normalized to control shRNA-treated cells and determined by Cell Profiler. (bar = 10mm).

See also Figure S7 in Chapter 2 of this thesis.

transduction of monocytes (Figure 6D and S7A, see Chapter 2 of this thesis), similar to the effects in the primary screen. As controls, we silenced CIITA and DM, obtaining the anticipated effects on L243 and CerCLIP levels, respectively. Gene silencing was confirmed by qPCR for representative shRNA constructs (Figure 6E).

Next, the effect of silencing the nine candidates on the distribution of MHC-II in imDCs was studied by confocal microscopy. A gallery of representative images is shown in Figure S7B in Chapter 2 of this thesis. Six candidates showed a significant redistribution of MHC-II from CD63-positive compartments to the plasma membrane, which mimics the distribution of MHC-II in mDCs (Figure 6F and S7C, see Chapter 2 of this thesis). Silencing of undefined proteins FLJ20249 (GPATCH4) and FLJ22595 (the small GTPase ARL14/ARF7) as well as the transcription factor MAFA strongly affected localisation. Redistribution of MHC-II was also observed for coat protein complex II protein SEC13L1 (SEC13), Golgi protein GOLPH3-like GPP34R and PDCD1LG1 (CD274), a molecule widely expressed on immune cells involved in the regulation of T cell responses.

Our strategy identified proteins controlling MHC-II transport in imDC that would not have been selected without an unbiased approach. Silencing these genes generated imDCs with an mDC-like MHC-II distribution. These proteins control one of the strongest specific responses in the immune system and therefore open up points to target manipulation strategies at.

A Pathway of the GTPase ARL14/ARF7 and actin-based Motor Myosin 1E controls MHC-II Transport in DC

We defined various proteins controlling MHC-II transport in DCs. One of these, the GTPase ARL14/ARF7 was detected on MHC-II vesicles in imDCs (Figure 7A) and selected as a starting point for building a pathway aimed at understanding the molecular basis of MHC-II transport in DCs. Guanine Exchange Factors (GEFs) activating ARF GTPases are specified by SEC7 domains [37]. We scanned the dataset of the primary screen (Figure 1) for proteins containing SEC7 domains that upregulated MHC-II expression, similar to ARL14/ARF7. Two candidate GEFs were identified. Their SEC7 domains were expressed as MBP-tagged proteins for *in vitro* GTP loading assays of GST-ARL14/ARF7 and GST-ARF6 as control. Only PSD4/EFA6B/TIC (selectively expressed in the immune system, z=2.22 in RNAi screen) promoted GTP loading of ARF6, as described [38] and ARL14/ARF7 (Figure 7B). The PH-domain of PSD4 was produced as GST-fusion protein and used in a lipid-binding assay which indicated specificity for various PIP2 species (Figure 7C). The candidates for controlling MHC-II transport in DC (Figure 6B) also included a regulatory subunit of PI3K (PIK3R2) [39] and PIP5K1A, which can generate PIP2. Overexpressed GFP-PIP5K1A localized to the plasma membrane and partly colocalized with intracellular MHC-II and ARL14/ARF7-mCherry vesicles in MelJuSo cells (Figure 7D) and phagosomes [40]. Collectively, this reveals part of a pathway where PIP5K1A and PIK3R2 create PIPs required for recruitment or activation of the GEF PSD4 which activates ARL14/ARF7.

GTPases require effectors to transmit function. We performed Yeast Two-Hybrid with ARL14/ARF7 as bait to identify C11ORF46 (now called ARF7 Effector Protein or ARF7EP) (Table S7, see Chapter 2 of this thesis). This 29 kDa protein does not have any detectable domains and is selectively expressed in the immune system. The interaction was confirmed by isolating ARL14/ARF7 with ARF7EP from lysates of MelJuSo expressing HA-ARF7EP and RFP-ARL14/ARF7 (Figure 7E). Immunostaining of MelJuSo cells expressing both proteins confirmed co-localization of ARL14/ARF7 and ARF7EP (Figure 7F).

Since ARF7EP does not provide any structural information that connects it to a biological pathway, we performed pull-down experiments with GST or GST-ARF7EP in cytosolic extracts of human PBMCs. Proteins found in the GST-ARF7EP isolate

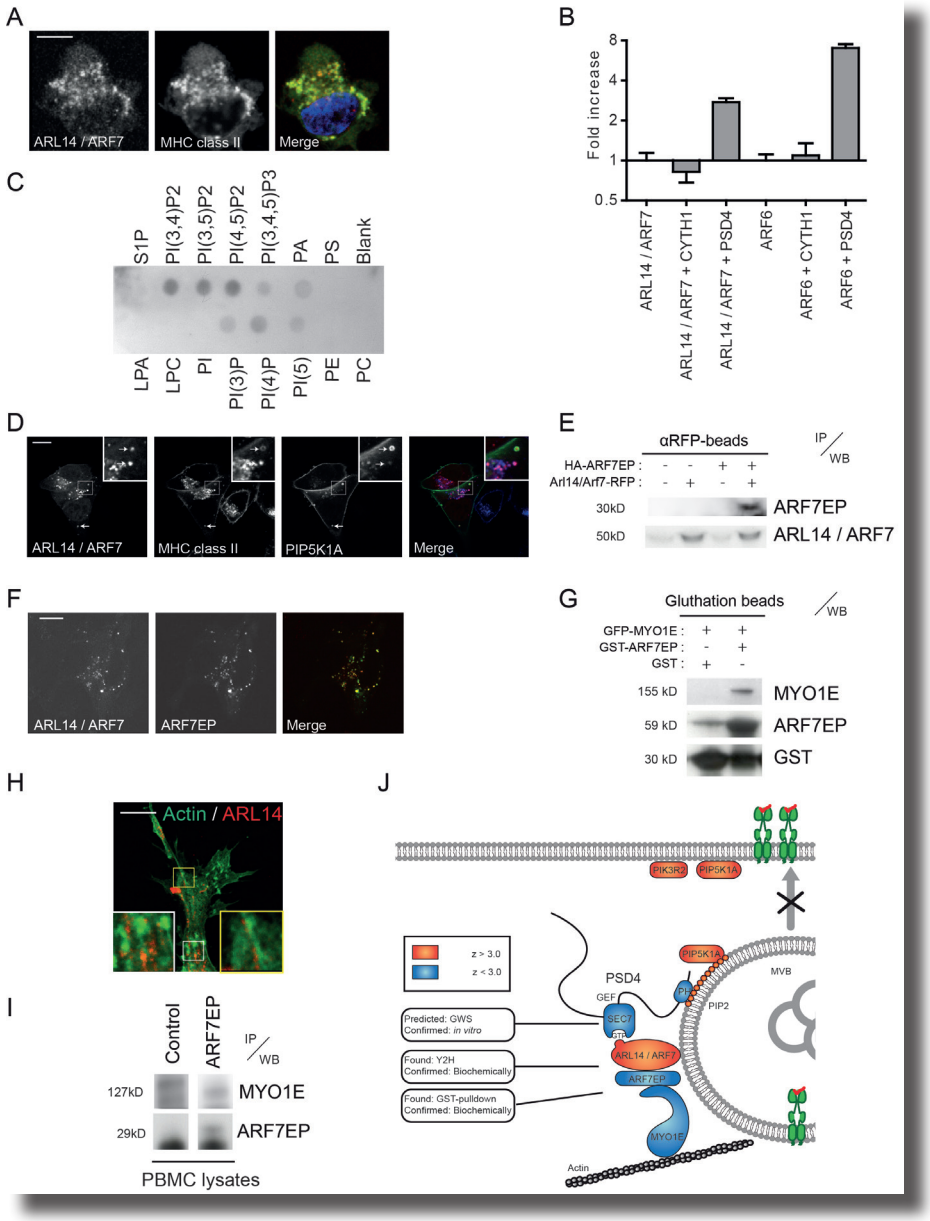

Figure 7 | Data-based Systems Determination of PIP5K-ARL14-MYO1E Pathway of MHC-II transport Control in imDC

A | Immature human monocyte-derived DCs were fixed and stained for nucleus (blue), MHC-II (green) and ARL14/ARF7 (2C8, red). (bar = 10 mm)

B | In vitro a32P-GTP loading of ARL14/ARF7 and ARF6 by SEC7 domains of predicted GEFs CYTH1 and PSD4. Results are normalized to spontaneous loading of the two GTPases. Shown are average and standard deviation of triplicate experiments.

C | Phospholipids spotted on a membrane were probed with the GST-purified PH domain of PSD4.

D | MelJuSo cells were transfected with ARL14/ARF7-RFP and GFP-PIP5K1A, fixed and stained for MHC-II. Arrows indicate colocalisation on vesicles. (bar = 10 mm)

Figure 7 | continued

E | Immunoprecipitation (IP) of ARL14/ARF7-RFP and HA-ARF7EP expressed in MelJuSo with anti-RFP. Immunoblots were probed with HA and ARL14.2 antibodies. Molecular weight standard is indicated. See also Table S7 in Chapter 2 of this thesis.

F | Immunofluorescence of MelJuSo expressing ARL14/ARF7-RFP and GFP-ARF7EP methanol-fixed and stained with ARF7EP antibody. (bar = 10 mm)

G | Pull-down of GFP-MYO1E expressed in HEK293T with recombinant GST-ARF7EP or GST (control) coupled to Glutathione beads. Immunoblots were probed with GST and GFP antibodies. Molecular weight standard is indicated.

H | imDC stained for endogenous actin and ARL14/ARF7 (ARL14.2). Two zoom-ins are shown. (bar = 10 mm).

I | IP of endogenous ARF7EP and MYO1E in human PBMC with anti-ARF7EP or anti-GFP (Control). Immunoblots were probed with MYO1E and ARF7EP antibodies. Molecular weight standard is indicated.

J | Summarized pathway of actin-based control of MHC-II in imDC. Red proteins; candidates from the screen with |z|>3; Blue proteins with |z|<3. Identification and confirmation of the various proteins is indicated. PI kinases create substrates for the GEF PSD4 required for ARL14/ARF7 activation. The effector ARF7EP and MYO1E connect to actin.

were identified by mass spectrometry as B-actin and actin-based motor protein myosin 1E (MYO1E). Pull–down experiments from HEK293T extracts showed specific recovery of GFP-tagged MYO1E by GST-tagged ARF7EP (Figure 7G). MYO1E is a single-headed actin-based motor highly expressed in the immune system. ARL14/ARF7 may connect to the actin network via ARF7EP-MYO1E to control export of MHC-II. To test this connection, human imDC were stained with anti-actin and anti-ARL14/ARF7 antibodies (Figure 7H) revealing ARL14/ARF7 containing vesicles aligning with actin cables. The interaction between ARF7EP and MYO1E was further confirmed by immune precipitation from extracts of human PBMC (Figure 7I).

Various assays were integrated with the results of the RNAi screen to place proteins in one immune specific pathway of actin-based control of MHC-II transport in imDC (Figure 7J). Manipulation of this pathway in imDCs to induce the characteristic MHC-II transport from intracellular stores to the plasma membrane could be the result of inactivation of the ARF7GEF PSD4 by changed behavior of PI3 and PI5 kinases. How these events are controlled in DCs during activation is unknown. By extensive dataset integration, we defined a pathway controlling one of the most essential steps in immune cell activation; the redistribution of MHC-II to the plasma membrane in DCs after maturation.

Discussion

We describe here the genome-wide analysis of an essential process in the immune system: antigen presentation by MHC-II. We identify 276 candidates with only 10% described thus far in the MHC-II pathway. Twenty-one candidates are linked to autoimmune diseases. As in our siRNA experiments, these genes may cause aberrant MHC-II expression in patients, which requires further experimental validation before consideration for therapeutic manipulation.

We have developed various methods to place the candidate genes in the systems of transcriptional and cell biological control of MHC-II antigen presentation. By flow cytometry we selected 45 genes affecting peptide loading only, including HLA-DM and components of the ESCRT machinery involved in multivesicular body formation. A limited set of genes could be placed in networks by computer-based pathway analysis, unlike the majority of genes, which have an unknown function. This represents an enigma in high-throughput screening yielding large datasets and often results in preselecting one gene for in-depth analysis with limited new understanding of biology.

There are two important unelucidated processes in MHC-II antigen presentation, which we addressed in our study in detail: the control of tissue specific expression of MHC-II and the regulation of MHC-II distribution in DCs. MHC-II expression is controlled by CIITA. How CIITA in turn is regulated is unclear. We discovered nine transcriptional regulators of MHC-II expression and performed cross-correlative qPCR to determine their interrelationships and their effects on CIITA expression. Five of these regulate the expression levels of CIITA in a complex feedback loop involving the (yeast meiosis) factor RMND5B and MAPK1 that phosphorylates and influences CIITA activity [41]. The remaining factors control MHC-II expression without affecting CIITA levels. This includes the HIV Tat interacting protein HTATIP, a histone modifier that may mediate Tat control of MHC-II expression [25, 42]. By combining experimental and literature data, we show that the activities of extracellular signalling, the cell cycle and chromatin modifications control the transcriptional network for immune tissue-restricted MHC-II expression. Of note, pathogens also

manipulate these pathways; HIV targets HTATIP and *L. monocytogenes* targets SMAD4 [25, 43]. Tissue selective expression of MHC-II is thus orchestrated by a series of unrelated input signals. The details of how these cooperate to induce proper MHC-II expression remain unclear.

To identify proteins controlling MHC-II distribution, we silenced all candidates and the effect on MHC-II distribution was visualized by microscopy. Candidate genes inducing a similar phenotype are expected to participate in one network, as illustrated in yeast screens that identified the ESCRT machinery [44]. We integrated our phenotypic clusters with databases like Humannet v. 1 to expand our networks and annotated these using GO analyses. Half of the genes in these clusters were predicted to control MHC-II trafficking but will require further experiments to validate their place in networks.

To select candidates involved in MHC-II redistribution in DCs, expression and functional RNAi datasets were combined to define six proteins controlling MHC-II transport. Silencing these resulted in imDCs with an mDC-like MHC-II distribution. These six candidates could act in one or parallel pathways.

One candidate, ARL14/ARF7, is a GTPase selectively expressed in immune cells. To build a pathway, we first localized ARL14/ARF7 on MHC-II compartments in imDC. Using domain predictions and *in vitro* assays, we defined the GEF for ARL14/ARF7 as PSD4. PSD4 contains a PH-domain with specificity for various PIP2 species which may result from activities of two other proteins proposed to control MHC-II distribution in DCs: PIK3R2 and PIP5K1A. While PI(3,5)P2 locates to late endosomes [45], the PH-domain of PSD4 has a broader specificity and can therefore not induce selective targeting of PSD4 to late endosomes. The 60 kDa N-terminal domain of PSD4 may induce targeting to endosomal vesicles [38]. When detecting PIP2, the PH domain of PSD4 might position the preceding SEC7 domain correctly for supporting GTP loading of ARL14/ARF7. To further expand the network, an interaction of the ARL14/ARF7 effector ARF7EP with the actin-based motor MYO1E was defined. This pathway connects general signalling events to actin-based transport control of MHC-II compartments in DCs.

While PIK3R2 and PIP5K1A upstream are broadly expressed proteins, the other proteins in this pathway are more immune system selective. Of note, another candidate for controlling MHC-II distribution in DCs, PDCD1LG1 (CD274, PD-L1) activates PI3K via its receptor PD-1. PD-1 delivers inhibitory signals regulating T cell activation and tolerance. Little is known about PD-L1 signalling [46] and this signalling may be irrelevant in mDC [47]. Tissue selective control of actin-based transport by GTPases has been shown before for melanosomes where GTPase RAB27a binds MYO5A via its effector Melanophylin [48]. MYO1E may be involved in granule secretion [49] as well as endocytosis by coupling to dynamin [50]. MYO1E may have multiple functions in actin-based processes depending on recruitment to specific locations. We define ARL14/ARF7-ARF7EP as a MYO1E receptor on MHC-II compartments for actin-based transport control. How the previously observed interaction between another actin-based motor MYH9 and MHC-II-associated Ii contributes to this process is unclear [51].

The four remaining proteins controlling MHC-II transport in imDC could not be placed in this pathway: MAFA is a transcription factor for insulin in pancreatic beta cells [52]. Our microarray data do not show any insulin production in DCs because the transcription co-factors Pdx-1 and NeuroD1 [53] are not expressed. SEC13L1 (SEC13) is a COPII protein controlling transport between ER and Golgi [54] which is a non immune-specific process in cells. GOLPH3L might have a similar function in the Golgi as GOLPH3 [55]. The function of the fourth protein, GPATCH4 is unknown. It remains to be elucidated whether and how GPATCH4 could manipulate MHC-II antigen presentation.

We describe here a genome-wide analysis of molecules acting on a central controller in the immune system: MHC-II. After a first candidate selection by flow cytometry, we applied two additional high-throughput techniques and integrated the data with expression and protein interaction databases, cross-correlative qPCR, Yeast Two-Hybrid and proteomics. We defined a transcriptional network for MHC-II and CIITA, and a cell biological pathway placing ARL14/ARF7, its effector ARF7EP and MYO1E in control of actin-based MHC-II transport in DCs. This study identifies new targets and pathways for chemical and biological manipulation of MHC-II expression in various diseases, including autoimmunity.

Experimental Procedures

siRNA Transfection, Flow cytometry and Microarray

Gene silencing was performed in the human melanoma cell line (MelJuSo) using DharmaFECT transfection reagent #1 and 50 nM siRNA (Human siGenome SMARTpool library, Dharmacon). Three days post-transfection, cells were analyzed by flow cytometry (BD FACSArray) using L243-Cy3 [22] and CerCLIP-Cy5 [21] monoclonal antibodies. The data was normalized (cellHTS, Bioconductor) and transformed into z-scores [56]. Expression levels of genes with $|z|>3$ were determined by microarray analysis (Illumina) in primary human monocytes, DCs and B cells; isolated and differentiated as previously

described [57, 58]. Mature DCs were generated by culturing for two days in the presence of 2.5 μg/ml LPS (Invivogen) and 1000 U/ml IFNγ (Immukine, Boehringer Ingelheim).
For statistical analysis, p-values were determined using the Student's t test.

Quantitative RT-PCR

Messenger RNA was extracted (mRNA Capture Kit) and reverse transcribed into cDNA (Transcriptor High Fidelity cDNA Synthesis Kit). The quantitative RT-PCR was performed using LightCycler® 480 SYBR Green 1 Master on the LightCycler® 480 Detection System (all Roche). Quantification was performed using the comparative CT method (ΔΔCT). Primer sequences are available upon request.

Confocal Microscopy

Distribution of MHC-II, early endosomes and Golgi was visualized by confocal microscopy (Leica AOBS microscope) using MelJuSo stably expressing HLA-DRB1-GFP, mCherry-GalT2 and stained with anti-EEA1 (BD transduction laboratories) and Hoechst (Invitrogen). DCs were stained using Hoechst, Phalloidin-Alexa568 (Molecular Probes), anti-ARL14 2C8 (BioConnect), anti-CD63 (NKI-C3) and anti-HLA-DR [3]. Images were analyzed using CellProfiler 1.0.5811 [32]. CPAnalyst 2 was used to determine the minimal set of parameters needed to describe the relevant phenotypes [33]. The "Measure Correlation" module of CellProfiler was used to determine the correlation between CD63 and MHC-II. MelJuSo cells were cultured with 3 ng/ml TGFβ for three days. Cells were stained with anti-SMAD4 (Santa Cruz) and anti-RMND5B (Abcam) antibodies.
Open and proprietary software was used for pathway analysis as described extensively in the Supplemental Experimental Procedures.

DC Manipulation

Human primary monocytes were transduced with lentiviral particles in the presence of 4 μg/ml polybrene (Millipore) at a MOI of 2. Viruses were produced by 293T cells transfected with packaging (pRSVrev, pHCMV-G VSV-G, pMDLg/pRRE) and pLKO.1shRNA constructs (Open Biosystems, Thermo Scientific) using Fugene 6 (Roche). Monocytes were subsequently cultured for six days in the presence of 800 U/ml IL-4 and 1,000 U/ml GM-CSF (Cellgenix) to generate imDCs. DC cell surface marker levels were determined by flow cytometry after staining with the following mouse anti-human antibodies: FITC CD14, APC DC-SIGN, PE HLA-DR (L243), FITC CD83, APC CD40, PE CD80, APC CD86 (all from BD).

Pathway building Techniques

Yeast Two-Hybrid was performed at DKFZ (Heidelberg) with ARL14-Q68L without myristoylation site cloned in pGBT9. ARF7EP was cloned in a bacterial expression vector as a GST-chimera and purified. Recombinant GST-ARF7EP and GST as a control were used to fish for endogenous MYO1E from cytosolic extracts of human PBMCs and bound fractions were analyzed by mass spectrometry. Biochemical GEF assays were performed with purified MBP-tagged SEC7 domains from CYTH1 and PSD4 and GST-purified ARL14 or ARF6 using a32P-GTP. The PH domain of PSD4 was isolated as a GST-PHPH protein from 293T cells and used to probe phospholipid membranes (tebu-bio). For antibodies used to immune precipitate see Supplemental Experimental Procedures in Chapter 2 of this thesis.

References

1. Reith, W., S. LeibundGut-Landmann, and J.M. Waldburger, *Regulation of MHC class II gene expression by the class II transactivator.* Nat.Rev. Immunol., 2005. **5**(10): p. 793-806.
2. Chaplin, D.D. and M.E. Kemp, *The major histocompatibility complex and autoimmunity.* Year.Immunol, 1988. **3**: p. 179-198.
3. Neefjes, J.J., et al., *The biosynthetic pathway of MHC class II but not class I molecules intersects the endocytic route.* Cell, 1990. **61**(1): p. 171-183.
4. Roche, P.A. and P. Cresswell, *Invariant chain association with HLA-DR molecules inhibits immunogenic peptide binding.* Nature, 1990. **345**(6276): p. 615-618.
5. Riberdy, J.M., et al., *HLA-DR molecules from an antigen-processing mutant cell line are associated with invariant chain peptides.* Nature, 1992. **360**(6403): p. 474-477.
6. Denzin, L.K., C. Hammond, and P. Cresswell, *HLA-DM interactions with intermediates in HLA-DR maturation and a role for HLA-DM in stabilizing empty HLA-DR molecules.* J.Exp.Med., 1996. **184**(6): p. 2153-2165.
7. Sloan, V.S., et al., *Mediation by HLA-DM of dissociation of peptides from HLA-DR.* Nature, 1995. **375**(6534): p. 802-806.
8. Zwart, W., et al., *Spatial separation of HLA-DM/HLA-DR interactions within MIIC and phagosome-induced immune escape.* Immunity, 2005. **22**(2): p. 221-233.
9. Boes, M., et al., *T-cell engagement of dendritic cells rapidly rearranges MHC class II transport.* Nature, 2002. **418**(6901): p. 983-988.
10. Chow, A., et al., *Dendritic cell maturation triggers retrograde MHC class II transport from lysosomes to the plasma membrane.* Nature, 2002. **418**(6901): p. 988-994.
11. Wubbolts, R., et al., *Direct vesicular transport of MHC class II molecules from lysosomal structures to the cell surface.* J.Cell Biol., 1996. **135**(3): p. 611-622.
12. Koppelman, B., et al., *Interleukin-10 down-regulates MHC class II alphabeta peptide complexes at the plasma membrane of monocytes by affecting arrival and recycling.* Immunity, 1997. **7**(6): p. 861-871.
13. Steimle, V., et al., *Regulation of MHC class II expression by interferon-gamma mediated by the transactivator gene CIITA.* Science, 1994. **265**(5168): p. 106-109.
14. Blander, J.M. and R. Medzhitov, *Toll-dependent selection of microbial antigens for presentation by dendritic cells.* Nature, 2006. **440**(7085): p. 808-812.
15. Thibodeau, J., et al., *Interleukin-10-induced MARCH1 mediates intracellular sequestration of MHC class II in monocytes.* Eur J Immunol, 2008. **38**(5): p. 1225-1230.
16. Ziegler, H.K. and E.R. Unanue, *Decrease in macrophage antigen catabolism caused by ammonia and chloroquine is associated with inhibition of antigen presentation to T cells.* Proc. Natl.Acad.Sci.U S A, 1982. **79**(1): p. 175-178.
17. Anderson, H.A. and P.A. Roche, *Phosphorylation regulates the delivery of MHC class II invariant chain complexes to antigen processing compartments.* J.Immunol., 1998. **160**(10): p. 4850-4858.
18. Kuipers, H.F., et al., *Statins affect cell-surface expression of major histocompatibility complex class II molecules by disrupting cholesterol-containing microdomains.* Hum.Immunol., 2005. **66**(6): p. 653-665.
19. Agrawal, S. and E.R. Kandimalla, *Role of Toll-like receptors in antisense and siRNA [corrected].* Nat Biotechnol, 2004. **22**(12): p. 1533-1537.
20. Reynolds, A., et al., *Induction of the interferon response by siRNA is cell type- and duplex length-dependent.* RNA., 2006. **12**(6): p. 988-993.
21. Denzin, L.K., et al., *Assembly and intracellular transport of HLA-DM and correction of the class II antigen-processing defect in T2 cells.* Immunity, 1994. **1**(7): p. 595-606.
22. Lampson, L.A. and R. Levy, *Two populations of Ia-like molecules on a human B cell line.* J.Immunol., 1980. **125**(1): p. 293-299.
23. Zhang, J.H., T.D. Chung, and K.R. Oldenburg, *A Simple Statistical Parameter for Use in Evaluation and Validation of High Throughput Screening Assays.* J Biomol Screen, 1999. **4**(2): p. 67-73.
24. Imai, A., et al., *Inhibition of endogenous MHC class II-restricted antigen presentation by tacrolimus (FK506) via FKBP51.* Eur J Immunol, 2007. **37**(7): p. 1730-1738.
25. Kamine, J., et al., *Identification of a cellular protein that specifically interacts with the essential cysteine region of the HIV-1 Tat transactivator.* Virology, 1996. **216**(2): p. 357-366.
26. Wu, C., et al., *BioGPS: an extensible and customizable portal for querying and organizing gene annotation resources.* Genome Biol, 2009. **10**(11): p. R130.
27. Snel, B., et al., *STRING: a web-server to retrieve and display the repeatedly occurring neighbourhood of a gene.* Nucleic Acids Res, 2000. **28**(18): p. 3442-3444.
28. Horton, R., et al., *Gene map of the extended human MHC.* Nat Rev Genet, 2004. **5**(12): p. 889-899.
29. Colland, F., et al., *Functional proteomics mapping of a human signaling pathway.* Genome Res, 2004. **14**(7): p. 1324-1332.
30. Dong, Y., et al., *The Smad3 protein is involved in TGF-beta inhibition of class II transactivator and class II MHC expression.* J Immunol, 2001. **167**(1): p. 311-319.
31. Shi, Y. and J. Massague, *Mechanisms of TGF-beta signaling from cell membrane to the nucleus.* Cell, 2003. **113**(6): p. 685-700.

32. Carpenter, A., et al., *CellProfiler: image analysis software for identifying and quantifying cell phenotypes.* Genome Biology, 2006. **7**(10): p. R100.
33. Jones, T.R., et al., *Scoring diverse cellular morphologies in image-based screens with iterative feedback and machine learning.* Proc Natl Acad Sci U S A, 2009. **106**(6): p. 1826-1831.
34. Cella, M., et al., *Inflammatory stimuli induce accumulation of MHC class II complexes on dendritic cells.* Nature, 1997. **388**(6644): p. 782-787.
35. Pierre, P., et al., *Developmental regulation of MHC class II transport in mouse dendritic cells.* Nature, 1997. **388**(6644): p. 787-792.
36. Kim, W.K., C. Krumpelman, and E.M. Marcotte, *Inferring mouse gene functions from genomic-scale data using a combined functional network/ classification strategy.* Genome Biol, 2008. **9 Suppl 1**: p. S5.
37. Casanova, J.E., *Regulation of Arf activation: the Sec7 family of guanine nucleotide exchange factors.* Traffic, 2007. **8**(11): p. 1476-1485.
38. Derrien, V., et al., *A conserved C-terminal domain of EFA6-family ARF6-guanine nucleotide exchange factors induces lengthening of microvilli-like membrane protrusions.* J Cell Sci, 2002. **115**(Pt 14): p. 2867-2879.
39. Deane, J.A. and D.A. Fruman, *Phosphoinositide 3-kinase: diverse roles in immune cell activation.* Annu Rev Immunol, 2004. **22**: p. 563-598.
40. Mao, Y.S., et al., *Essential and unique roles of PIP5K-gamma and -alpha in Fcgamma receptor-mediated phagocytosis.* J Cell Biol, 2009. **184**(2): p. 281-296.
41. Voong, L.N., et al., *Mitogen-activated protein kinase ERK1/2 regulates the class II transactivator.* J.Biol.Chem., 2008. **283**(14): p. 9031-9039.
42. Kanazawa, S., T. Okamoto, and B.M. Peterlin, *Tat competes with CIITA for the binding to P-TEFb and blocks the expression of MHC class II genes in HIV infection.* Immunity, 2000. **12**(1): p. 61-70.
43. Ribet, D., et al., *Listeria monocytogenes impairs SUMOylation for efficient infection.* Nature, 2010. **464**(7292): p. 1192-1195.
44. Teis, D., S. Saksena, and S.D. Emr, *Ordered assembly of the ESCRT-III complex on endosomes is required to sequester cargo during MVB formation.* Dev Cell, 2008. **15**(4): p. 578-589.
45. Vicinanza, M., et al., *Function and dysfunction of the PI system in membrane trafficking.* EMBO J, 2008. **27**(19): p. 2457-2470.
46. Keir, M.E., et al., *PD-1 and its ligands in tolerance and immunity.* Annu Rev Immunol, 2008. **26**: p. 677-704.
47. Breton, G., et al., *siRNA knockdown of PD-L1 and PD-L2 in monocyte-derived dendritic cells only modestly improves proliferative responses to Gag by CD8(+) T cells from HIV-1-infected individuals.* J Clin Immunol, 2009. **29**(5): p. 637-645.
48. Seabra, M.C. and E. Coudrier, *Rab GTPases and myosin motors in organelle motility.* Traffic, 2004. **5**(6): p. 393-399.
49. Schietroma, C., et al., *A role for myosin 1e in cortical granule exocytosis in Xenopus oocytes.* J Biol Chem, 2007. **282**(40): p. 29504-29513.
50. Krendel, M., E.K. Osterweil, and M.S. Mooseker, *Myosin 1E interacts with synaptojanin-1 and dynamin and is involved in endocytosis.* FEBS Lett, 2007. **581**(4): p. 644-650.
51. Vascotto, F., et al., *The actin-based motor protein myosin II regulates MHC class II trafficking and BCR-driven antigen presentation.* J Cell Biol, 2007. **176**(7): p. 1007-1019.
52. Olbrot, M., et al., *Identification of beta-cell-specific insulin gene transcription factor RIPE3b1 as mammalian MafA.* Proc Natl Acad Sci U S A, 2002. **99**(10): p. 6737-6742.
53. Cerf, M.E., *Transcription factors regulating beta-cell function.* Eur J Endocrinol, 2006. **155**(5): p. 671-679.
54. Tang, B.L., et al., *The mammalian homolog of yeast Sec13p is enriched in the intermediate compartment and is essential for protein transport from the endoplasmic reticulum to the Golgi apparatus.* Mol Cell Biol, 1997. **17**(1): p. 256-266.
55. Dippold, H.C., et al., *GOLPH3 bridges phosphatidylinositol-4- phosphate and actomyosin to stretch and shape the Golgi to promote budding.* Cell, 2009. **139**(2): p. 337-351.
56. Boutros, M., L.P. Bras, and W. Huber, *Analysis of cell-based RNAi screens.* Genome Biol., 2006. **7**(7): p. R66.
57. Souwer, Y., et al., *B cell receptor-mediated internalization of salmonella: a novel pathway for autonomous B cell activation and antibody production.* J Immunol, 2009. **182**(12): p. 7473-7481.
58. Ten Brinke, A., et al., *The clinical grade maturation cocktail monophosphoryl lipid A plus IFNgamma generates monocyte-derived dendritic cells with the capacity to migrate and induce Th1 polarization.* Vaccine, 2007. **25**(41): p. 7145-7152.

Chapter 2

A Genome-wide Multi-Dimensional RNAi Screen Reveals Pathways Controlling MHC Class II Antigen Presentation

Supplemental Information

Cell. 2011 Apr 15;145(2):268-83

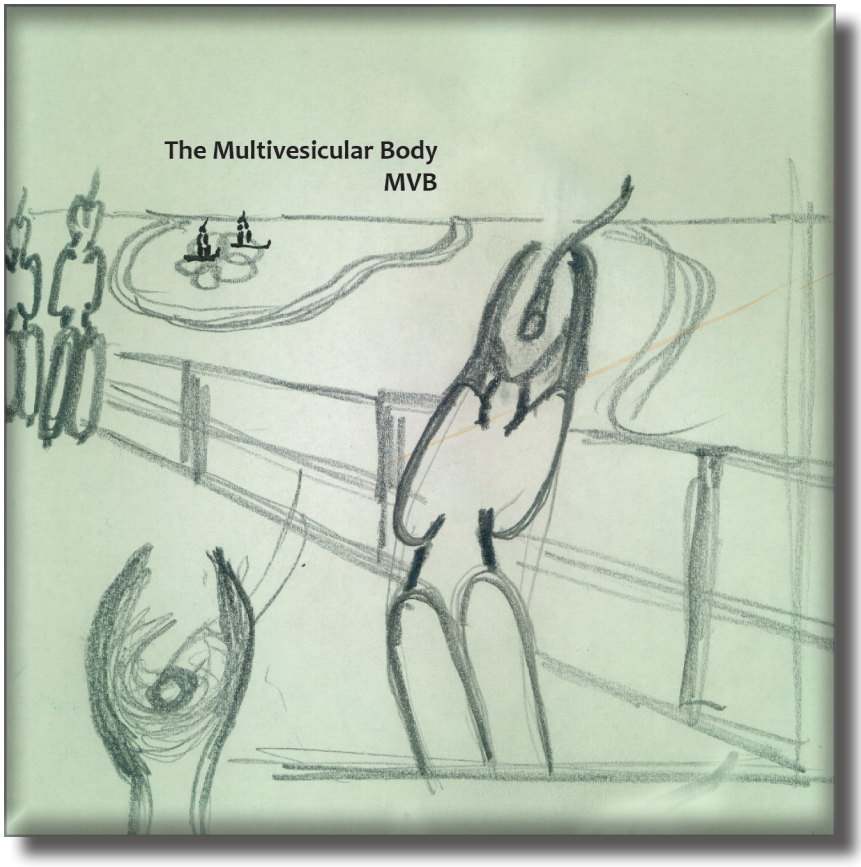

Supplemental Experimental Procedures

Cell Lines

Wild-type (wt) MelJuSo, human melanoma cell line, expressing HLA-DRB3 [17], was cultured in IMDM (Gibco) supplemented with 7.5% fetal calf serum (FCS, Greiner). MelJuSo were transfected with HLA-DRB1-GFP and mCherry-GalT2, stable clones were selected and cultured in IMDM/7.5% FCS supplemented with Penicillin/Streptomycin (Invitrogen), Hygromycin (Invitrogen) and Neomycin/G418 (Gibco). Human 293T cells were cultured in DMEM (Gibco) supplemented with 7.5% fetal calf serum (FCS, Greiner) and Penicillin/Streptomycin (Invitrogen).

Constructs

HLA-DRB1-GFP from pCDNA3-DR1B-GFP [18] was cloned into pCDNA3 via HindIII-XhoI. GalT2 was removed via EcoR1-BamH1 from GalNac-T2-GFP [19] construct (generous gift from T. Nilson) and placed into pmCherry-C1, where we replaced GFP from pEGFP-C1 [20] (Clontech) for mCherry via NheI and BglI.

The packaging constructs used for lentivirus production are as follows, pMDLg/pRRE, pRSV-Rev and pCMV-VSV-G [21], kindly provided by Dr. M. Soengas (University of Michigan, USA). The pLKO.1 plasmids containing shRNA hairpins targeting selected genes were purified from bacterial glycerol stocks (Open Biosystems, Thermo Scientific) using a large scale plasmid DNA purification kit (Qiagen). The vectors pLKO.1 empty, pLKO.1 EGFP shRNA, pLKO.1 TurboGFP shRNA, pLKO.1 Luciferase shRNA and pLKO.1 non-target shRNA served as negative controls.

ARL14/ARF7 Q68L missing the sequence coding for the myristoylation site (first two N-terminal amino acids) was amplified from IMAGE: 4747382 and cloned into pGBT9 via EcoRI and BamH1 restriction sites to use for Yeast Two-Hybrid assay. ARL14/ARF7 was cloned, using restriction sites EcoRI and BamHI, into pRP265 and mCherry-N1 via EcoRI and BamHI. ARF7EP was amplified form IMAGE clone 6062049 and cloned into pRP265 and p2HA-C1 via BglII and EcoRI (p2HA-C1 was retrieved from pEGFP-C1 (Clontech) where GFP was exchanged for HA-HA using Nhe1 and BglII cloning sites). Those constructs were used for protein production, co-immune precipitation and colocalization experiments. SEC7 domains of PSD4 (aa555-aa738) and CYTH1 (aa73-aa202) were amplified from IMAGE clone 5757431 (PSD4) and IMAGE clone 4755203 (CYTH1) and cloned into pMAL-c2X using BamHI and HinDIII restriction sites. Double PH-domains of PSD4 (aa776-aa892) were amplified and cloned into pRP265 and pEGFP-N1 using BglII, EcoRI and BamH1 for lipid binding. pGEX-Arf6 was a generous gift from Dr. C. D'Souza-Schorey (University of Notre Dame, FR). GFP-PIP5K1A GFP was a generous gift from Dr. N. Divecha (The University of Manchester,UK) [22]. Myo1E and Myo1E tail (aa710-aa1109) both amplified from IMAGE clone 30527536 were cloned into pEGFP-C1 using Asp718I and BamHI as restriction sites.

Antibodies

The hybridoma cell lines L243 (anti-HLA-DR complex, ATCC) and CerCLIP.1 (anti-CLIP24) have been described previously [23, 24]. Cells were maintained in IMDM/7.5% FCS, penicillin/streptomycin and gentamycin (Gibco). The monoclonal antibodies were purified, concentrated by HPLC and affinity purified using protein G-sepharose beads (Amersham Biosciences). L243 and CerCLIP antibodies were directly conjugated to Cy3 and Cy5 fluorophores, respectively and purified by size exclusion chromatography.

Mouse anti-human EEA1 (MAB 610457, BD transduction laboratories), Hoechst (2 µg/ml, 33342, Invitrogen), Phalloidin-Alexa568 (0.4 U/ml, Molecular Probes), mouse anti-human CD63 NKI-C3 [25], mouse anti-human Arl14 (BioConnect), mouse anti B-actin (AC-15, Sigma Aldrich) and rabbit anti-human HLA-DR [26, 27] were used to stain early endosomes, nuclei, actin, CD63, FLJ22595 (Arl14/ARF7), B-actin and HLA-DR, respectively, followed by secondary Alexa dye-coupled antibodies (Invitrogen) for detection by confocal microscopy.

Antibodies against human Arl14/Arf7 (ARL14.2) and human ARF7EP (used for immune precipitation, western blotting and immune fluorescence) were produced in rabbits after immunization with recombinant GST-Arl14/Arf7 and GST-ARF7EP respectively (GST was removed by Thrombin cleavage). Anti-HA (12CA5, gift from Dr. H. Ovaa, NKI, Amsterdam, NL) was used for co-immune precipitation assays. Rabbit anti-human Myo1E (H-60, Santa Cruz Biotechnology), mouse anti-GST (B14, Santa Cruz, sc-138), rabbit anti-mRFP, rabbit anti-GFP [28] and anti-HA-PO (Roche, 2013819001) were used for detection on Western Blot. Rabbit anti-mRFP was also used for immune precipitation.

Flow Cytometry HTS: RNAi Screen Layout

In the primary screen siRNAs (Human siGenome siRNA SMARTpool library - Genome, Dharmacon) were used to silence human genes in MelJuSo cells. In the deconvolution screen, the four siRNA duplexes of the smartpool of a potential candidate were tested separately. All steps were performed in triplicate. MelJuSo untreated and HLA-DM siRNA transfected were used as negative and positive

control (for CerCLIP), respectively.

Flow Cytometry HTS: siRNA Transfection

siRNA (50 nM final concentration) was aliquoted into 96-well plates (Greiner CELLSTAR® 96-well microplates, black, flat bottom) using a liquid handling robot (Hamilton ML STAR). Per well, 0.2 µl DharmaFECT1 (Dharmacon) and 9.8 µl IMDM was added to the siRNA, incubated for 20 minutes, followed by addition of 4,700 MelJuSo cells using a Microplate Dispenser (Matrix WellMate®) and culture for three days at 37°C and 5% CO2 before analysis.

Flow Cytometry HTS: Analysis

Cells were washed with PBS (Gibco), detached using 10 µl/well Trypsin-EDTA (Gibco) and incubated with 5 µg/ml L243-Cy3 and 6.7 µg/ml CerCLIP-Cy5 in 20 µl/well PBS/2% FCS for 30 minutes at 4°C. Samples were diluted to 200 µl with PBS/2% FCS, followed by 10 minutes incubation on ice before the mean fluorescence intensity (MFI) was determined using the BD FACSArray™ Bioanalyzer System (Becton Dickinson).

Flow Cytometry HTS: Normalization

Raw flow cytometry data (geometric mean fluorescence intensity of each antibody) was normalized using the CellHTS2 package of R2.6.0-based Bioconductor [29]. All data points were transformed into z-scores. The average z-score and standard deviation of untreated MelJuSo cells were calculated. Genes displaying a |z-score|>3 in at least two replicates were regarded as 'candidates'. In the deconvolution screen a candidate was considered confirmed, when at least two duplexes reproduced the phenotype observed in the primary screen.

Microarray Analysis

Human primary monocytes as well as immature and mature monocyte-derived DC were isolated and differentiated as described [30]. Human primary B cells were isolated from peripheral blood and activated as described [31]. Detailed protocols for RNA isolation, amplification, labeling, and hybridization can be found at **http://cmf.nki.nl/download/protocols.html**. The Sentrix Human-6_v.2 BeadChip (Illumina) was used for the whole genome gene expression study. The data underwent variance stabilizing transformation and robust spline normalization. Candidates were considered expressed in immune cells with a detection p-value of 0.01 or lower. Expression of a gene in at least one of five primary cell types led to incorporation in the deconvolution screen.

Data on overall gene expression in 79 human tissues was obtained from Novartis GNF SymAtlas (**http://biogps.gnf.org**). The GC-RMA package processed data was LOG-transformed. Expression maxima for immune versus normal tissues were determined and ranking upon the ratio was performed. Immune-specific expression threshold was set above a ratio of 1.09, which corresponded to that of CIITA.

Quantitative RT-PCR

Messenger RNA was extracted from cells using the mRNA Capture Kit (Roche) and reverse transcribed into cDNA using the Transcriptor High Fidelity cDNA Synthesis Kit (Roche). The qPCR was performed using LightCycler® 480 SYBR Green 1 Master (Roche) on the LightCycler® 480 Detection System (Roche). Primer sequences are available upon request. Quantification was performed using the comparative CT method (ΔΔCT). The results were expressed relative to GAPDH values; normalized to control siRNA treated cells and LOG-transformed. In case of lentiviral-transduced DC, results were expressed relative to 18S rRNA values and normalized to shControl treated cells

Confocal Microscopy HTS: siRNA Transfection

MelJuSo/HLA-DRB1-GFP/mCherry-GalT2 cells were transfected with siRNAs silencing all 276 candidates as described above and seeded on µ-Slide 18-well plates (flat ibiTreat, Ibidi). Control siRNA and RILP#3 siRNA, which separates the late endosomal Rab7-RILP receptor from the dynein motor resulting in scattered MHC class II-positive vesicles [32], were used as negative and positive control, respectively.

Confocal Microscopy HTS: Analysis

Cells were fixed with PBS/3.75% formaldehyde (free from acid, Merck), permeabilized with PBS/0.1% TritonX-100 (Sigma) and blocked with PBS/0.5% bovine serum albumin (BSA, Sigma). Cells were stained with anti-EEA1, goat anti-mouse-Alexa647 and Hoechst, washed with PBS and covered with 80% glycerol (Merck) in PBS. Stained cells were analyzed by a Leica AOBS microscope with appropriate filters for fluorescence detection. Pictures were taken using a HCX PL APO blue corrected 63x 1.32 object. Hoechst was excited at l=405nm and detected at l=416-470nm; GFP was excited at l=488nm and detected at l=500-550nm; mCherry was excited at l=561nm and detected at l=570-621 nm; Alexa-647 was excited at l=633nm and detected at l=642-742nm.

Confocal Microscopy HTS: CellProfiler and Clustering

Cell image analysis program CellProfiler 1.0.5811, as provided by the Broad Institute (Boston, USA), was used to extract multiple features from the cells in each image [33]. Briefly, nuclei were detected as primary objects. From these nuclei the cell was detected based on cytosolic background staining. EEA1 and MHC class II vesicles and the Golgi were detected as primary objects and then assigned to a cell containing this object (their parent). The membrane area was defined as the area between the cell perimeter expanded or shrunken by 10 pixels. The CP Analyst 2 program was used to determine the minimal number of parameters distinguishing and describing phenotypes of interest. During supervised machine learning seven bins for MHC class II, three for early endosome and five for Golgi features were designed. After cross-validation accuracy calculation (Figure S4B) six MHC class II parameters, two for EEA1 and five for Golgi were selected. All these features were z-score normalized in Excel (Table S4). The MHC class II related parameters were replicated four times and the Golgi related parameters were replicated two times to increase their weight in the consideration. A similarity matrix was calculated and the data were clustered using the Matlab Bioinformatics Toolbox. The phylogenetic tree was build in Matlab and imported into Cytoscape (2.6.3) with the PhyloTree (v.0.1) plug-in. The tree was plotted as an organic tree and nodes were coloured according to the z-score in the flow cytometry-based screen. The edge colour was determined by the changes in mRNA levels between im and mDCs (Table S1). The node size was determined by the mDC like phenotype, which is based on microscopy data (Table S4). Two bins were created in CP Analyst 2: one with wild type cells and one with cells resembling an mDC phenotype (MHC class II at the cell surface and little MHC class II inside). All cells for each candidate were scored for the enrichment of the mDC phenotype.

Confocal Microscopy HTS: Network Analysis

Humannet v. 1 [16] was used to predict genes that interact with candidate genes (neighbours). Two cut-off values were applied to be considered as an interacting gene: neighbours have a log-likelihood score ≥1 and a $|z| \geq 1.645$ in the flow cytometry screen. All candidates or clusters (with or without neighbours) were analyzed for enrichment in Gene Ontology terms (Cellular Component). Clusters were defined by having a distance of 153.6 from the root of the tree and at least 15 genes in the branch. Gene Ontology analysis was performed with the cytoscape plug-in BiNGO (v.2.3).

Lentivirus Production

Lentiviruses were produced as described previously [34] with following alterations. 293T cells were seeded at 3.5x106 per 10 cm dish 24 h before transfection in DMEM/7.5% FCS/PS. 293T cells were transiently transfected with the viral packaging constructs pMDLg/pRRE, pRSV-Rev and pCMV-VSV-G (ratio 1:1:1) in a ratio of 1:1 with the pLKO.1 vector harboring the respective shRNA sequence using 4 µl Fugene 6 transfection reagent (Roche) per µg of DNA. Per 10 cm dish, 2.33 µg of each packaging vector, 6.5 µg of pLKO.1 and 0.5 µg of pEGFP-C1 [20] (Clontech) were used. After 24 h the complete medium was replaced by serum-free DMEM. After another 24 h of culture, the supernatant was harvested and concentrated 100-fold by ultracentrifugation (Beckman Coultor Rotor SW28) at 20,000 rpm for 2 h at room temperature. The viral pellet was resuspended in Cellgro medium (Cellgenix), snap frozen in liquid nitrogen and stored at -80°C.

Dendritic Cell Transduction

Human primary monocytes were isolated from peripheral blood of healthy volunteers after informed consent as described [30], frozen and stored in liquid nitrogen. Thawed monocytes were plated at one million per well in 12 well plates (Falcon) and transduced with lentivirus at a MOI of 2 in 1 ml Cellgro medium in the presence of 4 µg/ml polybrene (Millipore). The medium was supplemented with 800 U/ml IL-4 and 1,000 U/ml GM-CSF (Cellgenix). After 24 h, 1 ml of Cellgro plus IL-4 and GM-CSF was added again. Cells were cultured for six days at 37°C and 5% CO_2 before analysis by flow cytometry. Maturation of DC was induced at day 5 by adding 10 ng/ml IL-1β, 10 ng/ml TNF-α, 1,000 U/ml IL-6 (Cellgenix) and 1 µg/ml PGE_2 (Sigma). For immunofluorescence, DC were seeded on µ-Slide 18-well plates (Ibidi) pre-coated with 20 µg/ml Fibronectin (Invitrogen) and incubated for seven hours. Slides were fixed with PBS/3.75% formaldehyde and stained with anti-HLA-DR and anti-CD63 antibodies, phalloidin and Hoechst. The "Measure Correlation" module of CellProfiler was used to determine the correlation between CD63 and MHC class II localisation. Correlation pixel plots were determined using the Leica Confocal Software.

Biochemical Experiments: Yeast Two-Hybrid Analysis

Arl14/ARf7 Q68L without myristoylation site was used as bait in a Yeast Two-Hybrid assay that was performed in a skeletal muscle cDNA library at DKFZ,

Heidelberg, Germany (information: **http://www.dkfz.de/gpcf/y2h.html**). Results are listed in Table S7.

Biochemical Experiments: Immune Precipitation and Pull-down

Cells (PBMC or MelJuSo) were lysed for 30 min in 0.8% NP-40 lysis buffer containing 50 mM NaCl, 50 mM Tris-HCl pH8.0, 5 mM $MgCl_2$ and phosphatase inhibitors (Roche Diagnostics, EDTA free). Supernatant after spinning (10 min at max. speed) was incubated with GST- or GST-ARF7EP-coupled Glutathione Sepharose beads 4G (GE Healthcare) or with anti-ARF7EP-, anti-mRFP- and anti-HA-coated Protein G-Sepharose beads 4 Fast flow (GE Healthcare) for one hour. Beads were washed four times before addition of Laemmli Sample Buffer followed by 5 min incubation at 100°C. Detection of co-immune-precipitated proteins was done via SDS-PAGE followed by western blotting and probing with respective antibodies to visualize proteins.

Biochemical Experiments: Immune Fluorescence

imDC were seeded on µ-Slide 18-well plates (Ibidi) pre-coated with 20 µg/ml Fibronectin (Invitrogen) and incubated for seven hours, fixed with 3.7% Formaldehyde in PBS or methanol and stained for MHC class II, Arl14/Arf7 and B-Actin. MelJuSo cells were transfected using FuGENE 6 (Roche Diagnostics) with DNA coding for Arl14/Arf7-mCherry and GFP-PIP5K1A followed by fixation with 3.7% formaldehyde in PBS two days post-transfection and staining for MHC class II.

Biochemical Experiments: GEF Assay

Ten µM GST-ARF6, GST-ARL14 or GST in loading buffer (1 mM EDTA, 4 mM $MgCl_2$, 50 mM HEPES pH7.6, 1 mM DTT) were incubated with 100 µM MBP-SEC7 domain of CYTH1 or PSD4 in loading buffer. Then, 3.3 µM) [α-32P]GTP (>5000 Ci/mmol) was added and incubated at 30°C for 20 min. The reactions were stopped by adding 500 µl cold stop buffer (100 mM NaCl, 10 mM $MgCl_2$, 20 mM HEPES pH7.6) and 20 µl Glutathione beads. The beads were washed five times with stop buffer to remove unbound [α-32P] GTP and measured by liquid scintillation counting. Free GST was taken as background and subtracted from all measurement values.

Biochemical Experiments: Lipid Binding Assay

HEK293T cells transiently overexpressing GST-PH-PH (PSD4) were harvested in 0.1% NP-40 lysis buffer, containing 50 mM Tris-Cl (pH7.4), 100 mM NaCl, 5 mM $MgCl_2$ and protease inhibitors. Cells were frozen at -80°C and thawed again followed by sonication. Lysis was extended for 45 min at 4°C. The supernatant after centrifugation was added to Glutathione Sepharose beads 4B to isolate GST-PH-PH (PSD4) from the lysate. Beads were washed two times, GST-PH-PH (PSD4) was eluted from beads using 100 mM Glutathione and used for the Lipid Binding assay.

PIP-StripsTM (tebu-bio) were blocked in PBS containing 3% fatty acid free BSA (Sigma # A-7030). The PIP-Strip was incubated with GST-PH-PH (PSD4) and the positive control (PLC-δ1 PH domain, PI(4,5)P_2 GRIPTM, tebu-bio) overnight. Binding to phosphoinositides was visualized by incubation with anti-GST antibody (B-14, Sc138 from Santa Cruz).

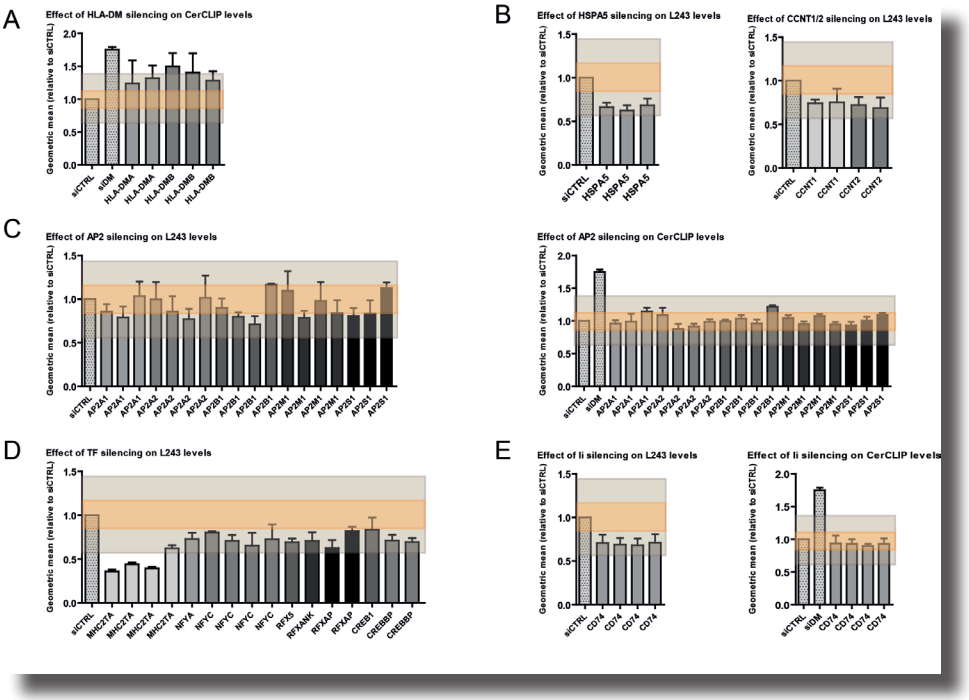

Figure S1 | Deconvolution of Genes known to affect the MHC Class II Pathway. Relates to Figure 2 (Chapter 1)
This figure explains the absence of genes known to be involved in the MHC class II pathway from our candidate list. Orange box: |z-score|<1; gray box: |z|<3. Representative, non-toxic siRNA duplexes are shown.
A | HLA-DM consists of an α and β chain and acts as a chaperone for MHC class II loading. While HLA-DMB showed a significant effect, HLA-DMA did not. For HLA-DMB, three siRNA duplexes show upregulation of CerCLIP labelling, two of which by a |z|>3 (our threshold). When silencing HLA-DMA only two duplexes gave an effect just below our threshold.
B | Some siRNA duplexes against HSPA5 (BiP, a chaperone in the ER that binds newly synthesized MHC class II) or CCNT1/CCNT2 (Cyclin T1/T2, both components of the transcriptional elongation complex PTEFb, which binds CIITA to turn on MHC class II transcription) showed a decrease in L243, but their effect was below the threshold.
C | Subunits of AP2 (Adaptor Protein 2 complex which is involved in the trafficking of MHC class II molecules) were not identified in the screen because silencing of individual subunits does not influence L243 or CerCLIP levels.
D | CIITA showed a pronounced effect, but the other factors involved in MHC class II transcription like NFY, RFX and CREB did not. As the deconvolution shows, silencing of these genes decreases L243 levels, but only with a z-score below our threshold of |z|>3.
E | Invariant chain (CD74) silencing also decreased L243 levels, but again below the threshold. No effect on CerCLIP levels was found.

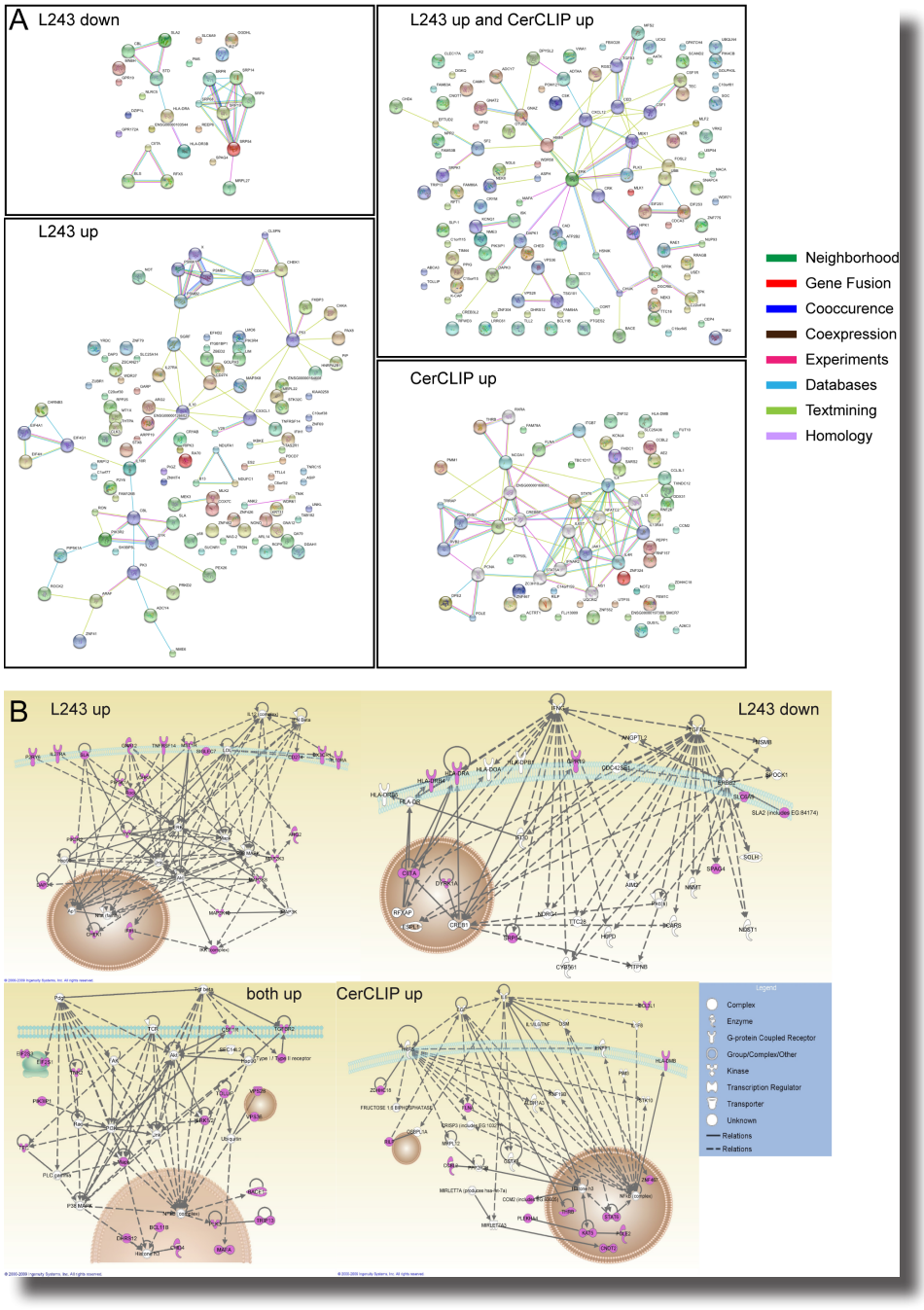

Figure S2 | Pathway Analysis of Targets grouped according to the Effects observed in the Primary Screen. Relates to Figure 2 (Chapter 1)

The 276 targets were grouped according to their effect on MHC class II at the cell surface. These four clusters (L243 up, L243 down, CerCLIP up and L243/CerCLIP up) were analyzed using the open source database and network program String (A) and the Ingenuity Pathways Analysis (IPA) program (B), resulting in networks summarized in this figure. Candidates identified in the screen are highlighted in pink in IPA-derived networks.

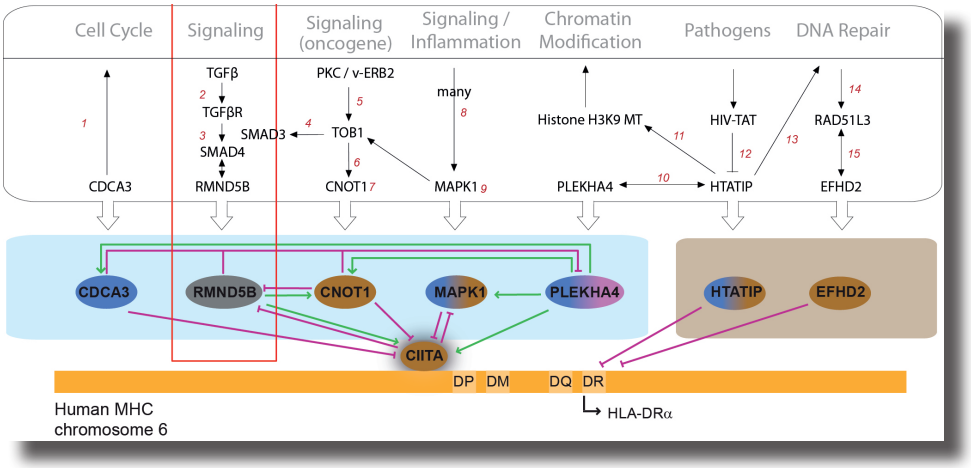

Figure S3 | Higher Order Control of the transcriptional Network. Relates to Figure 3 (Chapter 1)
Based on literature and experimental data (red box), factors interacting with candidates involved in transcriptional control and pathways were annotated in more general terms. Numbers correspond to Supplemental References [1-15].

A

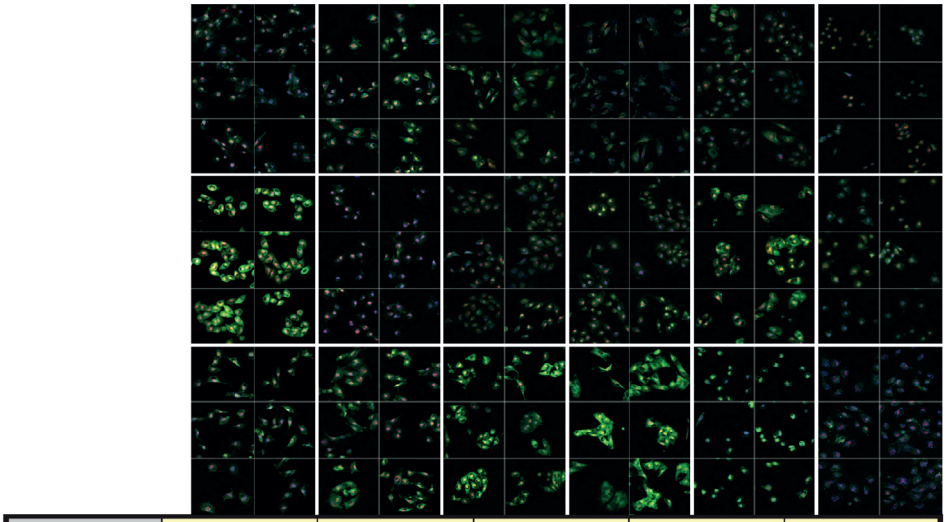

neg. control	HLA-DMB	THTPA	LOC403313	CHKA	DAPK3
pos. control	ASP	CAMK1	CDC2L5	PLK3	CSF1R
MAP3K11	MAP3K12	MAP3K14	MAP3K9	MAP4K1	MAPK1

B

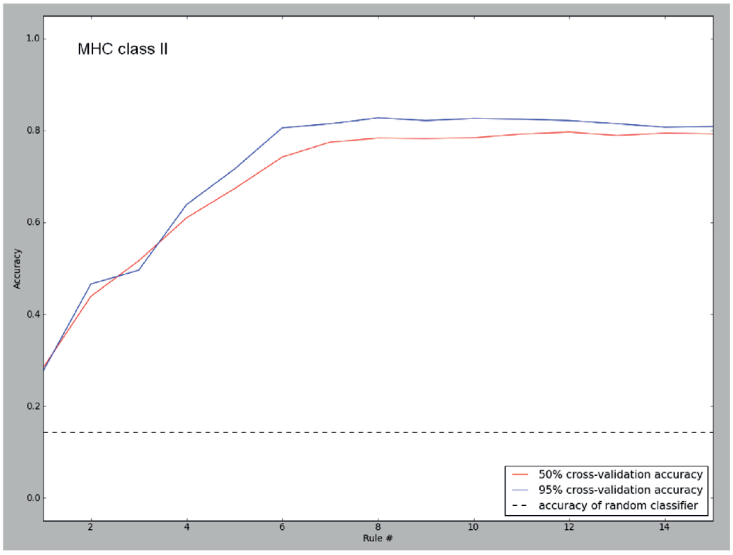

Figure S4 | Confocal Microscopy Image Analysis and 'Supervised Machine Learning'. Relates to Figure 4

A | MelJuSo/HLA-DRB1-GFP (green)/mCherry-GalT2 (red) cells were transfected with siRNAs silencing all 276 candidates and seeded on µ-Slide 18-well plates. After three days cells were stained for early endosomes (blue). On representative slide is shown. High resolution images of all slides can be found on ***http://www.neefjeslab.nl/****.*

B | Confocal images after gene silencing were analyzed by Cell Profiler. Prominent phenotypes were identified and the Cross-Validation Accuracy for MHC class II parameters after supervised machine learning in CP Analyst 2 was determined. Accuracy to distinguish defined phenotypes does not increase when more than six parameters are used.

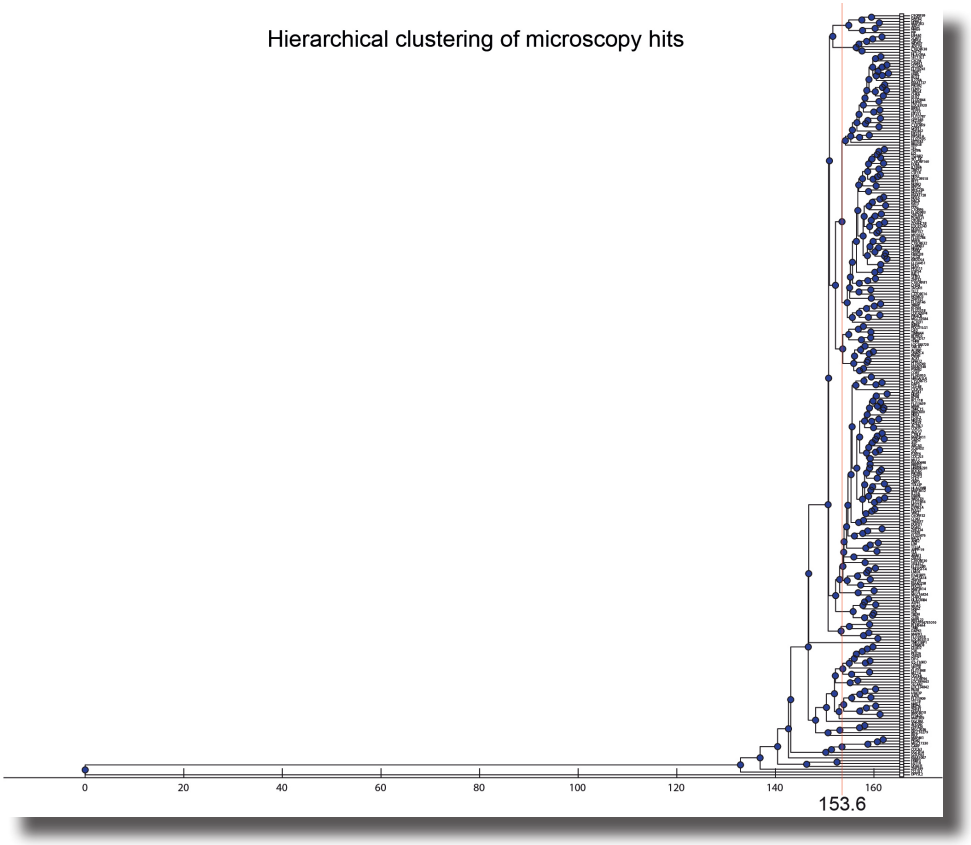

Figure S5 | Hierarchical Clustering of Microscopy Data. Relates to Figure 4C and 5 (Chapter 1)
The (dis)similarity between phenotypes upon knockdown of different genes is represented in this hierarchical clustering. A distance of 153.6 to the root of the tree was arbitrarily chosen as a cut-off value. Branches with more than 14 genes were used for further analysis (Figure 4C, Chapter 1).

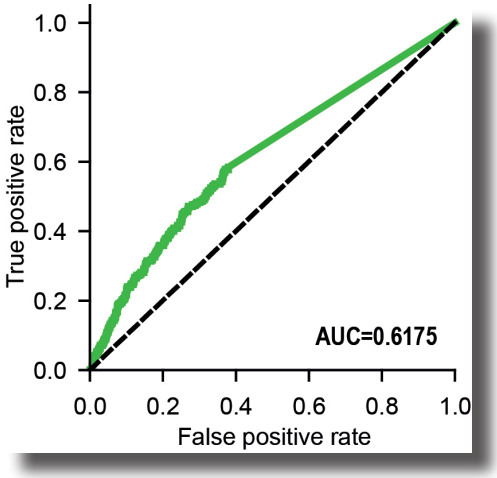

Figure S6 | The connectivity targets measured by the Area Under the Receiver Operating Characteristic (ROC) Curve (AUC) determined by program humannet v.1. Relates to Figure 5 (Chapter 1)
With an AUC of 0.6175 many of the connected genes (neighbours) are highly expected to interact in reality. Neighbours with a log-likelihood score ≥1 and a |z| ≥1.645 (p<0.1) in our original flow cytometry-based screen were considered for further analysis (Table S6).

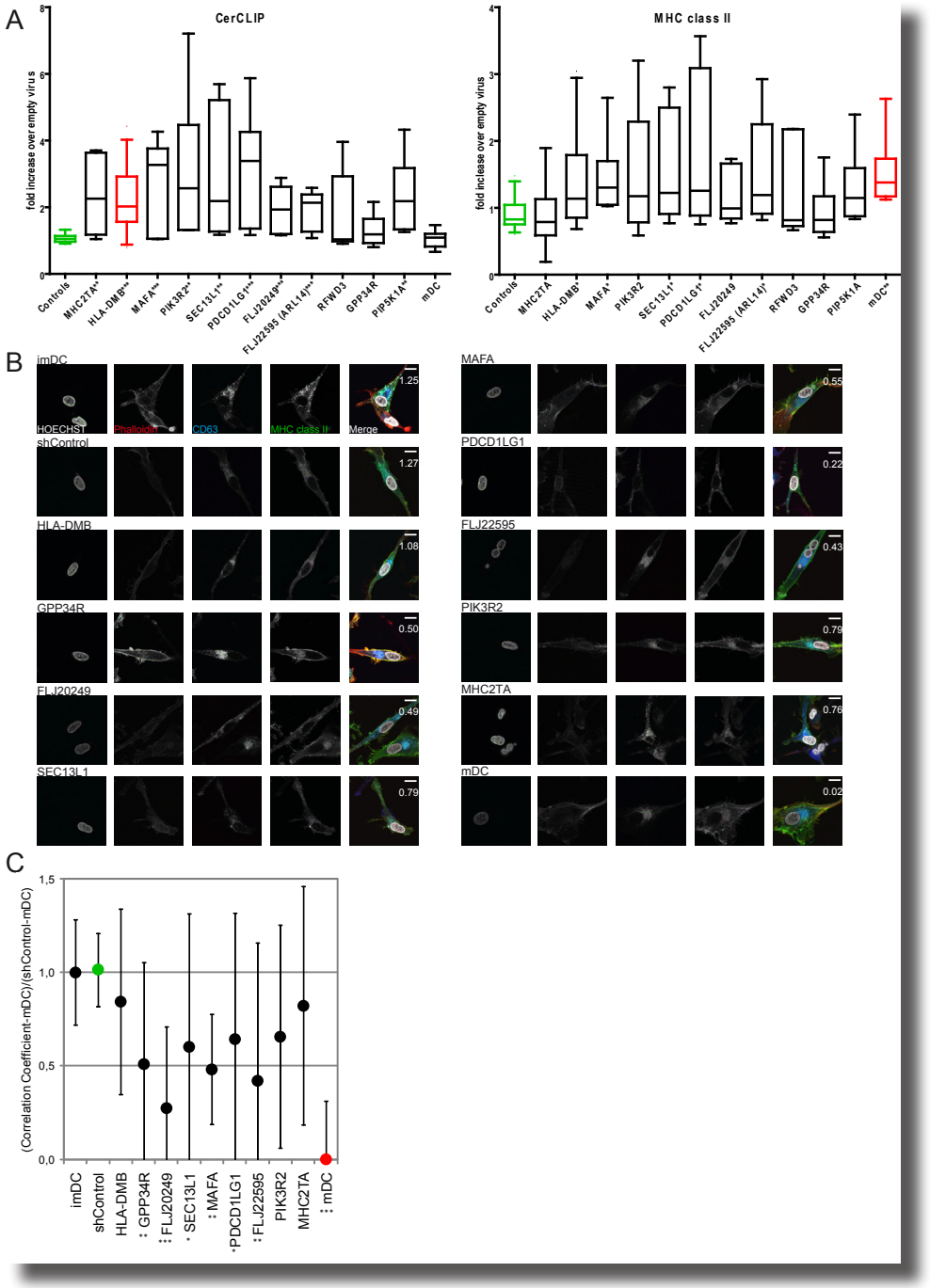

Figure S7 | Effect of selected Candidates on the Redistribution of MHC Class II in Dendritic Cells. Relates to Figure 6 (Chapter 1)

Monocytes were transduced with lentiviruses encoding shRNAs directed against seven candidate genes (four shRNA constructs per gene). After six days, imDCs generated from the transduced monocytes were analysed.

Supplemental Tables 1-7

available online at **http://dx.doi.org/doi:10.1016/j.cell.2011.03.023**

Table S1 | Expression of Candidates in human primary Immune Cells and Tissues, Relates to Figure 1 and 2 (Chapter 1)
mRNA of five different human primary immune cells (unstimulated and CD40L-activated B cells, primary monocytes, immature and mature monocyte-derived DC) was isolated and submitted to microarray analysis to investigate the expression levels of the candidates from the primary siRNA screen. The cells were characterized by flow cytometry for their lineage, MHC class II expression and activation status (data not shown). This table represents the average signal and the detection p-value of the microarray analysis. Probes for some of the hits were absent from the array as indicated at the bottom of the table. Gene expression data for 79 human tissues was retrieved from the GNF SymAtlas database. The detection signals are represented in this table divided into immune and non-immune tissues. The maxima for each group are determined and a ratio of 1.09 (as for CIITA) or higher is considered 'immune tissue-specific'. Sixty-nine hits fall into this group (highlighted in green).

Table S2 | Summary of the Results after Deconvolution, Relates to Figure 1 and 2 (Chapter 1)
The primary screen was performed using a pool of four siRNA duplexes per gene from a Dharmacon library. For deconvolution, the candidates were silenced using the four individual duplexes. This table summarizes the measured effects of each annotated siRNA pool and the number of duplexes confirming the phenotype in the pool of four siRNAs (for both L243 and CerCLIP, separately). The function and the cellular localization of the candidates were extracted from the Ingenuity Pathways Analysis program.

Table S3 | Description of Factors acting in a Transcriptional Network on the MHC Class II Locus identified by HTS qPCR, Relates to Figure 3 (Chapter 1)
Information based on published literature.

Table S4 | Summary of HTS Microscopy Results after Cell Profiler Calculation and CP Analyst 2 classification including mDC Phenotype Enrichment Score, Relates to Figure 4 (Chapter 1)
Six confocal microscopy pictures for each siRNA silencing situation were analyzed using Cell Profiler. After manual selection for prominent phenotypes and 'supervised machine learning', the most descriptive parameters for these phenotypes were determined. Per annotated gene, the values for the selected parameters used for clustering are listed in this table. Two bins were created in CPanalyst. One with wild type cells and one with cells resembling an mDC phenotype (MHC class II at the cell surface and little MHC class II inside). All cells for each candidate were scored for the presence of these two phenotypes. The p value for the mDC phenotype is indicated.

Table S5 | Gene Ontology Analysis of all our Candidate Genes. Relates to Figure 5 (Chapter 1)
The p value for 'cellular component' terms that are enriched in our dataset are given. The p values for 'cellular component' terms that are enriched in our dataset (extended with their neighbours) are given.

Table S6 | Genes connected to the Candidate Genes (Neighbours). Relates to Figure 5 (Chapter 1)
Humannet v. 1 was used to predict genes (Entrez Gene ID) that are likely to interact with candidate genes [16]. For each of the four clusters potentially interacting genes are indicated with the number 1. Each potentially interacting gene has at least a minimal absolute z-score of 1.645 (p=0.1) in the

Figure S7 | continued
A | Fold increase in CLIP-loaded MHC class II (CerCLIP) or general MHC II levels as detected by flow cytometry of three donors normalized to cells transduced with empty viral particles is shown. Four non-targeting shRNA sequences were used as shControl. HLA-DMB represents a positive control for the increase of CerCLIP, whereas L243 levels on mDCs can be considered as maximum. Shown is the 10-90 percentile with median value.
B | Representative images of all candidates silenced by lentiviral transduction of imDC, which confirmed their flow cytometry phenotype of MelJuSo cells in imDCs are shown. Confocal images stained for nucleus, actin (Phalloidin), CD63 and MHC class II were taken. The normalized correlation coefficient of CD63 and MHC class II is stated in the merged image (average of shControl treated DCs equals 1, average of mDCs equals 0). Bar = 10µm
C | The correlation between CD63 and MHC class II was quantified using Cell Profiler. Ten images were taken per construct per donor. Correlation coefficients were normalised to shControl treated cells. Mean of all donors ± s.e.m. is shown for one out of four constructs. The two controls (HLA-DMB and MHC2TA) show no significant effect, whereas all tested candidates (except PIK3R2) show a significant correlation towards a mature DC phenotype in their MHC class II distribution.
*A, C | * p<0.05, ** p<0.01, *** p<0.0001, Student's t test.*

genome wide flow cytometry screen for effects on L243 and/or CerCLIP.

Table S7 | Proteins binding to Arl14 as detected in Yeast Two-Hybrid Assay. Relates to Figure 7 (Chapter 1)

All different preys picked up in Yeast Two-Hybrid assay with constitutive Arl14 used as bait. C11orf46, shaded in green and called ARF7EP in this study, was picked up 10 times. Three other interacting proteins (yellow) were found only once. The false positive preys (promiscuous preys and fragments from the 3' UTR) are depicted in orange.

References

1. Xaus, J., et al., *The expression of MHC class II genes in macrophages is cell cycle dependent.* J Immunol, 2000. **165**(11): p. 6364-71.
2. Piskurich, J.F., et al., *Identification of distinct regions of 5' flanking DNA that mediate constitutive, IFN-gamma, STAT1, and TGF-beta-regulated expression of the class II transactivator gene.* J Immunol, 1998. **160**(1): p. 233-40.
3. Massague, J. and D. Wotton, *Transcriptional control by the TGF-beta/Smad signaling system.* EMBO J, 2000. **19**(8): p. 1745-54.
4. Xiong, B., et al., *Tob1 controls dorsal development of zebrafish embryos by antagonizing maternal beta-catenin transcriptional activity.* Dev Cell, 2006. **11**(2): p. 225-38.
5. Suzuki, T., et al., *Phosphorylation of three regulatory serines of Tob by Erk1 and Erk2 is required for Ras-mediated cell proliferation and transformation.* Genes Dev, 2002. **16**(11): p. 1356-70.
6. Miyasaka, T., et al., *Interaction of antiproliferative protein Tob with the CCR4-NOT deadenylase complex.* Cancer Sci, 2008. **99**(4): p. 755-61.
7. Rountree, M.R., K.E. Bachman, and S.B. Baylin, *DNMT1 binds HDAC2 and a new co-repressor, DMAP1, to form a complex at replication foci.* Nat Genet, 2000. **25**(3): p. 269-77.
8. Kyriakis, J.M. and J. Avruch, *Mammalian mitogen-activated protein kinase signal transduction pathways activated by stress and inflammation.* Physiol Rev, 2001. **81**(2): p. 807-69.
9. Yao, Y., et al., *ERK and p38 MAPK signaling pathways negatively regulate CIITA gene expression in dendritic cells and macrophages.* J Immunol, 2006. **177**(1): p. 70-6.
10. Stelzl, U., et al., *A human protein-protein interaction network: a resource for annotating the proteome.* Cell, 2005. **122**(6): p. 957-68.
11. Sapountzi, V., I.R. Logan, and C.N. Robson, *Cellular functions of TIP60.* Int J Biochem Cell Biol, 2006. **38**(9): p. 1496-509.
12. Creaven, M., et al., *Control of the histone-acetyltransferase activity of Tip60 by the HIV-1 transactivator protein, Tat.* Biochemistry, 1999. **38**(27): p. 8826-30.
13. Hejna, J., et al., *Tip60 is required for DNA interstrand cross-link repair in the Fanconi anemia pathway.* J Biol Chem, 2008. **283**(15): p. 9844-51.
14. French, C.A., C.E. Tambini, and J. Thacker, *Identification of functional domains in the RAD51L2 (RAD51C) protein and its requirement for gene conversion.* J Biol Chem, 2003. **278**(46): p. 45445-50.

15. Martin, V., et al., *Sws1 is a conserved regulator of homologous recombination in eukaryotic cells.* EMBO J, 2006. **25**(11): p. 2564-74.
16. Kim, W.K., C. Krumpelman, and E.M. Marcotte, *Inferring mouse gene functions from genomic-scale data using a combined functional network/ classification strategy.* Genome Biol, 2008. **9 Suppl 1**: p. S5.
17. Johnson, J.P., et al., *Surface antigens of human melanoma cells defined by monoclonal antibodies. I. Biochemical characterization of two antigens found on cell lines and fresh tumors of diverse tissue origin.* Eur.J.Immunol., 1981. **11**(10): p. 825-831.
18. Wubbolts, R., et al., *Direct vesicular transport of MHC class II molecules from lysosomal structures to the cell surface.* J.Cell Biol., 1996. **135**(3): p. 611-622.
19. Storrie, B., et al., *Recycling of golgi-resident glycosyltransferases through the ER reveals a novel pathway and provides an explanation for nocodazole-induced Golgi scattering.* J Cell Biol, 1998. **143**(6): p. 1505-1521.
20. Shaner, N.C., et al., *Improved monomeric red, orange and yellow fluorescent proteins derived from Discosoma sp. red fluorescent protein.* Nat Biotechnol, 2004. **22**(12): p. 1567-1572.
21. Dull, T., et al., *A third-generation lentivirus vector with a conditional packaging system.* J Virol, 1998. **72**(11): p. 8463-8471.
22. Divecha, N., et al., *Interaction of the type Ialpha PIPkinase with phospholipase D: a role for the local generation of phosphatidylinositol 4, 5-bisphosphate in the regulation of PLD2 activity.* EMBO J, 2000. **19**(20): p. 5440-5449.
23. Denzin, L.K., et al., *Assembly and intracellular transport of HLA-DM and correction of the class II antigen-processing defect in T2 cells.* Immunity, 1994. **1**(7): p. 595-606.
24. Lampson, L.A. and R. Levy, *Two populations of Ia-like molecules on a human B cell line.* J.Immunol., 1980. **125**(1): p. 293-299.
25. Vennegoor, C. and P. Rumke, *Circulating melanoma-associated antigen detected by monoclonal antibody NKI/C-3.* Cancer Immunol Immunother, 1986. **23**(2): p. 93-100.
26. Neefjes, J.J., et al., *The biosynthetic pathway of MHC class II but not class I molecules intersects the endocytic route.* Cell, 1990. **61**(1): p. 171-183.
27. Peters, P.J., et al., *Segregation of MHC class II molecules from MHC class I molecules in the Golgi complex for transport to lysosomal compartments.* Nature, 1991. **349**(6311): p. 669-676.
28. Rocha, N., et al., *Cholesterol sensor ORP1L contacts the ER protein VAP to control Rab7-RILP-p150 Glued and late endosome positioning.* J Cell Biol, 2009. **185**(7): p. 1209-1225.
29. Boutros, M., L.P. Bras, and W. Huber, *Analysis of cell-based RNAi screens.* Genome Biol., 2006. **7**(7): p. R66.
30. Ten Brinke, A., et al., *The clinical grade maturation cocktail monophosphoryl lipid A plus IFNgamma generates monocyte-derived dendritic cells with the capacity to migrate and induce Th1 polarization.* Vaccine, 2007. **25**(41): p. 7145-7152.
31. Souwer, Y., et al., *B cell receptor-mediated internalization of salmonella: a novel pathway for autonomous B cell activation and antibody production.* J Immunol, 2009. **182**(12): p. 7473-7481.
32. Jordens, I., et al., *The Rab7 effector protein RILP controls lysosomal transport by inducing the recruitment of dynein-dynactin motors.* Curr Biol, 2001. **11**(21): p. 1680-1685.
33. Carpenter, A., et al., *CellProfiler: image analysis software for identifying and quantifying cell phenotypes.* Genome Biology, 2006. **7**(10): p. R100.
34. Wang, X. and M. McManus, *Lentivirus production.* J Vis Exp, 2009(32).

Chapter 3

Routes to manipulate MHC Class II Antigen Presentation

van den Hoorn T*, Paul P*, Jongsma ML* and Neefjes J
* equal contribution

Current Opinion in Immunology, 2011 Feb;23(1):88-95

MHC class II molecules (MHC-II) present antigenic fragments acquired in the endocytic route to the immune system for recognition and activation of CD4+ T cells. This ignites a series of immune responses. MHC-II strongly correlates to most autoimmune diseases. Understanding the biology of MHC-II is therefore expected to translate into novel means of autoimmunity control or immune response improvement. Although the basic cell biology of MHC-II antigen presentation is well understood, many novel aspects have been uncovered in recent years including means of antigen delivery, preparation for MHC-II loading, transport processes and vaccination strategies. We will discuss past, present and future of these insights into the biology of MHC-II.

Introduction

Like all glycoproteins, MHC-II α- and β-chains are synthesized and assembled in the ER. Here they associate with Invariant Chain (Ii), which prevents premature binding of peptides to the MHC-II peptide-binding-groove and promotes exit from the ER and transport through the Golgi. The Ii contains a dileucine-based motif recognized by Adaptor Protein 2 (AP2) or AP3 complexes [1-3]. This motif is required for sorting at the Trans-Golgi-Network (TGN) and plasma membrane (PM) towards the MHC-II containing compartments (MIIC) [4-6] (pathway components discussed in this chapter are summarized in Figure 1). In the MIIC, residing proteases degrade antigens and Ii with the exception of a small fragment (called CLIP), protected by its embedding in the peptide-binding-groove of MHC-II. The CLIP fragment is exchanged for new (antigenic) peptides catalyzed by a unique and dedicated chaperone DM (H2-M in mice, HLA-DM in humans). DM is a MHC-II look-alike that interacts with MHC-II, stabilizing it in a state devoid of peptides, which would otherwise be prone to aggregation and degradation [7]. The peptide exchange reaction is stimulated by acidic pH and occurs in subdomains of the MIIC [8].

Probably, the MIIC does not have a 'Quality Control System' like the ER that allows exit of properly folded and assembled proteins only. The expression of MHC-II/CLIP complexes at the PM in the absence of DM illustrates this point. The MIIC moves to the PM for surface deposition of MHC-II, most likely after a certain intracellular residency time. In addition, MHC-II-bearing exosomes might be released conveying immunological information beyond the initial antigen presenting cell (APC).

The biology of antigen presentation by MHC-II has been studied for over 20 years by many groups and has yielded a fairly consistent view on the molecular basis underlying the successful acquisition of peptide fragments in the endocytic pathway for presentation at the PM. In general terms, assembly of MHC-II, their preparation for peptide loading, the generation of peptide fragments and transport processes are understood at almost atomic resolution. Yet many new findings complicate the initially simple biology. We will describe the state-of-art understanding based on recent insights. We will follow the general route of MHC-II from its birth in the endoplasmic reticulum (ER), through the endosomal pathway to the PM, exosomes and to their degradation. Along this path, we will not only describe new biological findings but also their application as new tools to manipulate MHC-II antigen presentation.

Delivery of Antigens to MIIC

Uptake of exogenous antigens can occur via several routes, reviewed by [9]. Each immune cell type has found its own one. B cells are poorly phagocytic, but they can take up IgM-coated Salmonella in a B cell receptor (BCR)-mediated pathway for antigen presentation in context of MHC-II [10]. The effectiveness of antigen presentation in dendritic cells (DC) depends on the cells' origin, maturation-stimulus and route of antigen uptake. These observations aid the understanding of immune response initiation and designing of vaccination strategies using DC and activated monocytes [11].

Recently it has been shown that DC continue to accumulate antigens via DEC205-mediated endocytosis and FcγR-mediated phagocytosis even after maturation, the latter involving the PIP5K isoforms α and γ [12]. Freshly synthesized or recycled MHC-II is loaded with the newly acquired antigens [13]. Endocytosis of DEC205 antibody-coupled peptides results in efficient uptake and delivery to the MIIC. This strategy has been applied to DC of melanoma patients resulting in effective peptide presentation. The stimulatory capacity of those DC was maintained after cryopreservation, which makes it an interesting approach for cancer immune therapy [14]. Antigen acquisition targeting Ig, Fc, complement or lectin receptors appears to be a feasible strategy to improve MHC-II antigen presentation and immune response outcome.

How cytosolic antigens reach MHC-II and why, although abundant, they only represent a minor fraction of all presented peptides (MHC ligand database; **http://www.syfpeithi.de**) [15], was unclear for a long time. Autophagy is a cell biological solution for the entry of cytosolic material into the lysosome. Membranes form and encapsulate parts of the cytosol forming autophagosomes, a process requiring ATG5 [16]. As reviewed by Nedjic and

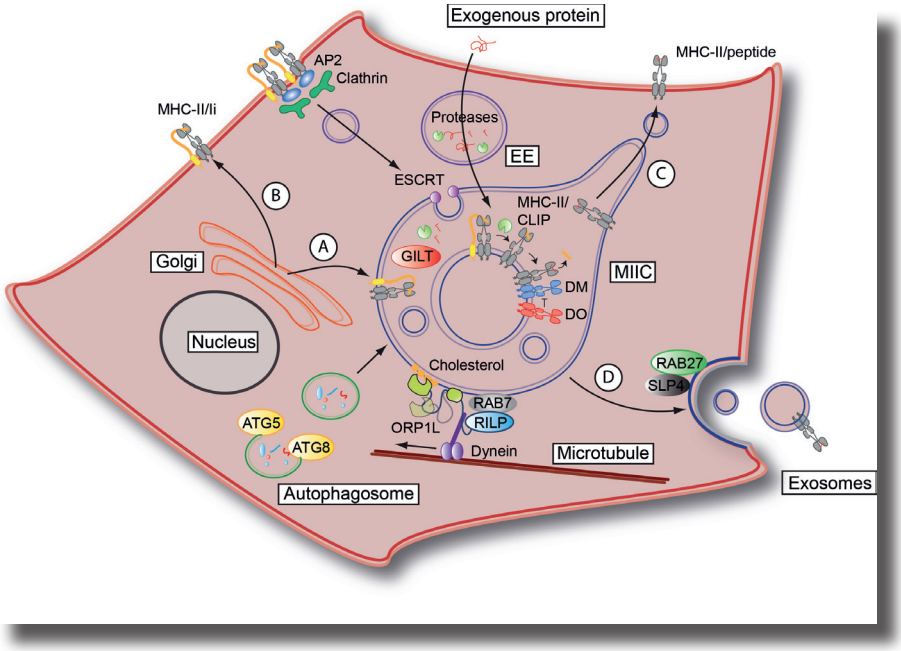

Figure 1 | The Transport Route of MHC Class II

After Ii binding in the ER, MHC-II is transported to the MIIC either directly (A) or via the PM (B) due to a dileucin motif in the associated Ii. In the MIIC, the Ii is degraded and the remaining CLIP fragment is exchanged for a new peptide in a process chaperoned by DM. After loading MHC-II is transported to the PM (C) or secreted on exosomes (D). MHC-II, MHC class II molecule; Ii, Invariant chain; AP2, Adaptor Protein 2; GILT, Gamma-interferon-inducible lysosomal thiol reductase precursor; DM, HLA-DM; DO, HLA-DO; ESCRT, Endosomal Sorting Complex Required for Transport; ATG, Autophagy related; ORP1L, oxysterol-binding protein; RILP, Rab7-interacting lysosomal protein; SLP4, Synaptotagmin-like protein 4; EE, early endosome; MIIC, MHC-II containing compartment.

colleagues, cortical thymic epithelial cells contain many autophagosomes [17] generating an array of different peptides, thereby shaping the self-tolerant T cell repertoire, as became clear from studies in ATG5-/- thymi [18]. ATG5-/- DCs are defective in phagosome-to-lysosome fusion, thereby inhibiting processing and presentation of extracellular microbial antigens [19]. Particular proteins are more selectively targeted to the autophagosome when coupled to ATG8/LC3, which in turn enhances their MHC-II presentation rate [20].

Antigen Processing in the MIIC

Antigens have to be unfolded for efficient degradation and peptide formation. One recently identified endosomal protein (called GILT) oxidizes disulfide linkages found in many extracellular proteins [21] and is essential for the presentation of a series of antigens [22]. GILT activity can strongly enhance antigen presentation of a melanoma antigen [23]. Acidic pH and chaperones might participate in further unfolding before substrates are processed by resident proteases. Many of these are cysteine proteases of the cathepsin family and are involved in inflammation, autoimmunity and cancer (reviewed by [24] and [25]). Nowadays, various cathepsin inhibitors are tested in primary immune cells as tools for immune response modulation in autoimmune diseases (Table 1).

Manipulating Peptide Loading of MHC-II in the MIIC

DM can stably associate with a unique co-chaperone DO (H2-O in mice, HLA-DO in humans), which is fairly selectively expressed in immature B cells and certain DC types. DO is also an MHC-II look-alike and functions as a pH sensor that alters the pH optimum of DM-mediated peptide loading of MHC-II to more acidic conditions and thereby changes the peptide repertoire presented by MHC-II [26]. In fact, presentation of many peptides is prevented by DO yielding more MHC-II/CLIP expression at the PM. Consequently, T cell help for B cells is reduced when DO is expressed [27]. DO may skew the DM support of MHC-II peptide loading to late and more

acidic endosomes, which are preferentially accessed by antigens taken up by BCR-mediated endocytosis. It is believed that this is preventing autoimmune responses by controlling the activation of B cells present peptides corresponding to antigens taken up by the BCR [26]. Indeed, NOD mice (susceptible to develop Type 1 Diabetes) overexpressing DO present an altered self-peptide repertoire which prevents activation of diabetogenic T cells and hence diabetes onset. DO possibly shapes the overall MHC-II self-peptide repertoire to improve T cell tolerance [28].
Small molecules affecting peptide loading of MHC-II can be of interest for autoimmunity (inhibitors) or vaccines (accelerators). Amines like chloroquine are known to neutralize MIIC and inhibit peptide loading [29]. Protease inhibitors affect the degradation of Ii or antigen (Table 1). More recently, a family of compounds was described to accelerate MHC-II peptide loading *in vitro*, without the help of DM, and promote peptide binding in APC *in vivo* [30]. Altered Peptide Ligands (APLs) are built to be more protease resistant, to reach the MIIC more easily and to be presented more efficiently (for review [31]). Manipulating MHC-II function becomes a realistic option to direct immune responses.

A topological Problem: Retrofusion or Exosomes?

MIIC consist of a limiting (outer) membrane and luminal vesicles (LV). It is still under debate whether LV are a stable structure or dynamically form and disappear again through retrofusion with the limiting membrane. The subdomains of MIIC differ. The LV contain tetraspanin molecules, cholesterol and the lipid LBPA, while the limiting membrane concentrates molecules like the GTPase RAB7, LAMP and the cholesterol transporter ABCA1. MHC-II and DM are detected on both membranes. Studies have shown that the LV are their preferred site of interaction [8]. MHC-II/DM complexes might be stabilized through association with the tetraspanin web (made of CD63, CD82 and others) [32, 33]. The interaction of MHC-II and DM on LV has interesting consequences for pathogens in phagosomes, such as *Salmonella*. Phagosomes do not have LV and MHC-II located at their limiting membrane fails to acquire peptides due to lack of DM support, therefore allowing immune escape of intracellular bacteria [8].
The LV can be secreted to the extracellular environment as exosomes. Mass spectrometry analysis of protein and lipid content of purified B cell exosomes verifies their origin from LV of MIIC (albeit at a considerably higher resolution) [34, 35]. The turn-over of MIIC takes only hours, whereas the half-life of MHC-II (8-48 hours) [36] or CD63 (2 days) [37] is considerably longer implying that the proteins have to be recovered from the LV not to be lost through exosome secretion. To our opinion, exosomes are the result of inefficient retrofusion of the LV to the limiting membrane of MIIC before fusion with the PM. How the process of retrofusion occurs is unclear. Alternatively LV might be stable nanocomplexes that survive necrosis, like proteasome and ribosome, which can be easily detected in tissue culture medium and body fluids [38]. Nonetheless, exosomes can have interesting functions.

Function and Application of MHC-II-bearing Exosomes

Exosomes are shed by almost all cell types and differ in content accordingly (reviewed in [39]). Exosomes contain cytosol. How the cytosolic contents are selected, is unknown. Exosomes resemble their cell of origin's topology and expose proteins like MHC-I and -II, CD1, tetraspanins, costimulatory molecules and adhesion molecules, such as ICAM-1. In fact, MHC-II-bearing exosomes can be considered 'nano immune cells' and have been found to exert both immune stimulatory and regulatory functions in intercellular communication (Figure 2). When shed by DC, exosomes can present antigen in context of MHC-II to activated T cells or T cell lines directly [40] or indirectly to naïve T cells when recaptured by recipient APCs [41]. Such recapture requires binding to host membranes mediated by LFA-1 and its ligand

Table 1 | Recently developed Cathepsin Inhibitors and their Effects

Inhibitor	Target	Effect
ZRLR	Cathepsin B	Enhances presentation of Tetanus Toxin-C (TTC) fragment to T-cells [70].
CatG Inhibitor	Cathepsin G	Reduces processing of TTC and Hemagglutenin (HA) peptides and their presentation to CD4+ T-cells [71].
Suc-VPF	Cathepsin G	Reduces processing of TTC and Hemagglutenin (HA) peptides and their presentation to CD4+ T-cells [71].
Compound 47	Cathepsin S	Inhibits processing of invariant chain [72, 73].
CAA0225	Cathepsin L	Involved in degradation of autophagosomal membrane markers [74].

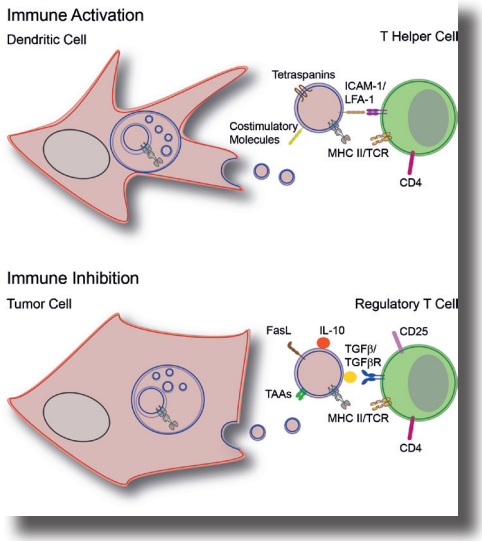

Figure 2 | Exosome Functions
Exosomes derived from dendritic cells can exert immune activating functions. Naïve T cells can be primed in an antigen-specific manner. Exosomes derived from tumor cells can exhibit immune regulatory functions by activating regulatory T cells. ICAM-1, intercellular adhesion molecule 1; LFA-1, lymphocyte function-associated antigen 1; TCR, T cell receptor; IL-10, interleukin-10; TGFβ, tumor growth factor β; TAA, tumor associated antigen

ICAM-1 on the exosome [42, 43]. Tumors are known to shed exosomes. Szajnik *et al.* have recently defined a new escape mechanism in cancer based on the activation of regulatory T cells (Tregs) in tumor patients [44]. Whether exosomes enter the recipient cells' MIIC for retrofusion, fuse with the PM or act as 'nano immune cells' is a fascinating subject and still unclear.

The immunogenetic potential of DC-derived exosomes has been demonstrated for vaccines against *Leishmania major* [45] and as cancer therapies *in vivo* in the past (reviewed in [46]). An alternative to the isolation of exosomes from patient-derived DCs might be the generation of artificial exosomes [47]. The advantage of exosome-based vaccines over other vaccination strategies remains to be proven in side by side comparative studies.

And out we go… MHC-II Transport to the Plasma Membrane

MHC-II is transported from the MIIC to the PM along microtubules in at least two different ways; 1. MIIC can move to the PM followed by fusion of the limiting membrane with the PM [48] 2. Tubules extend from MIIC towards the PM [49, 50], and vesicles may bud off to fuse with the PM [51]. This has been detected mainly in activated DC and not in other cell types. Close inspection of both routes shows that MIIC move in a bidirectional and stop-and-go manner by the activities of the dynein and kinesin motor proteins. Cholesterol, shown to influence MHC-II PM expression [52], controls the RAB7 effector ORP1L that controls RILP and the dynein motor. High cholesterol prevents the release of the dynein motor, inhibiting MIIC delivery to the PM [53]. How movement to the PM by kinesin motors is controlled, is unclear. Finally, MIIC have to fuse to the PM which probably requires the activity of RAB27A and its effector SLP4. This is directly correlated to the secretion of exosomes in HeLa cells [54]. Sorting of MHC-II to exosomes was shown to be ubiquitination-independent. Forced ubiquitination of MHC-II induces a decrease of MHC-II at the PM, but no enrichment on exosomes [55]. In the study of Buschow *et al.* it was shown that coculturing of DC with cognate T cells induced DC activation and exosome secretion independent of ubiquitination [56]. Although parts of MHC-II transport control are understood in detail, regulation of most other steps remains obscure and may be uncovered in the coming years.

Finally at the PM; Internalization and Recycling

It has been known for some time that the half-life of MHC-II at the PM is cell type dependent. When MHC-II associated to Ii arrives at the PM, they are internalized because of the dileucine motif in the Ii [57]. MHC-II, devoid of Ii, does not contain such internalization motifs and remains at the PM. Still, MHC-II has a longer lifespan on B cells than on monocytes, which is even further reduced following IL-10 exposure [36]. IL-10 upregulates a ubiquitin ligase called MARCH1, which modifies MHC-II and reduces its half-life [58]. The downregulation of MARCH1 expression in mature DC compared to immature DC corresponds to an increase in MHC-II half-life at the PM of the former [59] (Figure 3). Viruses and bacteria can use the ubiquitination machinery to manipulate MHC expression [60].

Salmonella typhimurium inhibits PM expression of MHC-II in DCs by ubiquitinating the HLA-DRβ chain using bacterial type III secretion system effectors rather than MARCH1 to directly modify HLA-DRβ [61-63]. HIV-Nef affects MHC-II expression and peptide loading by a different mechanism. The Nef protein triggers MHC-II internalization in a cholesterol dependent and clathrin- and dynamin-independent manner [64], but the exact details are unknown.

Upon internalization MHC-II has two options: 1. return to the PM prior to or after peptide exchange or 2. become degraded. In recycling endosomes, MHC-II can be loaded with new peptides in a DM-dependent [65] or independent manner [66] and transported back to the PM. This process involves at least ARF6, RAB35 and EHD1 [67]. Uptake of antigens in early endosomal compartments (that are relatively poor in proteases [68]) will allow presentation of other peptides than those generated in MIIC, hence broadening the peptide repertoire for the good or bad, which is unpredictable. Where MHC-II ends-up, when recycling fails, remains unclear. The reductase GILT (breaking disulfide bonds in the Ig domains of MHC-II) and cathepsins, such as cathepsin G, which degrades the MHC-II β-chain *in vitro* [69], might be involved. How the life of MHC-II is exactly terminated, however, remains an open question. Clearly, MHC-II is a cannibal presenting fragments of its deceased brothers or sisters. In fact, such MHC-II derived peptides are major constituents of the MHC-II peptide repertoire.

Conclusion

The cell biology of MHC-II has been studied for over two decades starting with the work of Unanue et al., who demonstrated inhibition of antigen presentation by chloroquine [29]. Since then many steps have been solved at the cell biological and atomic level. MHC-II antigen presentation comprises of processes like transport via various endosomal compartments, synthesis, ubiquitination and degradation. The routes of MHC-II involve many targets for manipulation to affect MHC-II expression and peptide loading, which is relevant for disease states like autoimmunity, infection and cancer.

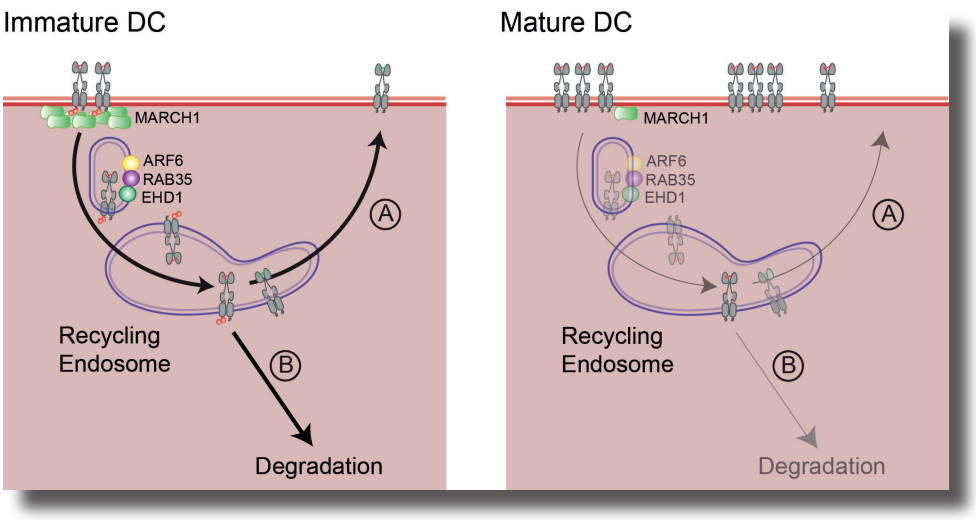

Figure 3 | MHC Class II Internalization, Recycling and Degradation
At the PM of immature DC, MHC-II can be ubiquitinated by MARCH1 and is transported via ARF6/RAB35/EHD1-positive tubular structures towards Recycling Endosomes (RE). After internalization, MHC-II may return to the PM (A) or proceed to degradation (B). In mature DC, MARCH1 expression is downregulated, resulting in decreased internalization, a long cell surface half-life and elongated presentation of antigen. PM, plasma membrane

References

- • of special interest
- •• of outstanding interest

1. Dugast, M., et al., *AP2 clathrin adaptor complex, but not AP1, controls the access of the major histocompatibility complex (MHC) class II to endosomes.* J Biol Chem, 2005. **280**(20): p. 19656-19664.
2. Gupta, S.N., et al., *Re-routing of the invariant chain to the direct sorting pathway by introduction of an AP3-binding motif from LIMP II.* Eur J Cell Biol, 2006. **85**(6): p. 457-467.
3. McCormick, P.J., J.A. Martina, and J.S. Bonifacino, *Involvement of clathrin and AP-2 in the trafficking of MHC class II molecules to antigen-processing compartments.* Proc Natl Acad Sci U S A, 2005. **102**(22): p. 7910-7915.
4. Neefjes, J.J., et al., *The biosynthetic pathway of MHC class II but not class I molecules intersects the endocytic route.* Cell, 1990. **61**(1): p. 171-183.
5. Peters, P.J., et al., *Segregation of MHC class II molecules from MHC class I molecules in the Golgi complex for transport to lysosomal compartments.* Nature, 1991. **349**(6311): p. 669-676.
6. Roche, P.A. and P. Cresswell, *Invariant chain association with HLA-DR molecules inhibits immunogenic peptide binding.* Nature, 1990. **345**(6276): p. 615-618.
7. Kropshofer, H., et al., *Editing of the HLA-DR-peptide repertoire by HLA-DM.* EMBO J, 1996. **15**(22): p. 6144-6154.
8. Zwart, W., et al., *Spatial separation of HLA-DM/HLA-DR interactions within MIIC and phagosome-induced immune escape.* Immunity, 2005. **22**(2): p. 221-233.
9. Burgdorf, S. and C. Kurts, *Endocytosis mechanisms and the cell biology of antigen presentation.* Curr.Opin.Immunol., 2008. **20**(1): p. 89-95.
10. Souwer, Y., et al., *B cell receptor-mediated internalization of salmonella: a novel pathway for autonomous B cell activation and antibody production.* J Immunol, 2009. **182**(12): p. 7473-7481.
11. Kamphorst, A.O., et al., *Route of antigen uptake differentially impacts presentation by dendritic cells and activated monocytes.* J Immunol, 2010. **185**(6):p. 3426-3435.

•• An extensive and thorough investigation of antigen processing and presentation capacities of differentially activated APC is presented here. The influence of various maturation stimuli on MHC-I and MHC-II antigen presentation is shown *in vivo.*

12. Mao, Y.S., et al., *Essential and unique roles of PIP5K-gamma and -alpha in Fcgamma receptor-mediated phagocytosis.* J Cell Biol, 2009. **184**(2): p. 281-296.
13. Platt, C.D., et al., Mature dendritic cells use endocytic receptors to capture and present antigens. Proc Natl Acad Sci U S A, 2010. 107(9): p. 4287-4292.

• Antigen uptake via DEC205-mediated-endocytosis and FcγR-mediated-phagocytosis remains efficient in mature DC. The acquired antigens are loaded onto a small pool of newly synthesized or recycled MHC-II

14. Birkholz, K., et al., Targeting of DEC-205 on human dendritic cells results in efficient MHC class II-restricted antigen presentation. Blood, 2010. 116(13): p. 2277-2285.

•• Endocytosis receptor DEC205 can deliver helper-epitopes to human monocyte-derived DC when coupled to an anti-DEC205 antibody. This results in effective MHC-II restricted antigen presentation in DC. This is a promising strategy for antigen-delivery for the immune therapy of various diseases.

15. Rammensee, H., et al., *SYFPEITHI: database for MHC ligands and peptide motifs.* Immunogenetics, 1999. **50**(3-4): p. 213-219.
16. Mizushima, N., et al., *Dissection of autophagosome formation using Apg5-deficient mouse embryonic stem cells.* J Cell Biol, 2001. **152**(4): p. 657-668.
17. Nedjic, J., et al., *Macroautophagy, endogenous MHC II loading and T cell selection: the benefits of breaking the rules.* Curr Opin Immunol, 2009. **21**(1): p. 92-97.
18. Nedjic, J., et al., Autophagy in thymic epithelium shapes the T-cell repertoire and is essential for tolerance. Nature, 2008. 455(7211):p. 396-400.

• Thymic epithelial cells, displaying MHC ligands for positive T cell selection, contain a high number of autophagosomes. An *in vivo* study of the MHC-II-restricted T cell receptor repertoire in mice with ATG5-deficient thymus revealed that autophagy supports positive T cell selection and tolerance induction.

19. Lee, H.K., et al., *In vivo requirement for Atg5 in antigen presentation by dendritic cells.* Immunity, 2010. **32**(2): p. 227-239.

• In mice, ATG5-/- DC are impaired in priming CD4+ T cells after Herpes Simplex virus infection. ATG5 not only functions in processing cytosolic antigens, but is also required for the processing and subsequent presentation of MHC-II peptides derived from phagocytosed microbial antigens.

20. Gannage, M. and C. Munz, *Monitoring macroautophagy by major histocompatibility complex class II presentation of targeted antigens.*

Methods Enzymol, 2009. **452**: p. 403-421.
21. Singh, R. and P. Cresswell, *Defective cross-presentation of viral antigens in GILT-free mice.* Science, 2010. **328**(5984): p. 1394-1398.
22. Arunachalam, B., et al., *Enzymatic reduction of disulfide bonds in lysosomes: characterization of a gamma-interferon-inducible lysosomal thiol reductase (GILT).* Proc Natl Acad Sci U S A, 2000. **97**(2): p. 745-750.
23. Rausch, M.P., et al., *GILT accelerates autoimmunity to the melanoma antigen tyrosinase-related protein 1.* J Immunol, 2010. **185**(5): p. 2828-2835.
24. Chapman, H.A., *Endosomal proteases in antigen presentation.* Curr Opin Immunol, 2006. **18**(1): p. 78-84.
25. Conus, S. and H.U. Simon, *Cathepsins and their involvement in immune responses.* Swiss Med Wkly, 2010. **140**: p. w13042.
• This review summarizes the role of cathepsins in innate and adaptive immunity. Furthermore, the involvement of cathepsins in the pathogenesis of (autoimmune) diseases is discussed.
26. van Ham, M., et al., *Modulation of the major histocompatibility complex class II-associated peptide repertoire by human histocompatibility leukocyte antigen (HLA)-DO.* J Exp Med, 2000. **191**(7): p. 1127-1136.
27. Draghi, N.A. and L.K. Denzin, *H2-O, a MHC class II-like protein, sets a threshold for B-cell entry into germinal centers.* Proc Natl Acad Sci U S A, 2010. **107**(38): p. 16607-16612.
28. Yi, W., et al., *Targeted regulation of self-peptide presentation prevents type I diabetes in mice without disrupting general immunocompetence.* J Clin Invest, 2010. **120**(4): p. 1324-1336.
29. Ziegler, H.K. and E.R. Unanue, *Decrease in macrophage antigen catabolism caused by ammonia and chloroquine is associated with inhibition of antigen presentation to T cells.* Proc. Natl.Acad.Sci.U S A, 1982. **79**(1): p. 175-178.
30. Call, M.J., et al., *In vivo enhancement of peptide display by MHC class II molecules with small molecule catalysts of peptide exchange.* J Immunol, 2009. **182**(10): p. 6342-6352.
31. Burster, T. and B.O. Boehm, *Processing and presentation of (pro)-insulin in the MHC class II pathway: the generation of antigen-based immunomodulators in the context of type 1 diabetes mellitus.* Diabetes Metab Res Rev, 2010. **26**(4): p. 227-238.
32. Hammond, C., et al., *The tetraspan protein CD82 is a resident of MHC class II compartments where it associates with HLA-DR, -DM, and -DO molecules.* J Immunol, 1998. **161**(7): p. 3282-3291.
33. Escola, J.M., et al., *Characterization of a lysozyme-major histocompatibility complex class II molecule-loading compartment as a specialized recycling endosome in murine B lymphocytes.* J Biol Chem, 1996. **271**(44): p. 27360-27365.
34. Wubbolts, R., et al., *Proteomic and biochemical analyses of human B cell-derived exosomes. Potential implications for their function and multivesicular body formation.* J Biol Chem, 2003. **278**(13): p. 10963-10972.
35. Buschow, S.I., et al., *MHC class II-associated proteins in B-cell exosomes and potential functional implications for exosome biogenesis.* Immunol Cell Biol, 2010.
36. Koppelman, B., et al., *Interleukin-10 down-regulates MHC class II alphabeta peptide complexes at the plasma membrane of monocytes by affecting arrival and recycling.* Immunity, 1997. **7**(6): p. 861-871.
37. Engering, A., et al., *Differential post-translational modification of CD63 molecules during maturation of human dendritic cells.* Eur J Biochem, 2003. **270**(11): p. 2412-2420.
38. Deutsch, E.W., et al., *Human Plasma PeptideAtlas.* Proteomics, 2005. **5**(13): p. 3497-3500.
39. Simpson, R.J., et al., *Exosomes: proteomic insights and diagnostic potential.* Expert Rev Proteomics, 2009. **6**(3): p. 267-283.
40. Arnold, P.Y. and M.D. Mannie, *Vesicles bearing MHC class II molecules mediate transfer of antigen from antigen-presenting cells to CD4+ T cells.* Eur J Immunol, 1999. **29**(4): p. 1363-1373.
41. Thery, C., et al., *Indirect activation of naive CD4+ T cells by dendritic cell-derived exosomes.* Nat Immunol, 2002. **3**(12): p. 1156-1162.
42. Nolte-'t Hoen, E.N., et al., *Activated T cells recruit exosomes secreted by dendritic cells via LFA-1.* Blood, 2009. **113**(9): p. 1977-1981.
43. Segura, E., et al., *CD8+ dendritic cells use LFA-1 to capture MHC-peptide complexes from exosomes in vivo.* J Immunol, 2007. **179**(3): p. 1489-1496.
44. Szajnik, M., et al., Tumor-derived microvesicles induce, expand and up-regulate biological activities of human regulatory T cells (Treg). PLoS One, 2010. 5(7): p. e11469.
• This study shows that upon coculture of CD4+ T cells with tumor-derived exosomes Tregs could be generated, which exhibited suppressor functions.
45. Schnitzer, J.K., et al., *Fragments of antigen-loaded dendritic cells (DC) and DC-derived exosomes induce protective immunity against Leishmania major.* Vaccine, 2010. **28**(36): p. 5785-5793.
46. Thery, C., M. Ostrowski, and E. Segura, Membrane vesicles as conveyors of immune responses. Nat Rev Immunol, 2009. 9(8):p. 581-593.
• This comprehensive review provides a good overview on the biology of exosomes of all cellular origins. It describes their properties and various functions reported thus far *in vitro* as well as *in vivo*.
47. De La Pena, H., et al., *Artificial exosomes as tools for basic and clinical immunology.* J Immunol Methods, 2009. **344**(2): p. 121-132.
48. Wubbolts, R., et al., *Opposing motor activities of dynein and kinesin determine retention*

and transport of MHC class II-containing compartments. J.Cell Sci., 1999. **112 (Pt 6)**: p. 785-795.

49. Boes, M., et al., *T cells induce extended class II MHC compartments in dendritic cells in a Toll-like receptor-dependent manner.* J Immunol, 2003. **171**(8): p. 4081-4088.
50. Chow, A., et al., *Dendritic cell maturation triggers retrograde MHC class II transport from lysosomes to the plasma membrane.* Nature, 2002. **418**(6901): p. 988-994.
51. Kleijmeer, M., et al., *Reorganization of multivesicular bodies regulates MHC class II antigen presentation by dendritic cells.* J Cell Biol, 2001. **155**(1): p. 53-63.
52. Kuipers, H.F., et al., *Statins affect cell-surface expression of major histocompatibility complex class II molecules by disrupting cholesterol-containing microdomains.* Hum.Immunol., 2005. **66**(6): p. 653-665.
53. Rocha, N., et al., *Cholesterol sensor ORP1L contacts the ER protein VAP to control Rab7-RILP-p150 Glued and late endosome positioning.* J Cell Biol, 2009. **185**(7): p. 1209-1225.
54. Ostrowski, M., et al., Rab27a and Rab27b control different steps of the exosome secretion pathway. Nat Cell Biol, 2010. 12(1): p. 19-30.

•• This paper identifies five RAB proteins that inhibit exosome secretion when silenced in CIITA-expressing HeLa cells without affecting normal protein secretion. The phenotype after silencing two of these RABs (RAB27A and RAB27B) is characterized and effectors are identified.

55. Gauvreau, M.E., et al., *Sorting of MHC class II molecules into exosomes through a ubiquitin-independent pathway.* Traffic, 2009. **10**(10): p. 1518-1527.
56. Buschow, S.I., et al., MHC II in dendritic cells is targeted to lysosomes or T cell-induced exosomes via distinct multivesicular body pathways. Traffic, 2009. 10(10): p. 1528-1542.

• This study demonstrates that upon coculturing of a T cell line with DC the number of exosomes secreted by the DC increases along with the levels of MHC-II on the microvesicles. By using a mutant MHC-II molecule that cannot be ubiquitinated, they demonstrate that the transfer of MHC-II to exosomes is independent of ubiquitination.

57. Simonsen, A., et al., *The leucine-based motif DDQxxLI is recognized both for internalization and basolateral sorting of invariant chain in MDCK cells.* Eur J Cell Biol, 1998. **76**(1): p. 25-32.
58. Thibodeau, J., et al., Interleukin-10-induced MARCH1 mediates intracellular sequestration of MHC class II in monocytes. Eur J Immunol, 2008. 38(5): p. 1225-1230.

• Immunosuppressant IL-10 reduces MHC-II expression in human monocytes by upregulating the ubiquitin ligase MARCH1.

59. de Gassart, A., et al., *MHC class II stabilization at the surface of human dendritic cells is the result of maturation-dependent MARCH I down-regulation.* Proc Natl Acad Sci U S A, 2008. **105**(9): p. 3491-3496.
60. Nathan, J.A. and P.J. Lehner, *The trafficking and regulation of membrane receptors by the RING-CH ubiquitin E3 ligases.* Exp Cell Res, 2009. **315**(9): p. 1593-1600.
61. Mitchell, E.K., et al., *Inhibition of cell surface MHC class II expression by Salmonella.* Eur J Immunol, 2004. **34**(9): p. 2559-2567.
62. Cheminay, C., A. Mohlenbrink, and M. Hensel, *Intracellular Salmonella inhibit antigen presentation by dendritic cells.* J Immunol, 2005. **174**(5): p. 2892-2899.
63. Lapaque, N., et al., *The HLA-DRalpha chain is modified by polyubiquitination.* J Biol Chem, 2009. **284**(11): p. 7007-7016.
64. Chaudhry, A., et al., HIV-1 Nef promotes endocytosis of cell surface MHC class II molecules via a constitutive pathway. J Immunol, 2009. 183(4): p. 2415-2424.

• This study demonstrates the role of HIV-1Nef in delaying MHC-II transport to the PM in monocytes. At the same time the rate of MHC-II removal from the cell surface is increased. The data in this paper suggest that Nef activates the normal MHC-II endocytosis route to reduce MHC-II antigen presentation.

65. Pathak, S.S., J.D. Lich, and J.S. Blum, *Cutting edge: editing of recycling class II:peptide complexes by HLA-DM.* J Immunol, 2001. **167**(2): p. 632-635.
66. Sinnathamby, G. and L.C. Eisenlohr, *Presentation by recycling MHC class II molecules of an influenza hemagglutinin-derived epitope that is revealed in the early endosome by acidification.* J Immunol, 2003. **170**(7): p. 3504-3513.
67. Walseng, E., O. Bakke, and P.A. Roche, *Major histocompatibility complex class II-peptide complexes internalize using a clathrin- and dynamin-independent endocytosis pathway.* J Biol Chem, 2008. **283**(21): p. 14717-14727.
68. Fernandez-Borja, M., et al., *HLA-DM and MHC class II molecules co-distribute with peptidase-containing lysosomal subcompartments.* Int Immunol, 1996. **8**(5): p. 625-640.
69. Burster, T., et al., *Masking of a cathepsin G cleavage site in vivo contributes to the proteolytic resistance of major histocompatibility complex class II molecules.* Immunology, 2010. **130**(3): p. 436-446.
70. Reich, M., et al., *Specific cathepsin B inhibitor is cell-permeable and activates presentation of TTC in primary human dendritic cells.* Immunol Lett,

2009. **123**(2): p. 155-159.
71. Reich, M., et al., *Application of specific cell permeable cathepsin G inhibitors resulted in reduced antigen processing in primary dendritic cells.* Mol Immunol, 2009. **46**(15): p. 2994-2999.
72. Cai, J., et al., *6-Phenyl-1H-imidazo[4,5-c]pyridine-4-carbonitrile as cathepsin S inhibitors.* Bioorg Med Chem Lett, 2010. **20**(15): p. 4350-4354.
73. Cai, J., et al., *2-Phenyl-9H-purine-6-carbonitrile derivatives as selective cathepsin S inhibitors.* Bioorg Med Chem Lett, 2010. **20**(15): p. 4447-4450.
74. Takahashi, K., et al., *Characterization of CAA0225, a novel inhibitor specific for cathepsin L, as a probe for autophagic proteolysis.* Biol Pharm Bull, 2009. **32**(3): p. 475-479.

Chapter 4

Studying MHC Class II Transport in Dendritic Cells

Paul P and Neefjes J

Methods in Molecular Biology, 2012 (in press)

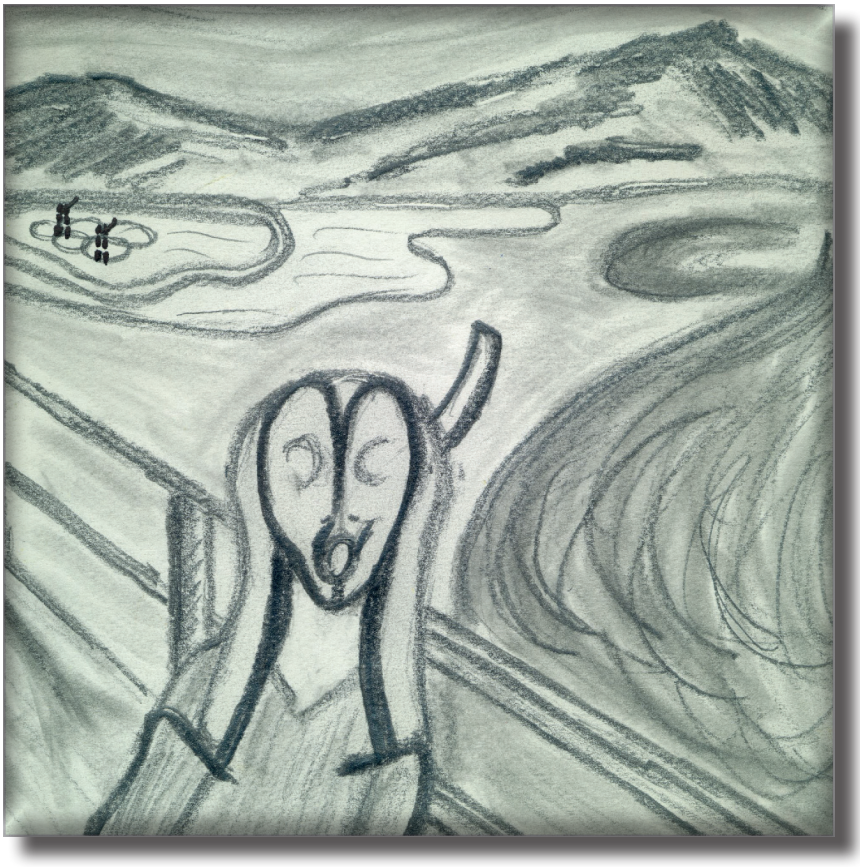

Professional antigen presenting cells, such as dendritic cells, are effective in activating T lymphocytes due to their unique ability to present antigens in the context of both MHC class I and II molecules. After successful loading with antigenic peptides MHC class II molecules traffic from the late endosomal loading compartment to the plasma membrane to exert their function of presenting peptides to T helper lymphocytes. Various processes play a role in this event, which are only partly understood to date. The following protocols demonstrate a strategy of how to integrate high throughput datasets to select candidates possibly involved in MHC class II transport for in depth studies. A combination of proteomics, RNAinterference and biochemical experimentation can uncover novel pathways regulating transport processes in primary dendritic cells.

1. Introduction

Dendritic cells (DC) are professional antigen presenting cells (APC) that regulate the adaptive immune response by stimulating naïve T cells (see [1] for review). Expression of peptide-loaded MHC class II molecules at the cell surface is the result of tightly regulated transport processes from late endosomal compartments (called MIIC [2-4]), where antigen loading takes place. For a detailed description of the MHC class II pathway see [5, 6]. In DC MHC class II transport to the cell surface is enhanced when danger signals are encountered [7, 8]. Various intracellular proteins have been associated with this process, such as iNOS and caspases [9]. The ubiquitin ligase MARCH1 modifies MHC class II in human immature DC (imDC) [10, 11], clathrin and AP2 orchestrate endocytosis [12], and cystatins regulate cathepsin activities [13]. Despite these findings, many open questions remain when it comes to the control of MHC class II transport in DC. For example, which motors are involved in MIIC transport? Little is known about this. Myosin II has been reported to interact with invariant chain (Ii) to control MHC class II transport in B cells [14]. Another actin-based motor, myosin 1E, has been recently implicated to be responsible for the positioning of MHC class II-positive vesicles in DC [15]. The dynein motor is recruited to MIIC via the small GTPase Rab7 [16].

One way of identifying new players in the MHC class II transport route is to select candidates following an RNAinterference (RNAi) screen and other high throughput cell biological assays. Gene knockdown is achieved by introducing small interfering RNA molecules (siRNA) or short hairpin RNA (shRNA) which are provided as either genome-wide or specialized libraries (kinases, phosphatases, G-protein coupled receptors, etc.). The resulting candidates can then be tested in smaller scale in primary DC. RNAi screens can be performed by microscopy as well as flow cytometry when appropriate antibodies are available. For a comparison of the two methods see Table 1. For the RNAi screen described here, changes in cell surface expression of MHC class II detected by flow cytometry serves as a primary read-out. In general, a robust read-out is essential. Negative and positive controls are required. See [17] for a review on tips and tricks of RNAi screening. Secondary screens may subsequently be used to cluster candidates into phenotypically similar pathways, which is essential for creating new biology.

Primary immune cells are often unsuitable for screening. They are limited in number, difficult to manipulate and prone to differentiate. Cell lines can serve as substitutes. For a list of MHC class II-positive cell lines see Table 2. For any of these cell lines, functionality and transfection efficiency need to be determined and optimized before large scale screening activities. In some cases activation with cytokines is required for efficient antigen processing and presentation.

Following the primary screen, microarray or deep sequencing studies on APCs provide information whether genes that influence MHC class II surface levels in cell lines are expressed in primary cells. The model cell line may be used for further high throughput (HT) experimentation: (1) Quantitative RT-PCR (qRT-PCR) following silencing of genes identified in the primary screen reveals whether the transcription rate of the MHC locus is altered. (2) Immunofluorescence and confocal microscopy provide vital information on alterations of the intracellular MHC class II distribution. The large

Table 1 | Characteristics of Flow Cytometry versus Microscopy

	Flow Cytometry	Microscopy
Readout	Intracellular or PM	Mainly intracellular
Analysis	Simple	Complex, software programs needed
Quantity	Many data points (cells)	Few data points
Detail	Little insight	Precise localization, many features detected

Table 2 | Possible Cell Lines for an MHC Class II-related RNAi Screen

Endogenous	Type	ATCC	Reference
MUTZ-3	Human		[25]
KG-1	Human	CCL-246	[26]
THP-1	Adherent, macrophage-like after stimulation with phorbol ester	TIB-202	[27]
LCL	Human Epstein Barr virus-transformed		Transformation protocol [28]
MelJuSo	Adherent human melanoma cell line		[29]
Ectopic	**Manipulation**	**ATCC**	**Reference**
RAW264.7	Adherent murine monocyte/macrophage cell line transfected with MHC class II	TIB-71	[30]
Fibroblasts	Transfected with MHC class II and Ii		[31]
HeLa	Transfected with CIITA	CCL-2	[32]

amount of images generated can be analyzed and clustered based on similarity using open software programs such as Cell Profiler and CP Analyst [18, 19]. To select candidates for in-depth follow-up studies, stringent criteria must be set. When addressing the question of what regulates MHC class II transport in DC, the following key points need to be considered. Silencing a gene that is a positive regulator of transport might result in reduced MHC class II levels at the plasma membrane. Knocking down a negative regulator, on the other hand, will result in higher cell surface expression levels. If this regulator is involved in the maturation-induced outward transport of MHC class II, its expression level might be lower in mature (m)DC compared to imDC, information that can be deduced from the gene expression data set. Finally, the intracellular distribution of MHC class II might be altered after silencing. For an example of HT data set integration and candidate selection strategy see [15].

The protocols described below are dedicated at how candidates selected from HT data sets can be validated and investigated in DC. First, the effects of silencing the candidate genes observed in the screen need to be confirmed in the primary immune cell. Lentiviral transduction is an efficient tool for the introduction of shRNA into human monocytes which can then be differentiated into imDC. In principle, such viral particles can also be used to introduce overexpression constructs. Once candidates that alter the transport of MHC class II are confirmed and changes of MHC class II gene transcription are excluded, the search for interaction partners/effectors can begin. Different methods can be applied for this purpose depending on which type of protein is selected. Yeast Two Hybrid (Y2H) technologies have been proven to be useful when looking for effectors of small GTPases. In our experience, for effector molecules of other protein classes (e.g. scaffold proteins) GST pulldown might be a more suitable method [20]. Kinases in general exceed very short lived interactions, which are difficult to detect in either assay. Any interaction identified using these methods needs to be confirmed by alternative methods, e.g. coimmunoprecipitation. All these techniques and considerations are required to build new pathways from high content screening data.

An RNAi screen only helps identifying potential candidate genes controlling a biological phenomenon. To understand the cell biology at a high content level, secondary HT screens can be applied. Subsequently, these are integrated with other datasets such as those from microarray, yeast two-hybrid and proteomics. When properly done, new pathways can be generated allowing definition of the control of MHC class II transport in primary DC.

2. Materials

2.1 Lentiviral Transduction of DC

- Human monocytes isolated from peripheral blood
- Cell line for lentivirus production (e.g. human 293T cells)
- Media and supplements: Cellgro medium (Cellgenix) or other medium for serumfree cultivation of dendritic cells, DMEM (GIBCO), fetal calf serum (FCS, Greiner), Phosphate-Buffered Saline (PBS, dissolve 1 tablet in 500 ml of distilled water, GIBCO) pH 7.4, trypsine-EDTA (GIBCO), IL-4 (Cellgenix), GM-CSF (Cellgenix), maturation trigger such as lipopolysaccharide LPS (Invivogen) and IFN-γ (Immukine,

Boehringer Ingelheim)
- Transfection reagent: Fugene 6 (Roche) or alike
- Plasmids: packaging constructs [e.g. pMDLg/pRRE, pRSV-Rev and pCMV-VSV-G [21]], control vectors (e.g. pLKO.1empty, pLKO.1shEGFP, pLKO.1shLuciferase, pLKO.1shSCRAMBLE), lentiviral plasmid containing shRNA of choice (pLKO.1 vectors from Open Biosystems, Thermo Scientific, usually 4-5 different sequences per gene)
- 0.45 µm filter units (Millipore)
- Polybrene (Millipore) dissolved in PBS
- Ultracentrifugation tubes (Beckman Coulter)
- Ultracentrifuge (Beckman Coulter Rotor SW28)

2.2 Flow Cytometry

- Wash Buffer: PBS containing 2% FCS
- Antibodies: PE anti-human HLA-DR (L243), FITC anti-human CD14, FITC anti-human CD83, PE anti-human CD80, APC anti-human CD86, APC anti-human CD40, APC anti-human DC-SIGN (all from BD Biosciences), diluted to 1-10 µg/ml in Wash Buffer
- FACS Calibur flow cytometer (BD Biosciences)

2.3 Immunofluorescence

- Cover glasses or µ-Slide 18-well plates (IBIDI)
- Coating: Fibronectin (Invitrogen) diluted to 20 µg/ml in PBS
- Fixation: PBS with 3,75% formaldehyde (free from acid, Merck)
- Permeabilization: PBS with 0.1% Triton X-100 (Sigma)
- Blocking: 0.5% bovine serum albumin (BSA, Sigma) in PBS
- Primary Antibody (AB): mouse anti-human CD63 (or any other late endosomal marker) and rabbit anti-HLA-DR [2] diluted in blocking buffer
- Fluorophore-conjugated Secondary Antibody (Invitrogen): diluted in blocking buffer, e.g. goat anti-mouse IgG Alexa 488
- HOECHST 33342 nuclear dye (Invitrogen) diluted to 2 µg/ml in secondary AB solution
- Phalloidin-Alexa568 (Molecular Probes) diluted to 0.4 U/ml in secondary AB solution
- Mounting medium: Vectashield (Vector Laboratories) or 80% glycerol (Merck) in PBS
- AOBS confocal microscope (Leica)

2.4 qRT-PCR

- Roche mRNA Capture Kit (Roche)
- Transcriptor High Fidelity cDNA Synthesis Sample Kit (Roche)
- Lightcycler 480 SYBR Green 1 Master (Roche)
- PCR-grade, RNAse-free water: DEPC-treated water (Invitrogen)
- Plates (Lightcycler 480 Multiwell 96, Roche)
- 10x primer solution: 3,3 µM of both forward and reverse primer in PCR-grade water; 18S rRNA reference primers: Forward 5'-CGGCTACCACATCCAAGGAA-3', Reverse 5'-GCTGGAATTACCGCGGCT-3'; HLA-DR α-chain primers: Forward 5'-CATGGGCTATCAAAGAAGAAC-3', Reverse 5'-CTTGAGCCTCAAAGCTGGC-3'
- PCR machine (Peltier Thermal Cycler, MJ Research)
- Light Cycler 480 Detection System (Roche)

2.5 Sample Preparation for Y2H and Glutathione-S-transferase(GST) Pulldown

- cDNA clone of gene of interest (e.g. IMAGE clone)
- Y2H suitable vector: e.g. pGBT9 (**http://www.dkfz.de/gpcf/y2h.html**)
- Cells of choice for GST pulldown, e.g. monocyte-derived imDC or mDC, peripheral blood mononuclear cells (PBMC)
- Lysis buffer: 50 mM NaCl (can be up to 500 mM to reduce unspecific binding), 50 mM Tris-HCl pH 8.0, 10 mM $MgCl_2$, 0.8% NP-40 and protease inhibitors (EDTA-free, Roche Diagnostics) in water
- Wash buffer: same as lysis buffer, but only 0.08% NP-40 and without protease inhibitors
- Recombinant GST-tagged protein of choice plus free GST for control purposes
- Glutathione Sepharose beads 4G (GE Healthcare)

2.6. Coimmunoprecipitation

- Cell line to be transfected with proteins identified to interact (e.g. MelJuSo or 293T) or primary immune cell type to study interaction of endogenous proteins
- Expression vectors encoding tagged proteins of interest (possible tags: GFP, HA, myc etc.)
- NP-40 lysis and wash buffers: see 2.5
- Antibodies: anti-GFP, anti-HA, anti-myc or antibodies raised against the proteins of interest
- Protein G Sepharose beads 4 Fast Flow (GE Healthcare)

2.7 SDS-PAGE and Western Blot

- 2x Sample Buffer: 4 ml distilled water (dH_2O), 10 ml 0.5 M Tris-HCl pH 6.8, 8 ml glycerol, 16 ml 10% SDS, few flakes of Bromphenol blue, store aliquots at -20°C, add 400 µl of β-mercaptoethanol per 3,8 ml of sample buffer before use.
- Resolving gel buffer: 1.5 M Tris-HCl pH 8.8, store

at 4°C
- Stacking gel buffer: 0.5 M Tris-HCl pH 6.8, store at 4°C
- 10% sodium dodecylsulphate (SDS) in dH2O
- Acrylamide/Bis-acrylamide: extremely toxic and carcinogenic! 40% (ratio 37.5:1, Biorad)
- TEMED (N,N,N,N-Tetramethylethylenediamine, Sigma)
- Initiator: 10% ammonium persulphate solution (APS) in dH2O, prepare just prior to use
- n-Butanol, water saturated: add dH2O, shake, let phases separate, use upper layer
- Electrophoresis buffer: 10x TGS (Biorad), final: 25 mM Tris, 192 mM glycine, 0.1% SDS, pH 8.3, dilute to 1x with dH2O
- Molecular weight standard: Page Ruler prestained protein ladder (Thermo Scientific)
- Gel fixative: 40% methanol and 10% acetic acid in dH2O
- Silver stain kit: SilverQuest (Invitrogen)
- Transfer buffer: 10x TG (Biorad), final: 25 mM Tris, 192 mM glycine, pH 8.3, dilute to 1x with dH2O and add 20% methanol
- PVDF membrane (Immobilon-P, Millipore)
- Blotting paper: Whatman (GE Healthcare)
- PBS/T: 0.1% Tween-20 (Sigma) in PBS
- Blocking buffer: 5% skim milk powder in PBS/T
- Primary AB: diluted in 1% blocking buffer
- Secondary AB: e.g. swine anti-rabbit IgG horse radish peroxidase-conjugated (Dako), diluted 1:5 000 in 1% blocking buffer
- Detection: Amersham ECL Detection Reagents (GE Healthcare)
- Biorad Mini Protean and Transfer System

3. Methods

3.1 Lentivirus Production

- 293T cells are grown in 150 cm^2 flasks in DMEM supplemented with 10% FCS.
- Cells are washed with PBS, trypsinized and seeded at 3.5 x 106 per 10 cm tissue culture dish. Per lentiviral shRNA construct four dishes are required.
- After 24 h cells are transfected. The three packaging constructs are mixed 1:1:1. The ratio of this packaging trio to shRNA construct (pLKO.1) is 1:1. To 1.4 ml of serum-free DMEM (room temperature) add 56 µl of Fugene 6. In a separate tube (see Note 1) mix 7 µg (see Note 2) of packaging vectors with 7 µg of pLKO.1shRNA. Combine Fugene/DMEM and DNA, incubate for 30 min at room temperature. Replace the medium in the 10 cm dishes with 12.6 ml of DMEM/FCS. Add DNA/Fugene dropwise.
- After 24 h change medium to 8 ml Cellgro. The cells should be 50% confluent. Handle them

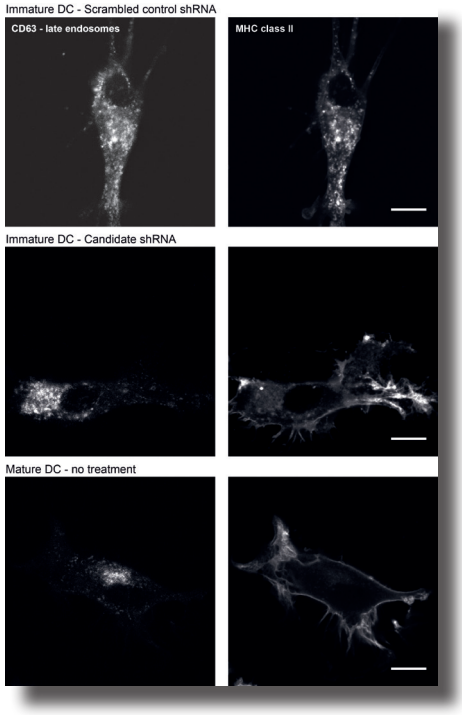

Figure 1 | Redistribution of MHC Class II after Candidate Gene Silencing
While MHC class II colocalises with the late endosomal marker CD63 on intracellular vesicles in immature DC (imDC, upper panel), most of MHC class II resides at the plasma membrane (PM) in mature DC (mDC, lower panel). When factors negatively influencing this transport process are silenced MHC class II molecules are redistributed to the PM, which resembles the phenotype of an mDC, while other maturation markers remain negative as is typical for an imDC (determined by flow cytometry). DC are fixed and stained with antibodies against CD63 and MHC class II. Fluorophore-conjugated secondary antibodies are used to visualize the localization of the two molecules by confocal microscopy. Bar = 10 µm.

carefully as they detach very easily.

- After another 24 h harvest the supernatant. Filter through a 0.45 µm filter. Concentrate the viral supernatant 100x by ultracentrifugation at 20.000 x g at room temperature for 2 h. Resuspend the viral pellet in 360 µl Cellgro (see Note 3) and snap freeze in liquid nitrogen. Store at -80 (see Note 4). The viral suspension obtained is enough to perform transduction of at least three different monocyte donors.
- Add another 7 ml of Cellgro to the 293T cells. A second harvest can be performed the day after.

3.2 Silencing Candidate Genes in DC

Human monocytes are transduced with lentivirus carrying shRNA constructs targeting the selected candidate genes followed by differentiation into imDC. Several control vectors should be used. An average of their phenotype serves as a reference point. The experiment should be performed in several donors as a big difference between individuals is usually observed when working with primary cells. General effects can be easily separated from MHC class II-specific ones by including additional cell surface markers such as MHC class I (for effects on the entire MHC locus), CD63 (for effects on recycling between PM and late endosomes) and transferrin receptor (for recycling in early endosomes).

- Thaw frozen monocytes. Wash 2x with Cellgro. Plate cells at 1 x 10^6 in 12-well plate in 900 µl Cellgro supplemented with IL-4 (800 U/ml final concentration), GM-CSF (1000 U/ml) and Polybrene (4 µg/ml). Add 100 µl of 100x viral supernatant.
- After 24 h remove 400 µl of medium and refresh with 1.4 ml of Cellgro/IL-4/GM-CSF.
- On day 5 mature a well of untreated imDC with LPS (2.5 µg/ml) and IFN-γ (1000 U/ml) to use as an mDC control.
- After 24 h determine the cell surface levels of MHC class II and other maturation markers by flow cytometry and the intracellular MHC class II distribution by immunofluorescence. To ensure that imDC were successfully generated monitor the reduction of CD14 and the increase of DC-SIGN cell surface levels compared to monocytes by flow cytometry. Furthermore, the cells are subjected to qRT-PCR to establish the level of knockdown and to rule out any effects on MHC class II gene transcription.

3.3 Phenotyping DC by Flow Cytometry

DC are semi-adherent and can be detached by repetitive pipetting and flushing the well.

- Approx. 50% of cells remain after differentiation from monocytes to imDC. Transfer approx. 100 000 DC per staining to a round-bottom 96-well plate. Spin cells down and discard supernatant. Wash cells one time with buffer and spin down.
- Add 20 µl of antibody cocktail (e.g. FITC-CD83, PE-MHCII, APC-CD40) and incubate for 30 min on ice in the dark. Wash cells with buffer followed by centrifugation.
- Resuspend pellet in 100 µl of wash buffer. Measure the cell surface expression of the respective markers using a plate reader attached to the flow cytometer.

3.4 Intracellular MHC Class II Distribution

In imDC MHC class II mainly resides in late endosomes where it colocalizes with CD63. When exposed to danger signals DC undergo striking morphological changes one of which is a redistribution of MHC class II to the plasma membrane. To determine whether any of the silenced candidate genes is responsible for maintaining MHC class II's endosomal location the colocalisation between CD63 and MHC class II is being determined (Figure 1).

- Coat µ-slides for 30 min at 37°C with fibronectin and rinse with PBS.
- Add 30 µl DC suspension and incubate in a wet chamber at 37°C for 6-7 h. All the following steps are carried out at room temperature.
- Fix cells with 3.75% formaldehyde for 15 min and wash by immersing the slide in a chamber filled with PBS. Slides may be stored for several days in PBS at 4°C.
- Permeabilize the cells with Triton-X for 10 min and wash with PBS.
- Unspecific binding is prevented by blocking with 0.5% BSA solution for 45 min.
- Add the primary antibody solution and incubate for 60 min. 15 µl of solution are enough to cover the entire surface area of one well.
- Wash the slides 3x for 5 min by placing the PBS-filled chamber on a shaking platform.
- Add the secondary antibody solution containing HOECHST as a nuclear dye and phalloidin to stain the actin cytoskeleton and incubate for 30 min in the dark.
- Wash the slides again 3x for 5 min and fill each well with 80% glycerol. The slides can be stored at 4°C for a few days until analysis with a confocal microscope. When using individual cover glasses perform all washing steps in

multi-well plates and mount the glasses in the end using a drop of mounting medium on a glass slide. Remove excess mounting medium by pressing the glass slide on tissue.
- Analyze the MHC class II distribution in DC by confocal microscopy.

3.2 Determination of mRNA Levels in DC by qRT-PCR

This method is used to determine the knockdown efficiency on one hand and to rule out any effects on transcriptional regulation of MHC class II on the other hand (see Note 5).

- Wash 50 000 DC 2x with cold PBS (see Note 6) and lyse in 50 µl lysis buffer (see Note 7).
- Add 4 µl of biotinylated oligo dT primer and anneal for 5 min at 37°C. Transfer lysate to a streptavidin-coated tube and incubate for another 5 min at 37°C (see Note 8).
- Add 200 µl of wash buffer and discard. Repeat washing step 3x. Leave the liquid of the last wash in the tube while preparing the cDNA synthesis master mix.
- Per reaction you will need: 6 µl 5x Reaction Buffer, 20 µl RNAse-free water, 0.5 µl RNAse Inhibitor, 2 µl nucleotides (dNTPs), 1 µl DTT, and 0.5 µl Reverse Transcriptase.
- Discard wash buffer completely. When pipetting away the liquid avoid touching the walls of the tube as this might destroy the layer of streptavidin. Add 30 µl of master mix.
- Reverse transcribe the captured mRNA into cDNA with a PCR program of 30 min 50°C and 5 min 85°C. Stop at 99°C. At such high temperature the bond between biotin and streptavidin is broken and the cDNA can be removed.
- Quickly remove the 30 µl of liquid and replace them with 50 µl of PCR-grade water. Incubate for 3 min at 99°C. Remove the liquid and combine it with the previous 30 µl. The cDNA can be stored at -20°C.
- For the qRT-PCR reaction 96-well plates are used. Per well add 5 µl of SYBR Green, 1 µl of 10x primer solution (3.3 µM each) and 1.5 µl of water. Add 2.5 µl of cDNA. Seal the plate and spin it to collect all fluid at the bottom of each well.
- Insert the plate in the LightCycler and start the run, which will take about 1 h 20 min.
- Analyze using the comparative CT method (ΔΔCT). Relate the results to the 18S rRNA values and normalize it to the average of control shRNA-treated cells.

3.3 Identification of Interaction Partners/ Effectors by Y2H

- The Y2H analysis can be outsourced (e.g. **http://www.dkfz.de/gpcf/y2h.html**). Alternatively, a protocol on how to perform Y2H can be found here [22].
- To prepare the sample for Y2H clone the cDNA of your gene of interest into a Y2H-combatible vector.
- Choose an appropriate cDNA library to screen (e.g. lymph node). Choose a cell type/tissue where your gene of interest is expressed under normal conditions. Information about tissue distribution can be found at **http://biogps.org** [23].

3.4 Identification of interaction partners/ effectors by GST pulldown

- To prepare a protein for GST pulldown clone the cDNA of your gene of interest into a GST expression vector. Produce the recombinant GST-tagged protein as well as free GST in e.g. *Escherichia coli* and purify them.
- Wash 120 µl of glutathione beads 3x in lysis buffer. Spin at 500 x g for 3 min. Remove liquid carefully (see Note 9).
- Couple 50 µg of recombinant protein dissolved in lysis buffer to the beads for 1 h. All subsequent incubation steps are performed at 4°C on a spinning wheel. Wash beads 3x in lysis buffer (see Note 10).
- Lyse 200 x 106 PBMC [cell number may vary depending on (1) the expression level of the protein of interest and (2) the availability of the cell type you want to use] in 750 µl lysis buffer for 30 min. Centrifuge for 10 min at maximum speed.
- Incubate beads with the supernatant of lysed cells for 1 h or overnight. Wash 1x in lysis buffer and 3x in wash buffer (see Note 10).
- Remove all liquid (see Note 9). Add 25 or 50 µl of 1x sample buffer (prepare by mixing equal volumes of water and 2x sample buffer), boil for 5 min at 100°C, centrifuge at max. speed and load supernatant on one or two gels, respectively.

3.5 SDS-PAGE and Mass Spectrometry

- Wash glass plates, clean with 70% ethanol and dry.
- Prepare two 1 mm 12% resolving gels by mixing 4.35 ml water with 2.5 ml resolving gel buffer, 0.1 ml 10% SDS solution and 3 ml acrylamide/bis-acrylamide solution. Start the polymerization by adding 50 µl of 10% APS solution and 5 µl of TEMED. Pour the gel leaving space for the

stacking gel. Overlay with n-butanol.
- After polymerization is complete pour away the butanol and rinse the gel with water. Absorb residual water using blotting paper.
- Prepare 4% stacking gel mixing 3.22 ml water with 1.25 ml stacking gel buffer and 50 µl 10% SDS solution and 0.5 ml acrylamide/bis-acrylamide solution. Start the polymerization by adding 25 µl of 10% APS solution and 5 µl of TEMED. Pour the liquid on top of the resolving gel and insert the comb.
- When polymerization is complete, assemble the gel unit, remove the combs, fill the unit with 1x electrophoresis buffer and flush each sample well using a long slender tip or syringe with needle.
- Load samples. Fill empty wells with 1x sample buffer. Include a weight marker in one lane.
- Close the unit and connect it to a power supply. Set the power supply to constant voltage and run at 90 V. When the sample front has passed the stacking gel the voltage may be increased to 110 V.
- When the SDS-PAGE run is finished, remove the gel and fix it for at least 20 min before proceeding to the silver staining.
- Perform mass spectrometric analysis to determine the proteins that have interacted with your protein of choice, but not with GST alone (see Note 11).

3.6 Confirmation of Interaction by Coimmunoprecipitation

Interactions identified by Y2H or GST pulldown need to be confirmed. If antibodies are available it is better to perform the coimmunoprecipitation (CoIP) with endogenous proteins in e.g. imDC or mDC. If such antibodies are not available ectopic expression of the proteins of interest in a cell line may be applied. By tagging the proteins with two different tags interactions can be studied.

- For CoIP either isolate the cell type of choice to confirm the interaction or transfect a cell line with plasmids encoding tagged versions of the two putative interaction partners. Use e.g. Fugene 6 for the transfection following the steps described under 3.1.
- Wash 50 µl of protein G beads 3x in lysis buffer. Spin at 500 x g for 3 min. Remove liquid carefully (see Note 9).
- Couple 5 µl (the amount might be reduced to as little as 1 µl depending on the strength of the antibody) of antibody (against interaction partner one or against the tag of interaction partner one) diluted in lysis buffer to the beads for 1 h. All subsequent incubation steps are performed at 4°C on a spinning wheel. Wash beads 3x (see Note 10).
- Lyse 5 x 106 transiently transfected cells (more primary cells are necessary when detecting endogenous proteins) in 750 µl lysis buffer for 30 min. Centrifuge for 10 min at maximum speed.
- Mix 50 µl of supernatant with an equal volume of 2x sample buffer, boil for 5 min at 100°C, centrifuge and store at -20°C. Load on a gel as a total lysate control.
- Incubate beads with the remaining supernatant of lysed cells for 1 h or overnight. Wash 1x in lysis buffer and 3x in wash buffer (see Note 10).
- Remove all liquid (see Note 9). Add 25 of 1x sample buffer (prepare by mixing equal volumes of water and 2x sample buffer), boil for 5 min at 100°C, centrifuge and load supernatant on a gel.
- Perform SDS-PAGE as described under 3.5.
- Prepare pieces of blotting paper and PVDF membrane slightly larger than the gel and soak the membrane in 100% methanol for 2-3 min.
- Fill a tray with 1x transfer buffer. Submerge the transfer cassette. Stack a foam pad and three pieces of blotting paper on the dark plastic side of the cassette. Remove the gel from the electrophoresis chamber, rinse with water, and place onto the filter paper. Place the membrane on the gel (avoid the introduction of bubbles. Add three pieces of blotting paper prewet in transfer buffer. Remove any bubbles in between the different layers by rolling a serological pipette over the stack. Place wet foam pad on top and close the cassette.
- Insert the cassette into the transfer tank. Black side of the cassette facing the black side of the tank. Double check that the membrane is placed between the gel and the anode (+). Proteins will migrate towards the anode. If inserted the opposite way proteins will be lost in the buffer.
- Place an ice block in the transfer tank and fill the tank with 1x transfer buffer. Add a magnetic stirrer.
- Place tank on a stirrer platform, close lid and perform transfer at constant current of 150 mA for 1.5 h. Alternatively, the transfer can be performed at constant 20 mA in the cold room overnight.
- Remove the PVDF membrane from the transfer unit (see Note 12). The prestained molecular weight marker should be clearly visible.
- Block the membrane in 10 ml of milk solution for 1 h at room temperature (RT) rocking on a shaking platform. Wash the membrane 3x with PBS/T for 5 min.

- Add the primary antibody solution (against interaction partner two or tag of interaction partner two) and incubate for at least one hour at RT or overnight at 4°C. Wash the membrane 3x with PBS/T for 5 min.
- Add the secondary antibody solution and incubate for 1 h at RT. Wash the membrane 3x with PBS/T for 10 min.
- Prepare the ECL reagents by mixing equal volumes of the two components. Remove the membrane from the washing solution. Remove excess buffer by blotting one corner of the membrane on tissue. Place membrane on clear plastic foil, cover with ECL mix and wrap in foil. Ensure complete coverage of the membrane by striking the liquid from one side to the other repeatedly.
- After 1 min remove excess liquid and wrap membrane in clean foil. Place membrane in a film cassette.
- In a dark room expose X-ray film to the chemiluminescence signals and develop afterwards. The exposure time needs to be adjusted to the signal strength.

3.7 Colocalisation Studies on putative Interaction Partners using Immunofluorescence Microscopy

Colocalisation observed by immunofluorescence (IF) represents an alternative method to support protein interaction data.

- Prepare primary cells as described under 3.4 or transiently transfected cells as described under 3.6.
- Determine the localization of the two putatively interacting proteins by staining them with antibodies directly or indirectly (anti-tag). See 3.4 for procedure.
- To place these interactions in context with MHC class II transport stain also for MHC class II or for the compartments involved in MHC class II antigen presentation (e.g. CD63 for late endosomes). Phalloidin is a stain for the actin cytoskeleton and will help to determine whether transport occurs along actin filaments. Furthermore, the microtubule network may be visualized using anti-tubulin antibodies.

3.8 Conclusion

An RNAi screen often results in a list of genes that are somehow affecting a biological process. To classify these 'hits' HT follow-up screens are needed. When all these individual datasets are integrated and stringent criteria are set a list of candidates emerges that might play a role in e.g. the control of MHC class II transport. To study and confirm these candidates experiments in primary immune cells (DC) need to be performed. Silencing can be achieved by introduction of shRNA constructs using lentivirus transduction. Changes in cell surface levels of MHC class II and its intracellular distribution are measured. To extend the findings of individual new players to whole pathways interaction partners and effectors can be identified using Y2H and proteomic approaches. All new findings require further confirmation applying alternative methods. Including appropriate controls ensures that the new findings are MHC class II-specific and do not affect any general transport or protein secretion pathway.

4. Notes

1. All tubes should be made from polyethylene to limit the rate of liposomes sticking to the tube's wall.
2. In order to monitor the transfection efficiency 0.5 µg of pEGFPC1 (Clontech) may be added to the packaging vector mixture. The amount of pLKO.1shRNA construct should be reduced to 6.5 µg respectively. More than 90% of 293T cells should be GFP-positive after 48 h.
3. Add Cellgro to pellet and leave it standing for a few minutes before pipetting up and down gently (try not to introduce bubbles).
4. To be able to set a certain mode of infection (MOI) the viral titer of your lentivirus preparation needs to be determined as transducing units per ml (TU/ml). Produce GFP-expressing lentiviral particles by introducing the pLKO.1TURBOGFP construct. Infect monocytes with decreasing volume of virus supernatant and determine the amount of GFP-positive colonies by microscopy after 48 h. Multiply this number with the dilution factor.
5. A useful program to design primers against your gene of interest for qRT-PCR is Perlprimer [24]. Adjust the settings according to what is being recommended with the SYBR Green you are using. BLAST the primer sequences to ensure they only recognize one gene.
6. To ensure RNAse-free working conditions wipe surfaces and tools with 70% ethanol. Use filter tips and RNAse-free tubes and reagents. Avoid working in a laminar flow hood as the flow of air will favor contamination with RNAses.
7. The solution is very viscous. One freeze-thaw cycle at -80°C helps to complete the lysis.
8. When working with the SA-coated tubes avoid the introduction of bubbles and scratching the wall of the tubes while pipetting!
9. Use a needle of diameter 0.4 mm. Liquid can be

entirely removed without loss of beads.

10. Transfer beads to a fresh tube during the last washing step. This will help eliminate proteins that unspecifically stick to the tube's wall.
11. Contamination of gels with keratine can cause problems during mass spectrometry. To ensure keratine-free conditions pre-cast gels can be used.
12. Use forceps to handle the membrane. The transfer of the prestained marker to the membrane gives an indication of the quality of protein transfer. To get an overview of protein transfer across the entire membrane stain with Ponceau S for a few minutes. Destain by rinsing with excess of water.

References

1. Lipscomb, M.F. and B.J. Masten, *Dendritic cells: immune regulators in health and disease.* Physiol Rev, 2002. **82**(1): p. 97-130.
2. Neefjes, J.J., et al., *The biosynthetic pathway of MHC class II but not class I molecules intersects the endocytic route.* Cell, 1990. **61**(1): p. 171-183.
3. Peters, P.J., et al., *Segregation of MHC class II molecules from MHC class I molecules in the Golgi complex for transport to lysosomal compartments.* Nature, 1991. **349**(6311): p. 669-676.
4. Roche, P.A. and P. Cresswell, *Invariant chain association with HLA-DR molecules inhibits immunogenic peptide binding.* Nature, 1990. **345**(6276): p. 615-618.
5. van den Hoorn, T., et al., *Routes to manipulate MHC class II antigen presentation.* Curr Opin Immunol, 2011. **23**(1): p. 88-95.
6. Neefjes, J., et al., *To a systems understanding of MHC class I and MHC class II antigen presentation* Nat Rev Immunol, 2011.
7. Cella, M., et al., *Inflammatory stimuli induce accumulation of MHC class II complexes on dendritic cells.* Nature, 1997. **388**(6644): p. 782-787.
8. Pierre, P., et al., *Developmental regulation of MHC class II transport in mouse dendritic cells.* Nature, 1997. **388**(6644): p. 787-792.
9. Wong, S.H., L. Santambrogio, and J.L. Strominger, *Caspases and nitric oxide broadly regulate dendritic cell maturation and surface expression of class II MHC proteins.* Proc Natl Acad Sci U S A, 2004. **101**(51): p. 17783-17788.
10. de Gassart, A., et al., *MHC class II stabilization at the surface of human dendritic cells is the result of maturation-dependent MARCH I down-regulation.* Proc Natl Acad Sci U S A, 2008. **105**(9): p. 3491-3496.
11. van Niel, G., et al., *Dendritic cells regulate exposure of MHC class II at their plasma membrane by oligoubiquitination.* Immunity, 2006. **25**(6): p. 885-894.
12. McCormick, P.J., J.A. Martina, and J.S. Bonifacino, *Involvement of clathrin and AP-2 in the trafficking of MHC class II molecules to antigen-processing compartments.* Proc Natl Acad Sci U S A, 2005. **102**(22): p. 7910-7915.
13. Pierre, P. and I. Mellman, *Developmental regulation of invariant chain proteolysis controls MHC class II trafficking in mouse dendritic cells.* Cell, 1998. **93**(7): p. 1135-1145.
14. Vascotto, F., et al., *The actin-based motor protein myosin II regulates MHC class II trafficking and BCR-driven antigen presentation.* J Cell Biol, 2007. **176**(7): p. 1007-1019.

15. Paul, P., et al., *A Genome-wide multidimensional RNAi screen reveals pathways controlling MHC class II antigen presentation.* Cell, 2011. **145**(2): p. 268-283.
16. Rocha, N., et al., *Cholesterol sensor ORP1L contacts the ER protein VAP to control Rab7-RILP-p150 Glued and late endosome positioning.* J Cell Biol, 2009. **185**(7): p. 1209-1225.
17. Sharma, S. and A. Rao, *RNAi screening: tips and techniques.* Nat Immunol, 2009. **10**(8): p. 799-804.
18. Carpenter, A., et al., *CellProfiler: image analysis software for identifying and quantifying cell phenotypes.* Genome Biology, 2006. **7**(10): p. R100.
19. Jones, T.R., et al., *Scoring diverse cellular morphologies in image-based screens with iterative feedback and machine learning.* Proc Natl Acad Sci U S A, 2009. **106**(6): p. 1826-1831.
20. Abu-Farha, M., F. Elisma, and D. Figeys, *Identification of protein-protein interactions by mass spectrometry coupled techniques.* Adv Biochem Eng Biotechnol, 2008. **110**: p. 67-80.
21. Dull, T., et al., *A third-generation lentivirus vector with a conditional packaging system.* J Virol, 1998. **72**(11): p. 8463-8471.
22. Kail, M. and A. Barnekow, *Identification and characterization of interacting partners of Rab GTPases by yeast two-hybrid analyses.* Methods Mol Biol, 2008. **440**: p. 111-125.
23. Wu, C., et al., *BioGPS: an extensible and customizable portal for querying and organizing gene annotation resources.* Genome Biol, 2009. **10**(11): p. R130.
24. Marshall, O.J., *PerlPrimer: cross-platform, graphical primer design for standard, bisulphite and real-time PCR.* Bioinformatics, 2004. **20**(15): p. 2471-2472.
25. Masterson, A.J., et al., *MUTZ-3, a human cell line model for the cytokine-induced differentiation of dendritic cells from CD34+ precursors.* Blood, 2002. **100**(2): p. 701-703.
26. Berges, C., et al., *A cell line model for the differentiation of human dendritic cells.* Biochem Biophys Res Commun, 2005. **333**(3): p. 896-907.
27. Tsuchiya, S., et al., *Induction of maturation in cultured human monocytic leukemia cells by a phorbol diester.* Cancer Res, 1982. **42**(4): p. 1530-1536.
28. Harding, C.V., D. Canaday, and L. Ramachandra, *Choosing and preparing antigen-presenting cells.* Curr Protoc Immunol, 2010. **Chapter 16**: p. Unit.
29. Johnson, J.P., et al., *Surface antigens of human melanoma cells defined by monoclonal antibodies. I. Biochemical characterization of two antigens found on cell lines and fresh tumors of diverse tissue origin.* Eur.J.Immunol., 1981. **11**(10): p. 825-831.
30. Hockett, R.D., et al., *Interferon-gamma differentially regulates antigen-processing functions in distinct endocytic compartments of macrophages with constitutive expression of class II major histocompatibility complex molecules.* Immunology, 1996. **88**(1): p. 68-75.
31. Stockinger, B., et al., *A role of Ia-associated invariant chains in antigen processing and presentation.* Cell, 1989. **56**(4): p. 683-689.
32. Poloso, N.J., L.K. Denzin, and P.A. Roche, *CDw78 defines MHC class II-peptide complexes that require Ii chain-dependent lysosomal trafficking, not localization to a specific tetraspanin membrane microdomain.* J Immunol, 2006. **177**(8): p. 5451-5458.

4

Discussion

Summary & Discussion
Nederlandse Samenvatting

Summary & Discussion

Major histocompatibility class II molecules (MHC class II) are one of the key regulators of adaptive immunity because of their specific expression by professional antigen presenting cells (APC). They present peptides derived from endocytosed material to T helper lymphocytes. Consequently, MHC class II is fundamental in orchestrating both cellular and humoral immune responses. A genetic association of certain MHC class II alleles with autoimmunity has long been established. The molecular mechanisms underlying this association are only poorly understood. An in depth understanding of the antigen presentation pathway by MHC class II is essential for the improvement of current therapies. General aspects of MHC class II antigen presentation and ways to manipulate it have been widely discussed in the Introduction Chapter and Chapter 3. Here, the tools to arrive at a systems understanding of MHC class II antigen presentation will be discussed. What are the advantages and disadvantages of a genome-wide screen? And how can a multi-dimensional, data-integrating approach increase the understanding of the systems biology of MHC class II?

In 2006, the Nobel Prize in Medicine was awarded to Andrew Fire and Craig Mello for their work on RNAinterference (RNAi) in C. elegans [1]. RNAi occurs in many eukaryotic organisms and is thought to be an antiviral mechanism triggered by double stranded (ds)RNA, which leads to sequence-specific mRNA degradation. Endogenously encoded micro (mi)RNA molecules target the 3' untranslated region (UTR) of mRNA and are involved in gene regulation. Nowadays, RNAi is applied in mammalian cells as means to silence the expression of genes of interest. As early as 2004, first efforts had been undertaken to perform genome-wide RNAi screens [2-4]. And this was just the beginning. Ever since its discovery, RNAi has been applied many a times to study signal transduction, cancer biology and host-pathogen interactions, to just name a few of the biological processes addressed (reviewed in [5]). The setup of these screens including the analysis methodology, however, varied greatly.

Different species of RNA can be used. Short hairpin RNA (shRNA) is often delivered by viral transduction, which has the advantage of stable integration in the genome and expression of selection markers. Libraries of shRNA are often provided in pools of several thousand different sequences, which makes it a more economic approach. Another very popular format is small interfering RNA (siRNA). These chemically synthesized 19-27 nucleotide long sequences can be easily introduced into cells by lipid-based transfection methods. Libraries of siRNA are often designed in an arrayed format with every well of a 96- or 384-well plate containing siRNAs targeting a single gene only. This naturally leads to a larger format; hence, automated liquid handling and high throughput analysis equipment are required. An siRNA species called enzymatically generated siRNA (esiRNA) can be easily produced by the researcher himself. For an overview of advantages and disadvantages of the various setups see [6].

Depending on the RNA format, the analysis assay might have to be performed in a high throughput manner. Robustness is a necessity. Various normalization procedures have been described [7, 8]. The cutoff levels are arbitrarily chosen and in turn influence the rate of false-positive and -negative candidates. Validation steps need to be applied to obtain a list of more reliable candidates. Again these have to be carefully chosen. Various reviews are available, which highlight tips, tricks and pitfalls for RNAi screening [6, 9, 10]. The take-home message is; clever design is crucial. By choosing proper controls one can get an idea of the 'screening window' (the maximum changes expected for a certain read-out), which will ultimately determine the robustness of the entire screen. A common normalization method is the so-called z-score [11], which is mainly dependent on the standard deviation of the control samples. The primary screen is often followed by one or several follow-up screens aiming at candidate validation. Furthermore, these screens may provide additional information about the candidate genes, which may become useful when plotting interaction networks. While other groups have established screening regimes suitable for the scientific questions they addressed [12-15], we have come up with a unique multi-dimensional approach that integrated various data sets to arrive at a more complete understanding of a crucial cellular process – MHC class II antigen presentation (described in Chapter 1 and 2 of this thesis).

Whenever an RNAi screen is set up one has to be aware of its strengths as well as its limitations. In our approach we ensured robustness using a melanoma cell line, which possesses a complete and functional MHC class II antigen presentation machinery [16]. A cell line facilitates reproducible transfection efficiency over long periods of time. There is virtually no limit in resources as opposed to primary cells (which would show donor to donor variation, thus affecting the statistical power of the assay). Two monoclonal antibodies were used to detect MHC class II on the cell surface in two different states, hence distinguishing target genes

involved in the regulation of overall surface levels and/or peptide loading. We have integrated these primary results with information on the intracellular distribution of MHC class II gathered in a secondary microscopy-based assay. Microscopy in combination with automated image analysis opens new venues to study complex cellular processes, such as intracellular trafficking [17], which are of great importance in MHC class II antigen presentation. It will certainly be further exploited in the near future, as high-resolution (semi)-automated microscopes and the corresponding image software undergo constant improvement.

MHC class II is selectively expressed on a subset of immune cells. Most of the genes discovered in our screen are affecting MHC class II expression at the cell surface when silenced. Therefore, they should contain those candidates that control tissue-specific MHC class II gene expression. The networks controlling these factors are unknown. We used our RNAi screen results to address this issue and unravel general cell biological terms defining tissue-selective expression of MHC class II. Therefore, high-throughput quantitative PCR was performed to investigate effects of gene silencing on the expression of the MHC class II locus. From this screen we were able to deduct a complex feedback regulated network of signaling molecules and transcription factors, which in turn regulate the levels of CIITA – the master regulator of MHC class II transcription. Further bioinformatics investigation revealed general cell biological cues such as signaling and chromatin modifications as modifiers of tissue-selective expression of MHC class II. Using RNAi to unravel transcriptional networks is being acknowledged as a powerful tool to uncover regulatory interactions that modulate transcription factor activity [18].

In general, the introduction of bias of any kind was prevented as much as possible by always investigating the list of candidates as a whole. We have subjected them to multiple assays, which we finally integrated to obtain networks of similarity in phenotype. To ensure that we are not studying artifacts due to the use of a melanoma cell line, we have additionally determined the expression levels of all genes in a panel of human primary immune cells. Only those candidates expressed in immune cells were considered for further studies.

Nevertheless, false-positive or -negative candidates can never be entirely excluded, without losing too many 'real hits'. Any screening setup has limitations which need to be taken into account. One major issue is the variability of knockdown efficiency achieved by different siRNA pools. The transfection method has been optimized beforehand targeting a few representative genes, but it will never be optimal for all. Often lethality caused by silencing particular genes (such as PLK1) can be observed and this has to be corrected for. Usually an arbitrary cut-off is chosen, and conditions of too low cell viability are excluded from the analysis. Despite the fact that the melanoma cell line MelJuSo has been shown to be properly presenting peptides bound to MHC class II [16] artifacts due to these cells' origin can never be entirely excluded. Hence, a thorough confirmation of selected candidates in primary APC has to be executed.

Dendritic cells (DC) have first been described in the 1970s [19], a discovery which has recently been awarded the Nobel Prize in Medicine for Ralph Steinman. DC are the main professional APC in our body. Starting in the early 1990s, culture methods have been described to obtain DC from bone marrow precursors or peripheral blood monocytes. Again these findings were pioneered by Ralph Steinman together with Kayo Inaba [20, 21].

We have used our integrated data sets (cell surface as well as intracellular MHC class II localization, expression in immune cells, and effects on MHC class II locus transcription) to select candidates that we think are involved in orchestrating the redistribution of MHC class II from intracellular late endosomal structures to the plasma membrane during DC activation (maturation). Establishing a lentiviral transduction method for delivery of shRNA constructs into monocytes that are then differentiated into immature DC enabled us to study the function of the selected candidates in human primary immune cells (described in Chapter 4 of this thesis). One striking finding was that the small GTPase ARL14 (sometimes referred to as ARF7) seems to be a negative regulator of outward transport of MHC class II. When silenced in immature DC, the majority of MHC class II molecules are redistributed to the plasma membrane leaving late endosome void of MHC class II. While those ARL14-silenced cells remain immature in terms of other activation markers they strikingly resemble a mature DC in regards to their MHC class II localization (see Chapter 1 and 2 of this thesis). This is a unique observation. By silencing one gene we have uncoupled two processes that were hitherto coupled: export of MHC class II and maturation of DC.

We then set out to unravel the mechanism underlying the MHC class II transport regulation by ARL14. Through a series of proteomic assays we have established various interaction partners, one of which is a so far unknown protein, now named ARF7 effector protein (ARF7EP). We propose that ARL14 is recruited to late endosomes by its guanine exchange factor PSD4, which binds to specific lipids on late

endosomes through its pleckstrin homology domain. ARL14 is linked to the actin cytoskeleton via ARF7EP and the motor myosin 1E. This complex seems to orchestrate the positioning of MHC class II-positive late endosomal vesicles along the cytoskeleton (see Chapter 1 and 2 of this thesis).
Other members of the ARF-like family of GTPases have recently been found to be implicated in lysosomal trafficking [22]. Lysosome-associated ARL8B was shown to regulate endosome to lysosome traffic of various cargos. It directly recruits, VPS41, a subunit of the HOPS (*ho*motypic fusion and *pro*tein sorting) complex. The HOPS complex has been well described in yeast, where it is involved in trafficking to the vacuole, an organelle similar to the lysosome [23]. The described function of ARL8B does not seem to be mediated by any of the known effectors of late endosome (LE) to lysosome trafficking. These are the small GTPase RAB7, RILP (RAB7 interacting lysosomal protein) [24], the cholesterol sensor ORP1L and the ER-resident protein VAP [25]. Lately, this machinery has been linked to the HOPS complex too. RILP seems to act as a bridge between two LE decorated with the RAB7/RILP/HOPS complex [Rik van der Kant, personal communication]. While the GTPase ARL14 is involved in positioning LE along the actin cytoskeleton, the GTPases ARL8B, RAB7 and possibly others seem to control late endosome and lysosome vesicle tethering and fusion.

RNAi screening will become a more and more affordable and feasible tool for the understanding of molecular processes in immune cells as the development of high-throughput techniques and automated analysis software progresses [26]. Studying the MHC class II pathway on a genome-wide scale opens up many opportunities of manipulation (see Chapter 3 in this thesis). Understanding antigen presentation in more detail will ultimately lead to new strategies of inhibiting unwanted immune responses (e.g. in autoimmune diseases) as well as boosting immunity (e.g. in cancer or vaccine development).
Yet, defining novel factors using the new technologies described in this thesis (Chapters 1, 2 and 4) should be considered as a basis for a deeper understanding of biology, which still requires much and hard work. The findings presented here may be further supported by the large data sets that appear in the public domain. We believe that an integration of wet-lab and computer-based biology will guide future cell biology and immunology to a deep understanding of important biological processes and to new ways to manipulate these in disease. Manipulating MHC class II may be of relevance for auto-immune diseases, transplantation as well as vaccination strategies and I hope that my work may provide a basis for novel insights and improvement.

References

1. Fire, A., et al., *Potent and specific genetic interference by double-stranded RNA in Caenorhabditis elegans.* Nature, 1998. **391**(6669): p. 806-11.
2. Berns, K., et al., *A large-scale RNAi screen in human cells identifies new components of the p53 pathway.* Nature, 2004. **428**(6981): p. 431-7.
3. Brummelkamp, T.R., et al., *Loss of the cylindromatosis tumour suppressor inhibits apoptosis by activating NF-kappaB.* Nature, 2003. **424**(6950): p. 797-801.
4. Paddison, P.J., et al., *A resource for large-scale RNA-interference-based screens in mammals.* Nature, 2004. **428**(6981): p. 427-31.
5. Mohr, S., C. Bakal, and N. Perrimon, *Genomic screening with RNAi: results and challenges.* Annu Rev Biochem, 2010. **79**: p. 37-64.
6. Campeau, E. and S. Gobeil, *RNA interference in mammals: behind the screen.* Brief Funct Genomics, 2011. **10**(4): p. 215-26.
7. Konig, R., et al., *A probability-based approach for the analysis of large-scale RNAi screens.* Nat Methods, 2007. **4**(10): p. 847-9.
8. Birmingham, A., et al., *Statistical methods for analysis of high-throughput RNA interference screens.* Nat Methods, 2009. **6**(8): p. 569-75.
9. Sigoillot, F.D. and R.W. King, *Vigilance and validation: Keys to success in RNAi screening.* ACS Chem Biol, 2011. **6**(1): p. 47-60.
10. Sharma, S. and A. Rao, *RNAi screening: tips and techniques.* Nat Immunol, 2009. **10**(8): p. 799-804.
11. Boutros, M., L.P. Bras, and W. Huber, *Analysis of cell-based RNAi screens.* Genome Biol., 2006. **7**(7): p. R66.
12. Orvedahl, A., et al., *Image-based genome-wide siRNA screen identifies selective autophagy factors.* Nature, 2011. **480**(7375): p. 113-7.
13. Collinet, C., et al., *Systems survey of endocytosis by multiparametric image analysis.* Nature, 2010. **464**(7286): p. 243-9.
14. Chevrier, N., et al., *Systematic discovery of TLR signaling components delineates viral-sensing circuits.* Cell, 2011. **147**(4): p. 853-67.
15. Snijder, B., et al., *Population context determines cell-to-cell variability in endocytosis and virus infection.* Nature, 2009. **461**(7263): p. 520-3.
16. Wubbolts, R., et al., *Direct vesicular transport of MHC class II molecules from lysosomal structures to the cell surface.* J.Cell Biol., 1996. **135**(3): p. 611-622.

17. Conrad, C. and D.W. Gerlich, *Automated microscopy for high-content RNAi screening.* J Cell Biol, 2010. **188**(4): p. 453-61.
18. Mattila, J. and O. Puig, *Insights to transcriptional networks by using high throughput RNAi strategies.* Brief Funct Genomics, 2010. **9**(1): p. 43-52.
19. Steinman, R.M. and Z.A. Cohn, *Identification of a novel cell type in peripheral lymphoid organs of mice. I. Morphology, quantitation, tissue distribution.* J Exp Med, 1973. **137**(5): p. 1142-62.
20. Randolph, G.J., et al., *Differentiation of phagocytic monocytes into lymph node dendritic cells in vivo.* Immunity, 1999. **11**(6): p. 753-61.
21. Inaba, K., et al., *Generation of large numbers of dendritic cells from mouse bone marrow cultures supplemented with granulocyte/macrophage colony-stimulating factor.* J Exp Med, 1992. **176**(6): p. 1693-702.
22. Garg, S., et al., *Lysosomal trafficking, antigen presentation, and microbial killing are controlled by the Arf-like GTPase Arl8b.* Immunity, 2011. **35**(2): p. 182-93.
23. Nickerson, D.P., C.L. Brett, and A.J. Merz, *Vps-C complexes: gatekeepers of endolysosomal traffic.* Curr Opin Cell Biol, 2009. **21**(4): p. 543-51.
24. Johansson, M., et al., *Activation of endosomal dynein motors by stepwise assembly of Rab7-RILP-p150Glued, ORP1L, and the receptor betalll spectrin.* J Cell Biol, 2007. **176**(4): p. 459-71.
25. Rocha, N., et al., *Cholesterol sensor ORP1L contacts the ER protein VAP to control Rab7-RILP-p150 Glued and late endosome positioning.* J Cell Biol, 2009. **185**(7): p. 1209-1225.
26. Chow, A., B.D. Brown, and M. Merad, *Studying the mononuclear phagocyte system in the molecular age.* Nat Rev Immunol, 2011. **11**(11): p. 788-98.

Nederlandse samenvatting

Major Histocompatibility Complex klasse II moleculen (MHC klasse II) zijn belangrijke regulatoren van de adaptieve immuun respons. Ze komen specifiek tot expressie in professioneel antigen presenterende cellen (APC) waar ze peptiden, afkomstig van opgenomen materiaal, presenteren aan T helper lymphocyten. MHC klasse II is fundamenteel voor het dirigeren van zowel de cellulaire als de humorale immuun respons.

Sinds lange tijd is bekend dat er een genetisch verband bestaat tussen bepaalde MHC klasse II allelen en bepaalde auto-immuunziekten, maar tot nu toe is er nog geen goede verklaring voor het moleculaire mechanisme achter dit verband. Meer kennis over MHC klasse II antigeen presentatie is essentieel om de huidige behandelmethodes voor auto-immuunziekten te verbeteren.

Wij hebben een unieke methode ontwikkeld waarin verschillende datasets met elkaar zijn geïntegreerd om een compleet beeld te krijgen van dit belangrijke cellulaire proces, MHC klasse II antigeen presentatie (zie hoofdstuk 1 en 2 van dit proefschrift).

Bij het opzetten van een RNAi screen is het belangrijk de voordelen, maar ook de nadelen van de techniek te kennen. In onze aanpak hebben we voor robuustheid gezorgd door gebruik te maken van een melanoma cel lijn, welke een functionele MHC klasse II antigeen presentatie route bezit. Door gebruik te maken van twee monoclonale antilichamen konden we onderscheid maken tussen twee verschillende vormen van MHC klasse II aan de cel oppervlakte. Dit gaf ons de mogelijkheid genen te identificeren die betrokken zijn bij de regulatie van ofwel de totale MHC klasse II levels ofwel de peptide belading van MHC klasse II aan het cel oppervlak. Deze gegevens hebben we geïntegreerd met gegevens uit een tweede screen, in welke we gekeken hebben naar de lokalisatie van intracellulaire MHC klasse II moleculen met behulp van confocale microscopie. Daarnaast hebben we ook op grote schaal door middel van kwantitatieve PCR gekeken naar het effect van gen onderdrukken op de expressie niveaus van de MHC klasse II locus. Met behulp van de data die deze screen opleverde, konden we een complex CIITA regulerend netwerk tekenen, bestaande uit signaalmoleculen en transcriptiefactoren, met vele feedbackloops. CIITA is de belangrijkste regulator van MHC klasse II transcriptie.

Door geen voorselectie te maken, maar telkens de gehele lijst met kandidaat genen te gebruiken voor follow-up experimenten, hebben we uiteindelijk een unbiased dataset verkregen. De kandidaat genen zijn onderworpen aan verschillende testen/screens. Door de verschillende resultaten te integreren hebben we deze kandidaat genen kunnen clusteren naar gelijkende effecten op de MHC klasse II antigeen presentatie route.

Deze geïntegreerde dataset is gebruikt om kandidaat genen te selecteren die naar onze mening betrokken zijn bij het dirigeren van MHC klasse II moleculen van intracellulaire laat endosomale membranen naar het plasma membraan tijdens dentritische cel (DC) activatie (maturatie). Voor een aantal van deze genen hebben we de betrokkenheid bij dit proces kunnen bevestigen. Eén van deze genen, ARL14 hebben we in meer detail bestudeerd. Met behulp van proteomics hebben we interactiepartners van ARL14 geïdentificeerd. Dit ARL14 complex lijkt belangrijk te zijn voor de lokalisatie van MHC klasse II positieve laat endosomale vesicles langs het cytoskelet (zie hoofdstuk 1 en 2 van dit proefschrift). Het beter begrijpen van de systeembiologie van MHC klasse II presentatie is slechts één manier om nieuwe targets te vinden voor de behandeling van bijvoorbeeld auto-immuunziekten. De afgelopen tien jaar zijn verschillende methodes beschreven waarop de presentatie van antigeen door MHC klasse II gemoduleerd kan worden. Deze zijn uitgelicht in hoofdstuk 3 van dit proefschrift.

DCs hebben een grote bijdrage in immuun regulatie en antigeen presentatie. Daarom komt er bij het bestuderen van MHC klasse II moleculen altijd een moment waarop DCs een rol gaan spelen. In hoofdstuk 4 van dit proefschrift worden methoden beschreven die de onderzoeker in staat stellen de MHC klasse II route te bestuderen in dit professionele antigeen presenterende cel type.

Appendices

Curriculum vitae
List of Publications
Acknowledgements

Curriculum vitae

Petra Paul was born in Vienna (Austria) on October 10, 1980. In 2000, she graduated with distinction from the Secondary College for Chemical Technology (Specialization: Biochemistry and Biochemical Technology). In the same year, she enrolled in the Molecular Biology program at the University of Vienna. In 2001, she began to work part-time in the tumor immunology group of Priv. Doz. Dr. Thomas Felzmann at the Children's Cancer Research Institute in Vienna. This occupation lasted until 2006 and was finalized by the Master thesis entitled "The cellular biology of cross-presentation: Two-step maturation of dendritic cells".
During the summer of 2003, she joined the group of Dr. Ornella Parolini, director of the Centro di Ricerca E. Menni in Brescia (Italy), for a three month internship supported by a Leonardo da Vinci fellowship. During this internship Petra investigated the tolerogenic potential of cells of human amnion and chorion.
In March 2006, she graduated with distinction in Molecular Biology (Specialization: Cell Biology, Immunology and Molecular Medicine) from the University of Vienna. In July 2006, she joined the group of Prof. Dr. Jacques Neefjes at the Department of Cell Biology at the Netherlands Cancer Institute in Amsterdam (The Netherlands), where she performed the research described in this thesis.

List of Publications

Paul, P. and Neefjes, J., *Studying MHC class II transport in dendritic cells.* Methods Mol Biol, 2012. (in press)

Hoorn, T.v., **Paul, P.**, Janssen, L., Janssen, H. and Neefjes, J., *Dynamics within tetraspanin pairs affect MHC class II expression.* J Cell Sci, 2012. **125**(2): p. 328-339.

Neefjes, J., Jongsma, M.L., **Paul, P.** and Bakke, O., *Towards a systems understanding of MHC class I and MHC class II antigen presentation.* Nat Rev Immunol, 2011. **11**(12): p. 823-836.

Paul, P., van den Hoorn, T., Jongsma, M.L., Bakker, M.J., Hengeveld, R., Janssen, L., Cresswell, P., Egan, D.A., van Ham, M., Ten Brinke, A., Ovaa, H., Beijersbergen, R.L., Kuijl, C. and Neefjes, J., *A Genome-wide multidimensional RNAi screen reveals pathways controlling MHC class II antigen presentation.* Cell, 2011. **145**(2): p. 268-283.

van den Hoorn, T., **Paul, P.**, Jongsma, M.L. and Neefjes, J., *Routes to manipulate MHC class II antigen presentation.* Curr Opin Immunol, 2011. **23**(1): p. 88-95.

Dohnal, A.M., Luger, R., **Paul, P.**, Fuchs, D. and Felzmann, T., *CD40 ligation restores type 1 polarizing capacity in TLR4-activated dendritic cells that have ceased interleukin-12 expression.* J Cell Mol Med, 2009. **13**(8B): p. 1741-1750.

Hüttner, K.G., Breuer, S.K., **Paul, P.**, Majdic, O., Heitger, A. and Felzmann, T., *Generation of potent anti-tumor immunity in mice by interleukin-12-secreting dendritic cells.* Cancer Immunol Immunother, 2005. **54**(1): p. 67-77.

Felzmann, T., Hüttner, K.G., Breuer, S.K., Wimmer, D., Ressmann, G., Wagner, D., **Paul, P.**, Lehner, M., Heitger, A. and Holter, W., *Semi-mature IL-12 secreting dendritic cells present exogenous antigen to trigger cytolytic immune responses.* Cancer Immunol Immunother, 2005. **54**(8): p. 769-780.

Felzmann, T., Witt, V., Wimmer, D., Ressmann, G., Wagner, D., **Paul, P.**, Hüttner, K. and Fritsch, G., *Monocyte enrichment from leukapharesis products for the generation of DCs by plastic adherence, or by positive or negative selection.* Cytotherapy, 2003. **5**(5): p. 391-398.

Bailo, M., Soncini, M., Vertua, E., Signoroni, P.B., Sanzone, S., Lombardi, G., Arienti, D., Calamani, F., Zatti, D., **Paul, P.**, Albertini, A., Zorzi, F., Cavagnini, A., Candotti, F., Wengler, G.S. and Parolini, O., *Engraftment potential of human amnion and chorion cells derived from term placenta.* Transplantation, 2004. **78**(10): p. 1439-1448.

Acknowledgements

Six years of PhD project are coming to an end; years of ups and downs, utter excitement when a hypothesis is proven, as well as fear of drowning in piles of high throughput data. A driving force and major factor of motivation has been my supervisor. Jacques, I would like to thank you for your continuous trust in me, ever since you hired me back in 2006. I am grateful that you always encouraged me to tackle the various challenges of a genome-wide screen. You are an endless source of inspiration. Often crosslinking approaches from various fields, which I have enjoyed and learned from a lot. I admire (and sometimes dread) how you are always up-to-date with everyone's experiments. Thank you for granting me independence and giving me trust in my own capabilities.

All the screening efforts would not have been manageable without the combined forces of our 'screen team'. Thank you, Marlieke and Tineke, for fruitful discussions, pep talks and countless hours of collaborative efforts in the lab. Coen, I would like to thank you for your valuable input in the design of our screening strategy, especially, when it came to bioinformatics. A big thanks also goes to two talented students, who helped with the primary screen, Mark and Rutger.
I have incredibly enjoyed those years working in a lively, friendly and loyal group. Dear current and former Neefixes, I thank you very much: Tom, Alex, Marije, Joost, Christoph, Nuno, Vero, Wilbert, Coen, Vicky, Tineke, Izhar, Lennert, Baoxu, Jeroen, Xiaohang, Ilana, Gosia, Tizi, Rik, Amy, Marlieke, Charlotte, Ruud, Sjoerd, Robbert, and Inge. Thank you Lennert, for keeping the lab up and running and for the cloning of various constructs!

Life in our department would be chaotic wasn't it for the dedication of Hans and Marieke. Thank you for all your help with various administrative issues!
I would also like to thank all other members of former H4 and current B6 for discussions, help and the amicable atmosphere.
What would daily life be without your office buddies? I have always had a great bunch of people surrounding me. Thanks, Vicky, Erik, Diane, Tineke, Marlieke, Farid, Anass, Amy, and Reggy for all the laughter, good music and Dutch lessons ;-)

Furthermore, I would like to acknowledge the three people that have kept an eye on my progress during those years, and who have always come up with useful suggestions and encouraging words: Thank you, Jannie, Ton and Reuven.

In those past years, my work has relied on the help and services of many of the facilities in the NKI. Herewith, I would like to express my gratitude to Roderick, Dave, Pasi, Ben, Frank and Anita, Lenny and Lauran, Ron and Lodewijk. I would also like to thank the numerous labhelpers! What a great initiative.

This project would not have been possible without the advice, materials and help of our collaborators. Thank you, Pete, Anja, Marieke, Huib, and Oddmund. Numerous colleagues in the NKI have provided valuable input in my work over those years. Thank you all for teaching me methods, sharing your knowledge and your suggestions.

At the NKI, I have not only found a great environment to perform research, but also a great crowd of people. Many experiences throughout these years have left their impressions, which I hope to take with me in the future. Thank you, Eitan, Nuno, Vero, Katy, Ulli, Sascha, Guillaume, Vicky, Baoxu, Xiaohang, Rik, Dalila, Fra, Ari, Charlotte, Tizi, Cristiane, Xanthippi, Patricia, Christelle, Katrin, Dilek, Alessia, Cesare, Zeliha and Suresh for Weekendjes weg and other excursions, especially the culinary ones during the International Dinners. Talking of eating, every working day has a lunch break, and I believe that ours are special. Thank you, Appiah, for your smile and positive energy!!!

At home I have been sharing my house with two great persons. Katrin, vielen Dank für die nette Zeit. Ich wünsche dir alles Gute für die Zukunft!
Vicky, those three years living together have been so much fun. I miss it! All the best to your lovely little family and good luck with your new job!

I would like to thank my two paranimfs (paranimfen, paranimfi,… or whatever the plural of that word is) for their support in the preparation phase and on the day of my thesis defense. Grazie, Fra! Dankeschön, Schwesterherz!

Dear Ana, thank you for your friendship. You are a true partner in crime whether it may be science, travelling, or food,... All the best for your PhD!
Klein, aber fein, ist mein Kreis an Freunden aus der Heimat. Vielen Dank, dass ihr trotz Distanz und oftmalig längerer Sendepause immer für mich da seid. Ich hoffe, das bleibt auch in Zukunft so, wohin auch immer es mich verschlägt. Meine Haustür steht jederzeit für Besuche offen. Danke für Eure Freundschaft: Vera, Mareike, Schutzi, Evi, Romy, Nina, und Tamara.

Zu guter Letzt möchte ich meinen Eltern danken. Für die Unterstützung über all die Jahre endloser Ausbildung. Es ist vollbracht, jetzt kann der Ernst des Lebens beginnen. Danke, dass ihr mein Streben immer unterstützt habt, auch wenn es mich weit weg von daheim geführt hat. Aufmunternde Worte haben mir durch so manche Krise geholfen.

Liebe Sarah, 2644 km weit weg, aber doch immer ganz nah. Ich vermisse dich, aber ich freu mich auch, dass es dir in der Türkei so gut gefällt. Ich verspreche, meine nächste Destination hat besseres Wetter.

Dear Marcello, every day I am grateful to have met you. I am excited about what the future might hold for us. Thank you for your love and support!

I apologize to those of you I might have forgotten in the rush and excitement of wrapping up my thesis. My sincere thanks go out to everyone who has supported me in those last six years.

Petra